

**UNCLASSIFIED**

---

**AD 401 142**

*Reproduced  
by the*

**DEFENSE DOCUMENTATION CENTER**

**FOR**

**SCIENTIFIC AND TECHNICAL INFORMATION**

**CAMERON STATION, ALEXANDRIA, VIRGINIA**



---

**UNCLASSIFIED**

NOTICE: When government or other drawings, specifications or other data are used for any purpose other than in connection with a definitely related government procurement operation, the U. S. Government thereby incurs no responsibility, nor any obligation whatsoever; and the fact that the Government may have formulated, furnished, or in any way supplied the said drawings, specifications, or other data is not to be regarded by implication or otherwise as in any manner licensing the holder or any other person or corporation, or conveying any rights or permission to manufacture, use or sell any patented invention that may in any way be related thereto.

AEDC-TDR-63-88

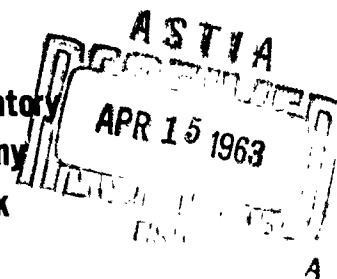
63-3-2



**MOLECULAR FLUX DISTRIBUTION  
IN AN AEROSPACE CHAMBER –  
ANALYSIS OF GAS KINETICS –  
SUMMARY REPORT**

By

**C. A. Tsonis  
General Engineering Laboratory  
General Electric Company  
Schenectady, New York**



**TECHNICAL DOCUMENTARY REPORT NO. AEDC-TDR-63-88**

**April 1963**

**AFSC Program Area 850E, Project 7778, Task 777801**

(Prepared under Contract No. AF 40(600)-954 by the General Engineering Laboratory, General Electric Company, Schenectady, New York)

**ARNOLD ENGINEERING DEVELOPMENT CENTER  
AIR FORCE SYSTEMS COMMAND  
UNITED STATES AIR FORCE**

# ***NOTICES***

Qualified requesters may obtain copies of this report from ASTIA. Orders will be expedited if placed through the librarian or other staff member designated to request and receive documents from ASTIA.

When Government drawings, specifications or other data are used for any purpose other than in connection with a definitely related Government procurement operation, the United States Government thereby incurs no responsibility nor any obligation whatsoever; and the fact that the Government may have formulated, furnished, or in any way supplied the said drawings, specifications, or other data, is not to be regarded by implication or otherwise as in any manner licensing the holder or any other person or corporation, or conveying any rights or permission to manufacture, use, or sell any patented invention that may in any way be related thereto.

MOLECULAR FLUX DISTRIBUTION  
IN AN AEROSPACE CHAMBER -  
ANALYSIS OF GAS KINETICS -  
SUMMARY REPORT

By

C. A. Tsonis

General Engineering Laboratory

General Electric Company

Schenectady, New York

(The reproducibles used in the reproduction  
of this report were supplied by the author.)

April 1963

### FOREWORD

The work described in this report was performed at the General Engineering Laboratory, General Electric Company for the Missile and Space Vehicle Department, General Electric Company under MSD Requisition Number AF 40(600)-954.

### ACKNOWLEDGEMENT

The author wishes to express his gratitude to the personnel of the Computer Section at AEDC for their efforts in programming the mathematical problem on molecular kinetics and in producing the computer results of the test cases indicated in the text.

### ABSTRACT

The purpose of this investigation was to determine analytically the molecular incidence rates on the various surfaces of the space simulator. The mathematical model of the space simulator consists of two concentrically located spherical surfaces corresponding to the chamber wall outside and to the vehicle inside. The analysis is divided into two phases.

Phase I deals with conditions of uniform pumping and outgassing on each surface. A square pulse of outgassing is assumed to occur and the total number of molecular hits is determined for each surface. These results are extended to a steady state uniform flow and the molecular incidence rates are obtained.


Phase II is an analysis of the nonuniform case introduced by surface discontinuities of axisymmetric type. The procedure followed is to determine the various probabilities that a molecule leaving a surface will hit spherical zones on either surface. Using these probabilities the molecular incidence rates can be determined. While the probabilities have been found, analytic expressions for molecular incidence determination are very difficult to obtain.

The problem, therefore, was approached from a computer point of view enabling us to obtain computer solutions with a high degree of accuracy.

### PUBLICATION REVIEW

This report has been reviewed and publication is approved.

  
Donald D. Carlson  
Lt Col, USAF  
Chief, Space Systems Office

  
Jean A. Jack  
Colonel, USAF  
DCS/Test

## CONTENTS

	<u>Page</u>
1.0 INTRODUCTION -----	1
1.1 The Vehicle in Space -----	1
1.2 The Vehicle in a Chamber -----	2
1.3 Molecular Kinetics -----	3
1.4 Molecular Flux Distribution -----	4
2.0 COSINE DISTRIBUTION -----	5
3.0 UNIFORM PUMPING (PHASE I) -----	7
3.1 Directional Flow (Pulse) -----	7
3.1.1 Difference Equations -----	7
3.1.2 Special Cases -----	9
3.1.3 Molecular Pumping -----	10
3.2 Steady State Uniform Flow -----	10
3.2.1 Rate Determination of Molecular Incidence -----	11
3.2.2 Special Cases of Rate Determination -----	12
3.3 Resume -----	12
4.0 SINGLE SURFACE DISCONTINUITY (PHASE II) -----	13
4.1 Analysis Approach to the Probability Equations of Molecular Transfer -----	13
4.1.1 From the Chamber Wall to the Vehicle -----	14
4.1.2 From the Vehicle to the Chamber Wall -----	24
4.1.3 From the Chamber Wall to the Chamber Wall -----	27
4.2 Recapitulation -----	31
5.0 COMPUTER LOGIC -----	34
5.1 Partition -----	34
5.2 Probability Equations -----	35
5.3 Probability Flow Charts -----	36
5.3.1 From Chamber Wall to Vehicle -----	36
5.3.2 From Chamber Wall to Chamber Wall -----	37
5.4 Molecular Transfer Flow Charts -----	40



	<u>Page</u>
5.5 Modified Approach to the Computer Solution -----	41
5.5.1 Matrix Notation -----	42
5.5.2 Molecular Transfer -----	44
5.5.3 Molecular Flux Distribution -----	45
6.0 COMPUTER RESULTS -----	46

FIGURES

## SYMBOLS

Subscripts v and c refer to vehicle and chamber wall, respectively. In case we specify a portion on either of these two surfaces, v and c will be employed accordingly.

- $a_x$  = pumping coefficient on surface x (where x = v or c)
- $P_{xy}$  = probability that a molecule leaving surface x will hit surface y (=cor v) without an intermediate collision. Clearly  $P_{vc} = 1$ ,  $P_{vv} = 0$
- $H_{xy}$  = total number of molecular hits against the non-pumping surface y due to a flow originated at surface x.
- $H_x$  = total number of molecular hits against the non-pumping portion of surface x (x = v or c)
- $M_x(n)$  = number of molecules pumped out on surface x during the interval  $n\tau \leq t < (n+1)\tau$ ,  $n=1, 2, \dots$
- $M_x$  = total number of molecules pumped out on surface x
- $f_x(n)$  = number of molecules leaving surface x during the interval  $n\tau \leq t < (n+1)\tau$ ,  $n=1, 2, \dots$
- $F_x$  = steady state uniform flow per unit area per unit time originating at surface x
- $R_x$  = rate of molecular incidence on surface x per unit area
- $r_x$  = radius of surface x
- $\gamma$  = angle between the tangent vector to the vehicle and the radial vector both vectors drawn from a point on the chamber wall.

In considering the probability  $P_{xy}$  of a point p (see Figures 2,3,4,5,6,7)

- $\theta_p$  = latitude of the point p
- $C_{\theta_p}$  = boundary of the surface region on y illuminated from p
- $\theta_o$  = latitude on surface y
- $G_{\theta_o}$  = subregion of the illuminated region on y bounded by  $C_{\theta_p}$  and/or  $\theta_o$  for which the latitude  $\theta$  of any point in that subregion satisfies the relation  $\theta \geq \theta_o$

### Spherical Zone Probabilities

- $P_{xy}(\theta_i, \theta_j)$  = probability that a molecule departing from a point on surface  $x$  with latitude  $\theta_i$  will hit the surface region on surface  $y$  bounded below by the latitude  $\theta_j$ . This region may or may not be illuminated completely from that point (see Figures 8 - 15).
- $P_{x_i y_j}$  = probability that a molecule departing from a spherical zone  $X_i$  will hit the spherical zone  $Y_j$ .
- $\rho(x_i)_n$  = number of molecules leaving the spherical zone  $x_i$  during  $n\tau \leq t < (n+1)\tau$
- $X_i$  =  $i$ 'th spherical zone on surface  $X$
- $N_1$  = spherical zone on the chamber wall whose upper boundary is the discontinuous line.

### Single Surface Discontinuity

- $a_{v_i}$  =  $a_v$  for all  $i$
- $a_{c_i}$  =  $a_{c_1}$   $\begin{cases} 1 \leq i \leq N_1 \\ n_1 + 1 \leq i \leq 2N \end{cases}$
- $g_1$  = flow rate per unit area introduced on the part of the chamber wall for which  $a_{c_i} = a_{c_1}$
- $g_2$  = flow rate per unit area introduced on the part of the chamber wall for which  $a_{c_i} = a_{c_2}$
- $g$  = flow per unit area introduced on the vehicle
- $X, Y, Z$  = usual cartesian coordinate system
- $r, \theta, \phi$  = usual spherical coordinate system
- $\alpha$  = complement of  $\theta$
- $\beta$  = same as  $\phi$
- $(\theta_i, \theta_j)$  = spherical zone on either surface bounded by the latitudes  $\theta_i$  and  $\theta_j$
- $\theta_d$  = latitude of discontinuous line on chamber wall
- $N$  = number of spherical zones of a hemisphere
- $N_2$  =  $\gamma/\Delta\theta$
- $\theta_I$  = lower latitude of the  $I$ 'th spherical zone
- $\overline{\text{Lim}} C_{\theta_I}$  = maximum latitude of  $C_{\theta_I}$
- $\underline{\text{Lim}} C_{\theta_I}$  = lower latitude of  $C_{\theta_I}$

## 1.0 INTRODUCTION

As a necessary consequence of the space age, it has become mandatory to plan for ground testing of space vehicles, components and materials. The duplication of all the spatial environments is obviously impossible. Many papers have been written defining those environments which could be simulated and the degree to which simulation is required. Among those listed as necessary and feasible is the low pressure environment of outer space. It is frequently stated that a pressure of  $10^{-5}$  Torr is sufficient to simulate the thermal radiation environment and the high electrical impedance of space. This statement alone does not define where the pressure is measured, nor in fact what is meant by pressure in the highly directional conditions of both true space and a space environmental simulator. A serious evaluation of the nature of the molecular flux in both cases is necessary in order to evaluate what is meant by simulation.

### 1.1 THE VEHICLE IN SPACE

Two altogether different gaseous sources surround the vehicle in space. First, there is the natural environment which was there prior to the entry of the space vehicle, and secondly, the gas sources which have been contributed by the vehicle.

The atmosphere of the planet earth at altitudes above 1500 km consists primarily of hydrogen ions, decreasing in density with increase in altitude. Below this level, the atmosphere consists principally of oxygen and nitrogen in atomic, ionized, or molecular states, depending on the altitude. Between 200 and 1500 km the density decreases with increasing altitude from about  $10^{10}$  to  $10^5$  particles per cubic centimeter. The corresponding mean free paths range from a few miles to several hundred thousand miles, distances which are huge relative to the dimensions of any space craft. The velocity of these molecules ranges from 1 to 2 km/sec. Yet, the velocity of an earth satellite ranges from 7.5 to 11 km/sec. The vehicle then appears to be rushing through a relatively stationary low density gas medium, most of the collisions being on the leading edge of the space craft. We note then that the molecular incidence rate, and the pressure, depends on the velocity of the vehicle and varies over the surface of the vehicle.

In addition to the planet atmosphere, the sun is thought to emit a variable stream of protons and electrons (solar wind) having a density of 600 to 10,000 protons per cubic centimeter near the earth. The velocity of these protons varies from 500 to 2000 km/sec. depending on the solar activity. The incidence rate is from  $5 \times 10^{10}$  to  $2 \times 10^{12}$  particles per second per square centimeter, which is comparable to the incidence rate of molecules from the planet atmosphere at high altitudes. Since the velocity of the solar wind is so much higher than that of the vehicle, the collisions are all on the side facing the sun. The extremely high energy is sufficient to cause sputtering or other surface phenomena. Again we note that there is no uniformity over the surface of the vehicle, nor can we simply define a pressure equivalent of altitude.

In addition to the environmental gases, the vehicle itself is a major source of gas, in the form of outgassing and leakage. This gas is given off by the vehicle with thermal energies relative to the vehicle. The outgassing occurs in all directions, but may well vary over the surface of the vehicle, depending on the variations in the vehicle structure and material composition. The outgassing products will travel many miles in a straight line before making collisions with an environmental molecule, hence for all practical purposes, the molecules which leave the vehicle are permanently gone. Space may therefore be considered as pumping molecules as fast as they are produced. This pumping action is not related to the conventional concept of effusion velocity of an orifice of a fixed speed per unit area, as no fixed area of space can be defined as the pumping surface.

In almost all space vehicle situations, the outgassing of the vehicle represents a far greater density than that contributed by either the planet environment or the solar wind. Hence, the gas density surrounding the vehicle is almost entirely made up of the composition of the outgassing products. Yet this gas is all moving away from the vehicle and does not contribute to the gas returning to the vehicle. The returning gas is still defined by the velocity of the vehicle and the normal environment through which it is moving.

## 1.2 THE VEHICLE IN A CHAMBER

When a vehicle is placed in a space simulation chamber, it is again exposed to two different sources of gas: 1) The natural environment or background of the chamber, and 2) The gas contributions due to the outgassing and leakage of the vehicle.

For true duplication of the atmosphere of space, the chamber background should match that of the upper atmosphere in gas type, density and energy. In addition, it should be properly oriented to account for the relative velocity of the vehicle through the stationary gas, and the solar wind. While such conditions are not completely impossible, they are sufficiently difficult and expensive, that realistic evaluations are required to determine the necessity of such duplication. In the normal space chamber, the residual gas is made up of the outgassing products of the walls of the chamber and leaks which may exist to the outside atmosphere or to various internal fluid sections such as cryogenic lines. The composition of this gas will vary in different chambers, and may include such gas types as: water vapor, hydrogen, carbon dioxide, carbon monoxide, nitrogen and helium. The gas is not ionized, and in general is at a temperature of about 100°K. In addition, there may be directional effects in the event that discontinuities exist on the chamber wall. For example, the presence of a large area solar simulator may contribute a high outgassing rate from a particular section of the chamber wall.

When the vehicle is in a chamber, just as when it is in space, the outgassing of the vehicle is the predominate gas present. However, in the

case of the chamber an altogether different situation exists. In order to duplicate the effectively infinite pumping speed of outer space the chamber must have walls which are perfect condensers for all incident molecules. Since such perfect condensers are not presently feasible, a great majority of the outgassing from the vehicle is reflected from the chamber wall and returns to the vehicle. In almost all instances, this returning gas flux is far larger than the original chamber background. Again we note that this gas flux does not have the characteristic properties of the permanent space background. The gas is predominately water and nitrogen. The temperature is between 100 and 300°K. Anomalous directional effects may exist if large areas of non pumping walls are present.

The foregoing differences between a chamber and space may not be of importance in the superficial condition of simulating for heat transfer and electrical discharge effects. However, if any surface phenomena is involved, such as friction or sputtering, entirely different results may be obtained in the two cases.

### 1.3 MOLECULAR KINETICS

Considering the foregoing differences between true space and so-called space simulators, it is apparent the simple question "What altitude has been simulated?" is almost impossible to define. In the simplest case it creates a serious controversy of philosophy, measuring equipment, and people. The Molecular Kinetics program was started to study the various problems of gas-vehicle collisions in space and in a chamber, to produce a yardstick for measuring simulation, and to define the effects or limitations of various chamber parameters on the degree of simulation achieved. This program is divided into a number of different phases, each covered in a different report. The common denominator of all phases of the Molecular Kinetics program is the dealing with highly directional gas flows, in terms of measuring, controlling, or defining simulation.

In order to derive a language to be used in the interpretation of space simulation, and which is compatible with the parameters present in space simulator, it is first necessary to define the ground rules to be used. We first note that the vehicle is the point of interest for discussing simulation, and further it is the molecules arriving at the vehicle which are of importance. Any measurement or consideration of molecular fluxes or pressures on the chamber wall are of importance only in so far as they can be interpreted at the vehicle proper. The second important factor to be determined is the term to be used for discussing gas particles in the simulator. Three different terms are immediately apparent: pressure, density, and particle flux.

While density is very meaningful for the random gas in space in the absence of a vehicle, it has little meaning for the vehicle when a large amount of outgassing products from the vehicle are included in the measurement. The density concept does not define the direction of the gas and hence cannot be related to the molecules striking the vehicle, either in space or in a chamber.

A consideration of the earlier discussions on the extreme directional effects both in space and in a chamber indicates that molecular incidence and energy level are the important factors in assessing simulation. It is apparent that there is a considerable difference in the temperatures in space and in a simulator. A theoretical assessment of the temperature of the molecules received by the vehicle in a space chamber is almost impossible due to the variations in the temperature within the chamber and the differences in the accommodation coefficient for different gases. While pressure is related to both energy and incidence rate, the true measurement of pressure is likewise a very difficult problem. From both the analysis and the measurements point of view it is far easier to consider the rate at which molecules are striking a surface. Except for cases of extreme energy (such as the solar wind) the surface reactions are more dependent on the gas type than on the variations of energy which exist. For these, and other reasons which will be more apparent in the different reports, the concept of molecular flux has been chosen for all analysis. Molecular flux is defined as the number of molecules per square centimeter per second arriving or leaving a given surface.

#### 1.4 MOLECULAR FLUX DISTRIBUTION

This part of the Molecular Kinetics program has to do with the mathematical analysis of computing the molecular flux on every part of the space vehicle and the chamber walls as a result of outgassing occurring from either the vehicle or the chamber wall. The program further considers the effects of a surface discontinuity, such as a solar region, on the flux distribution. In solving this problem probability equations were first derived for an axial symmetry, and equations were generated for the limiting conditions of every possible configuration. In all cases a cosine distribution was assumed for the leaving molecules. The general problem of a single surface discontinuity was then handled by means of a computer program. The program considers the case of a spherical vehicle in a spherical chamber, one of which contains a spherical cap of different properties. The surfaces are then divided into circular sections about a common axis congruent with the axis of the single surface discontinuity. A value of sticking coefficient and outgassing rate is assigned to each surface. The computer program counts the molecules arriving and leaving each and every surface until a steady state flow condition is obtained. This final value then defines the molecular flux to the different parts of the system as a result of the assumed outgassing rates.

## 2.0 COSINE DISTRIBUTION

In the molecular migration from one surface to another, it will be assumed that all molecules follow a "Cosine Distribution"; that is, the probability that a molecule will travel in a certain direction when it leaves from a point on a surface is proportional to the cosine of the angle between this direction and the normal to the surface at the point in question. Thus, molecules have the greatest tendency to leave a surface in a direction normal to the surface. The statistical concept of this law is presented in the following discussion.

Let  $da_1$  be a surface element on a surface  $S_1$  and let us assume that it is required to find the probability that the molecular flow emitted from that surface element will hit a specified area  $A_2$  on a surface  $S_2$ . If the element area  $da_1$  is taken sufficiently small we may speak, in a sense, of a point  $p$  instead of the element  $da_1$  as if the total flow from  $da_1$  was emitted from the point  $p$ . If a sphere  $S$  of arbitrary radius  $r$  (unit radius will be convenient) is constructed with center the point  $p$ , the directional vector from the point  $p$  to the boundary of area  $A_2$  will describe a closed curve  $s$  on the surface  $S$ . Let  $A$  be the area enclosed by  $s$ . If  $dA$  is an area element of  $A$  we have

$$dA = r^2 \cos\theta d\phi d\theta$$

Let  $\theta = f(\phi)$  be the equation of the curve  $s$ . The angle between the normal to  $S_1$  at  $p$  and the vector to any point of  $s$  from  $p$  is  $\frac{\pi}{2} - \theta$ . Since we assume a cosine distribution it follows that the molecular flow through  $dA$  will be

$$\begin{aligned} dA K \cos\left(\frac{\pi}{2} - \theta\right) &= Kr^2 \cos\theta \sin\theta d\phi d\theta \\ &= Kr^2 \sin\alpha \cos\alpha d\beta d\alpha \end{aligned}$$

where

$$\alpha = \frac{\pi}{2} - \theta, \beta = \phi \text{ and } K \text{ is a proportionally constant}$$

Thus

$$(\text{Total Flow thru } A) = \int d\beta \int_0^{\frac{\pi}{2} - f(\beta)} Kr^2 \cos\alpha \sin\alpha d\alpha$$

On the other hand

$$(\text{Total Flow thru hemisphere}) = \int d\beta \int_0^{\frac{\pi}{2}} Kr^2 \cos\alpha \sin\alpha d\alpha = K\pi r^2$$



Then the probability P of hitting the area A from the point p is

$$P = \frac{(\text{Total flow thru A})}{(\text{Total flow thru hemisphere})} = \frac{1}{\pi} \int_0^{\frac{\pi}{2}} d\beta \int_0^{f(\beta)} \cos\alpha \sin\alpha d\alpha$$

Thus, the probability that a molecule emitted from a point on a sphere of radius  $r_c$  will hit an inside sphere of radius  $r_v$  is

$$P = \frac{1}{\pi} \int_0^{2\pi} d\beta \int_0^{\gamma} \cos\alpha \sin\alpha d\alpha = \sin^2 \gamma$$

### 3.0 UNIFORM PUMPING

The objective of this section is to determine the rate of molecular incidence on either surface under the most simplified conditions. In this analysis, the most simplified model of space simulator is considered; i.e., a spherical test vehicle located concentrically in a spherical test chamber. The walls of both the vehicle and the chamber are assumed to have uniform properties and the pumping coefficients on each of these two surfaces are assumed uniformly distributed. To be more specific, if we define the pumping coefficient  $a_x$  by:

$$a_x = A_1/A$$

where  $A_1$  is the pumping portion of area  $A$ ,  $a_x$  remains constant throughout the surface  $x$ . Furthermore, in order to cover every special case we consider the general case where  $a_c \neq a_v \neq 0$ .

The analysis is made on the basis of a pulse of molecules being admitted uniformly from either the vehicle or the chamber wall or both surfaces. The results, however, are equally applicable to a steady state flow as it will be shown in a derivation below.

With this mathematical model we have

$$P_{cv} = \sin^2 \gamma = P, P_{vc} = 1$$

#### 3.1 DIRECTIONAL FLOW (PULSE)

##### 3.1.1 Difference Equations

The following difference equations are easily derived

$$f_v(n+1) = P(1-a_v)f_c(n) \quad (3.1)$$

$$f_c(n+2) = (1-a_c)(1-P)f_c(n+1) + (1-a_c)f_v(n+1) \quad (3.2)$$

Substituting 3.1 into 3.2 we obtain

$$f_c(n+2) - (1-a_c)(1-P)f_c(n+1) - (1-a_c)(1-a_v)Pf_c(n) = 0 \quad (3.3)$$

The general solution of 3.3 is

$$f_c(n) = C_1 r_1^n + C_2 r_2^n \quad (3.4)$$

where  $C_1$  and  $C_2$  are arbitrary constants which have to be defined from the boundary conditions, and  $r_1$  and  $r_2$  are the roots of the characteristic equation

$$\psi(r) = r^2 - (1-a_c)(1-P)r - (1-a_c)(1-a_v)P = 0 \quad (3.5)$$

#### Boundary Conditions

If the flow is introduced on both surfaces,  $f_c(1)$  will not depend on  $f_c(0)$  exclusively but on both  $f_c(0)$  and  $f_v(0)$ . If the flow is introduced on surface  $x$  only then  $f_v(0)=0$  for  $y \neq x$ . In any case we assume  $f_c(0)$  and  $f_c(1)$  given covering thus all special cases.

Then from 3.4 by setting  $n = 0, 1$  we obtain the following system of equations

$$\begin{cases} f_c(0) = C_1 + C_2 \\ f_c(1) = C_1 r + C_2 r_2 \end{cases} \quad (3.6)$$

Determining the constants  $C_1$  and  $C_2$  from 3.6 and putting them in 4) we obtain finally

$$f_c(n) = \frac{f_c(0)r_1 r_2 (r_1^{n-1} - r_2^{n-1})}{r_2 - r_1} - \frac{f_c(1)(r_1^n - r_2^n)}{r_2 - r_1} \quad (3.7)$$

However the number of molecules leaving the chamber wall during  $n\tau \leq t < (n+1)\tau$  is the same as the number of molecular hits on the nonpumping part of the chamber wall during  $n\tau \leq t < (n+1)\tau$ . Hence, the total number of molecular hits on the chamber wall is

$$H_c = \sum_{n=1}^{\infty} f_c(n) = \frac{f_c(1) - r_1 r_2 f_c(0)}{(1-r_1)(1-r_2)} \quad (3.8)$$

Similarly, from equation 3.1 and 3.8 we obtain

$$\begin{aligned} H_v &= \sum_{n=0}^{\infty} f_v(n+1) = P(1-a_v) \sum_{n=0}^{\infty} f_c(n) \\ &= P(1-a_v) \left[ \frac{f_c(1) - r_1 r_2 f_c(0)}{(1-r_1)(1-r_2)} + f_c(0) \right] \\ &= P(1-a_v) \frac{f_c(0) [1 - (r_1 + r_2)] + f_c(1)}{(1-r_1)(1-r_2)} \\ &= P(1-a_v) [H_c + f_c(0)] \end{aligned} \quad (3.9)$$

Another form of equations 3.8 and 3.9 in terms of  $f_c(0)$  and  $f_v(0)$  can be obtained by making the following substitution

$$\begin{aligned} f_c(1) &= (1-a_c)(1-P)f_c(0) + (1-a_c)f_v(0) \\ &= (r_1+r_2)f_c(0) + (1-a_c)f_v(0) \end{aligned}$$

Then 3.8 and 3.9 become

$$H_c = \frac{(r_1+r_2-r_1r_2)f_c(0) + (1-a_c)f_v(0)}{(1-r_1)(1-r_2)} \quad (3.10)$$

$$H_v = \frac{f_c(0) + (1-a_c)f_v(0)}{(1-r_1)(1-r_2)} \quad P(1-a_v) \quad (3.11)$$

### 3.1.2 Special Cases

Two special cases are of interest, namely,

$$f_c(1) = (1-P)(1-a_c)f_c(0) = (r_1+r_2)f_c(0), \quad f_v(0) = 0$$

$$f_c(1) = (1-a_c)f_v(0), \quad f_c(0) = 0$$

Substituting these two equations in equations 3.8 and 3.9 or just simply setting  $f_c(0)$  or  $f_v(0)$  equal to zero in equations 3.10 and 3.11 we obtain the following special cases.

$$H_{cc} = \frac{r_1+r_2-r_1r_2}{(1-r_1)(1-r_2)} f_c(0) \quad \left. \vphantom{H_{cc}} \right\} f_v(0) = 0 \quad (3.12)$$

$$H_{cv} = \frac{P(1-a_v)}{(1-r_1)(1-r_2)} f_c(0) \quad \left. \vphantom{H_{cv}} \right\} f_v(0) = 0 \quad (3.13)$$

$$H_{vc} = \frac{(1-a_c)}{(1-r_1)(1-r_2)} f_v(0) \quad \left. \vphantom{H_{vc}} \right\} f_c(0) = 0 \quad (3.14)$$

$$H_{vv} = \frac{-r_1r_2}{(1-r_1)(1-r_2)} f_v(0) \quad \left. \vphantom{H_{vv}} \right\} f_c(0) = 0 \quad (3.15)$$

### 3.1.3 Molecular Pumping

The number of molecules pumped on either surface during  $n\tau \leq t < (n+1)\tau$  is given by:

$$M_c(n) = \frac{a_c}{1-a_c} f_c(n) \quad (3.16)$$

$$M_v(n) = \frac{a_v}{1-a_v} f_v(n) \quad (3.17)$$

The total number of molecules pumped is

$$M_c = \sum_{n=1}^{\infty} M_c(n) = \frac{a_c}{1-a_c} H_c \quad (3.18)$$

$$M_v = \sum_{n=1}^{\infty} M_v(n) = \frac{a_v}{1-a_v} H_v \quad (3.19)$$

Note that we must have

$$M_c + M_v = f_c(0) + f_v(0)$$

since eventually all the introduced molecules must be pumped out. This can be verified to be the case.

## 3.2 STEADY STATE UNIFORM FLOW

The results obtained in 3.1 can be extended to the case where a steady state molecular flow is established instead of a pulse under the following assumptions.

a) The rate of molecular incidence is determined after a long period of time since the time when the uniform steady state flow was initiated.

b) Time duration between two successive hits of each molecule is taken to be a statistical average time interval  $\tau$ .

Consider now a square pulse of flow into the system of time duration starting at  $t = 0$  and suppose that we want to determine the number of molecular hits during the time interval  $n\tau \leq t < (n+1)\tau$ .

According to assumption b), the number of molecule hits during the time interval  $n\tau \leq t < (n+1)\tau$  will depend on how many molecules are present in the space simulator during the time interval  $(n-1)\tau \leq t < n\tau$ . Thus, our problem is to determine the number of molecular hits  $f(n)$  during  $n\tau \leq t < (n+1)\tau$  due to a

square pulse established during the time interval  $0 \leq t < \tau$ , or saying the same thing in a different way, to find the number of molecular hits during  $0 \leq t < \tau$  due to a square pulse established  $-n\tau$  ago. If we had two identical pulses established at  $t = n\tau$  and  $t = -(n+m)\tau$ , each pulse of duration  $\tau$  then by superposition, the total number of molecular hits during  $0 \leq t < \tau$  due to these two pulses will be  $f(n) + f(n+m)$ . Now we are ready to pass to a steady uniform flow. If the flow is considered to consist of square pulses, the total number of molecules present during the time interval  $0 \leq t < \tau$  is

$$\sum_{n=0}^{\infty} f(n) \quad \text{where } N \text{ is very large}$$

If, however,  $f(n)$  converges very rapidly (as indeed is the case) we may replace  $N$  by infinity. Then

$$\sum_{n=0}^N f(n) \sim \sum_{n=0}^{\infty} f(n)$$

Incidentally, it is obvious that any transient conditions of the flow at the beginning will have negligible effects.

Now let  $H$  be the number of molecular hits during  $0 \leq t < \tau$  due to  $\sum_{n=0}^{\infty} f(n)$  molecules present during  $-\tau \leq t < 0$ . Then the rate of molecular incidence during  $0 \leq t < \tau$  is  $\frac{H}{\tau}$ .

### 3.2.1 Rate Determination of Molecular Incidence

Clearly

$$f_c(0) = (1-a_c)F_c \tau 4\pi r_c^2$$

$$f_v(0) = (1-a_v)F_v \tau 4\pi r_v^2$$

Substituting these in equations 3.10 and 3.11 we obtain

$$R_c = \frac{(r_1 + r_2 - r_1 r_2)F_c + (1-a_v)F_v P}{(1-r_1)(1-r_2)} \quad (3.2.1)$$

$$R_v = \frac{(1-a_c)F_c + (1-a_c)P(1-a_v)F_v}{(1-r_1)(1-r_2)} \quad (3.2.2)$$

### 3.2.2 Special Cases of Rate Determination

a)  $f_v = 0$  (flow originated at chamber wall)

$$R_c = \frac{(r_1 + r_2 - r_1 r_2) F_c}{(1 - r_1)(1 - r_2)} \quad (3.2.3)$$

$$R_v = \frac{(1 - a_c) F_c}{(1 - r_1)(1 - r_2)} \quad (3.2.4)$$

If  $a_v = 0$ , equations 3.2.3 and 3.2.4 reduce to

$$R_c = R_v = \frac{(1 - a_c) F_c}{a_c} \quad (3.2.5)$$

b)  $f_c = 0$  (flow originated at vehicle)

$$R_c = \frac{(1 - a_v) P F_v}{(1 - r_1)(1 - r_2)} \quad (3.2.6)$$

$$R_v = \frac{r_1^2 F_v}{(1 - r_1)(1 - r_2)} \quad (3.2.7)$$

If  $a_v = 0$ , equations 3.2.6 and 3.2.7 reduce to

$$R_c = \frac{P F_v}{a_c} \quad (3.2.8)$$

$$R_v = \frac{(1 - a_c) P F_v}{a_c} \quad (3.2.9)$$

### 3.3 RESUMÉ

The results obtained by admitting a square pulse of molecular flow on either surface are represented by equations 3.8 and 3.9 or 3.10 and 3.11 and special cases are represented by equations 3.12 - 3.15. The total number of molecules pumped followed immediately from equations 3.18 and 3.19. Then the transition from a pulsed to a steady state continuous uniform flow was made in section 3.2 and the rates of molecular incidence were determined from equations 3.2.1 and 3.2.2. Particular cases appear in section 3.2.2. This completes Phase I of the analysis of the project.

#### 4.0 SINGLE SURFACE DISCONTINUITY

A surface discontinuity is established by either a discontinuity in the molecular flow or discontinuity in the pumping coefficient or both. Specifically, the function representing a discontinuous flow or a discontinuous pumping coefficient will be in the form of a step function. Further, the discontinuous line or lines on a surface will be a circle or parallel circles on the surface. One line discontinuity will be referred to as "single surface discontinuity" and many line discontinuity as "multiple surface discontinuity". Except for these discontinuities, the molecular flow as well as the pumping coefficient will be assumed uniformly distributed on each surface. The spherical configuration of the chamber-vehicle system and the types of discontinuities considered give rise to an axisymmetric case which simplifies somewhat the mathematical analysis of the problem. As a result of this axisymmetry, it is intuitively true that the distribution of molecular hits on a surface  $x$  depends only on the angle  $\theta$  between the axis of symmetry and the radius vector from the co-center of the system to any point on the surface  $x$ .

The following analysis deals with a single surface discontinuity on the chamber wall separating two spherical caps. The molecular flow and the pumping coefficient in each cap are uniformly distributed but differ from one cap to the other.

##### 4.1 ANALYSIS APPROACH TO THE PROBABILITY EQUATIONS OF MOLECULAR TRANSFER

The mathematical analysis of the single surface discontinuity is divided into two parts. Part I deals with setting up the various probability equations of molecular migration from one surface to specified regions on the same surface or on another surface. These regions are spherical caps bounded below by a latitude  $\theta_0$ . Then the probability that a molecule of a surface will hit a spherical zone on either surface will be the absolute value of the difference of two probabilities associating the point  $p$  with two spherical caps. Accordingly, there are three cases discussed.

The first case is when the point  $p$  is considered on the chamber wall and the specified region on the vehicle.

The second case is when both the point  $p$  and the specified region are on the chamber wall.

The third case is when the point  $p$  is considered on the vehicle and the specified region on the chamber wall. Thus, Part I will supply us all the information needed to proceed to Part II.

Part II deals with computer solutions of the problem. Both surfaces are divided into a sufficiently large number of spherical zones and the molecular flux density on each spherical zone on both surfaces is determined at any time interval. The purpose of these solutions is to provide us with



sufficient information so that we can determine the molecular flux distribution and the incidence rate at various parts of the vehicle and chamber wall as a result of two different steady state uniform flows, one introduced at one part of the discontinuous surface and the other on the other part of the discontinuous surface.

#### 4.1.1 From the Chamber Wall to the Vehicle

The transformation of coordinates from one orthogonal system to another can be accomplished by means of the following table

	i	j	K	
$\bar{a}$	$\frac{1}{h\alpha} \frac{\partial x}{\partial \alpha}$	$\frac{1}{h\alpha} \frac{\partial y}{\partial \alpha}$	$\frac{1}{h\alpha} \frac{\partial z}{\partial \alpha}$	
$\bar{b}$	$\frac{1}{h\beta} \frac{\partial x}{\partial \beta}$	$\frac{1}{h\beta} \frac{\partial y}{\partial \beta}$	$\frac{1}{h\beta} \frac{\partial z}{\partial \beta}$	
$\bar{c}$	$\frac{1}{h\gamma} \frac{\partial x}{\partial \gamma}$	$\frac{1}{h\gamma} \frac{\partial y}{\partial \gamma}$	$\frac{1}{h\gamma} \frac{\partial z}{\partial \gamma}$	(4.1)

where  $i, j, K$  are unit vectors in the direction of  $x, y, z$  in one system and  $\bar{a}, \bar{b}, \bar{c}$  are unit vectors in the directions of  $\alpha, \beta$  and  $\gamma$  in the other system, while  $h\alpha, h\beta, h\gamma$  are defined as:

$$h\alpha = \frac{\partial s}{\partial \alpha}, \quad h\beta = \frac{\partial s}{\partial \beta}, \quad h\gamma = \frac{\partial s}{\partial \gamma}$$

Now, let  $P$  be a point on the chamber wall with position  $\phi_P$  and  $\theta_P$  and let  $\alpha, \beta, \gamma$  be taken in the directions of increasing  $\phi, \theta$  and  $r$  at  $P$ . Then  $\gamma$  coincides with the normal to the surface at  $P$  drawn outwards, and the plane  $(\alpha, \beta)$  becomes the tangent plane at  $P$ . The element of length on a sphere of radius  $r$  is given by

$$ds_1^2 = r^2 \cos^2 \theta d\phi^2 + r^2 d\theta^2$$

The element of length at  $P$  is given by  $ds^2 = dr^2 + ds_1^2$  where  $ds_1$  is an arc element on the sphere passing through  $P$ .

Hence

$$ds^2 = dr^2 + r^2 \cos^2 \theta d\phi^2 + r^2 d\theta^2$$

and  $h\alpha = r \cos \theta$ ,  $h\beta = r$ ,  $h\gamma = 1$

follow immediately.

The equation of a sphere is

$$\bar{X} = r [\cos \phi \cos \theta \mathbf{i} + \sin \phi \cos \theta \mathbf{j} + \sin \theta \mathbf{k}]$$

Then on the sphere at P

$$\begin{aligned} \partial x / \partial \alpha &= -r \sin \phi \cos \theta & \partial y / \partial x &= r \cos \phi \cos \theta \\ \partial x / \partial \beta &= -r \cos \phi \sin \theta & \partial y / \partial \beta &= -r \sin \phi \sin \theta \\ \partial x / \partial \gamma &= \cos \phi \cos \theta & \partial y / \partial \gamma &= \sin \phi \cos \theta \\ \partial z / \partial \alpha &= 0, \partial z / \partial \beta = r \cos \theta, \partial z / \partial \gamma &= \sin \theta \end{aligned}$$

and the table (4.1) becomes

	i	j	K
$\bar{a}$	$-\sin \phi$	$\cos \phi$	0
$\bar{b}$	$-\cos \phi \sin \theta$	$-\sin \phi \sin \theta$	$\cos \theta$
$\bar{c}$	$\cos \phi \cos \theta$	$\sin \phi \cos \theta$	$\sin \theta$

(4.2)

As a result of axiometry, the probability that a molecule will hit the spherical zone  $(\theta_i, \theta_j)$  is independent of  $\phi$ . Thus we may set  $\phi = 0$  in the table (4.2) to obtain

	i	j	K
$\bar{a}$	0	1	0
$\bar{b}$	$-\sin \theta_p$	0	$\cos \theta_p$
$\bar{c}$	$\cos \theta_p$	0	$\sin \theta_p$

(4.3)

In order to preserve the notation used previously in connection with this project,  $\alpha$  will denote the angle between the radius vector from P and  $-\bar{c}$  and  $\beta$  will be the angle between  $\bar{a}$  and the projection of the radius vector from P on the plane  $(\bar{a}, \bar{b})$ .

Then (see Figure 1) by means of table (4.3) we obtain

$$\begin{aligned} \bar{X} &= r \sin \theta \cos \theta \bar{a} \\ &+ r \left[ -\cos \phi \cos \theta \sin \theta_p + \sin \theta \cos \theta_p \right] \bar{b} \\ &+ r \left[ \cos \phi \cos \theta \cos \theta_p + \sin \theta \sin \theta_p \right] \bar{c} \end{aligned} \quad (4.4)$$

$$\bar{y}_1 = R \cos \gamma \left[ \cos \beta \sin \gamma \bar{a} + \sin \beta \sin \gamma \bar{b} - \cos \gamma \bar{c} \right] \quad (4.5)$$

Now let the heads of vectors  $\bar{x}$  and  $\bar{y}$  coincide. They  $\bar{y} = \bar{PO} + \bar{x}$  which yields

$$\begin{aligned} \bar{y} &= r \sin \phi \cos \theta_o \bar{a} \\ &+ r \left[ -\cos \phi \cos \theta_o \sin \theta_p + \sin \theta_o \cos \theta_p \right] \bar{b} \\ &+ \left\{ r \left[ \cos \phi \cos \theta_o \cos \theta_p + \sin \theta_o \sin \theta_p \right] - R \right\} \bar{c} \end{aligned} \quad (4.6)$$

The intersection of C and  $\theta_o$  can be found if we set  $\bar{y}_1 = y$

Then we obtain

$$\begin{aligned} \text{a) } \sin \phi \cos \theta_o &= \cos \gamma \cos \beta \\ \text{b) } -\cos \phi \cos \theta_o \sin \theta_p + \sin \theta_o \cos \theta_p &= \cos \gamma \sin \beta \\ \text{c) } \cos \phi \cos \theta_o \cos \theta_p + \sin \theta_o \sin \theta_p &= \sin \gamma \end{aligned} \quad (4.7)$$

from 4.7c we obtain

$$\cos \phi = \frac{\sin \gamma}{\cos \theta_o \cos \theta_p} - \tan \theta_o \tan \theta_p \quad (4.8)$$

substituting 4.8 into 4.7b and solving for  $\sin \beta$  we obtain

$$\sin \beta = \frac{\sin \theta_o - \sin \gamma \sin \theta_p}{\cos \gamma \cos \theta_p} \quad (4.9)$$

If we take the dot product of the vectors  $\bar{y}$  (eq. 4.6) and  $\bar{PO}$  we obtain

$$\cos^2 \alpha = \frac{\left\{ R - r \left[ \cos \phi \cos \theta_o \cos \theta_p + \sin \theta_o \sin \theta_p \right] \right\}^2}{|\bar{y}|^2}$$

But from 4.6 we have also

$$|\bar{y}|^2 = R^2 \left[ 1 + \sin^2 \gamma - 2 \sin \gamma (\cos \phi \cos \theta_o \cos \theta_p + \sin \theta_o \sin \theta_p) \right]$$

Hence

$$\sin^2 \alpha = \frac{\sin^2 \gamma \left[ 1 - (\cos \phi \cos \theta_o \cos \theta_p + \sin \theta_o \sin \theta_p)^2 \right]}{1 + \sin^2 \gamma - 2 \sin \gamma (\cos \phi \cos \theta_o \cos \theta_p + \sin \theta_o \sin \theta_p)} \quad (4.10)$$

from equation 4.6 we obtain

$$r \sin\phi \cos\theta_o = |\bar{y}| \cos\beta \sin\alpha$$

$$r \left[ -\cos\phi \cos\theta_o \sin\theta_p + \sin\theta_o \cos\theta_p \right] = |\bar{y}| \sin\beta \sin\alpha$$

Hence

$$\tan\beta = \frac{-\cos\phi \cos\theta_o \sin\theta_p + \sin\theta_o \cos\theta_p}{\sin\phi \cos\theta_o} \quad (4.11)$$

differentiating 4.11 with respect to  $\phi$  we obtain

$$d\beta = \frac{\cos\theta_o \left[ \sin\theta_p \cos\theta_o - \cos\phi \sin\theta_o \cos\theta_p \right] d\phi}{1 - (\cos\phi \cos\theta_o \cos\theta_p + \sin\theta_o \sin\theta_p)^2} \quad (4.12)$$

Summarizing the above results:

The points of intersection of the curves  $C_{\theta_p}$  and  $\theta_o$  are given by:

$$\cos\phi = \frac{\sin\gamma - \sin\theta_o \sin\theta_p}{\cos\theta_o \cos\theta_p} \quad \text{in terms of } \phi \quad (4.13)$$

$$\sin\beta = \frac{\sin\theta_o - \sin\gamma \sin\theta_p}{\cos\gamma \cos\theta_p} \quad \text{in terms of } \beta \quad (4.14)$$

On  $\theta_o$

$$\sin^2\alpha = \frac{\sin^2\gamma \left[ 1 - (\cos\phi \cos\theta_o \cos\theta_p + \sin\theta_o \sin\theta_p)^2 \right]}{1 + \sin^2\gamma - 2\sin\gamma (\cos\phi \cos\theta_o \cos\theta_p + \sin\theta_o \sin\theta_p)} \quad (4.15)$$

and

$$d\beta = \frac{\cos\theta_o \left[ \sin\theta_p \cos\theta_o - \cos\phi \sin\theta_o \cos\theta_p \right] d\phi}{1 - (\cos\phi \cos\theta_o \cos\theta_p + \sin\theta_o \sin\theta_p)^2} \quad (4.16)$$

Let  $\max C_{\theta_p}$ ,  $\min C_{\theta_p}$  denote the maximum and minimum latitudes of curve  $C_{\theta_p}$  which occur at  $\phi = 0$  or  $\phi = \pi$ .

When  $-\frac{\pi}{2} < \theta_p < -\gamma$  from Eq. 4.8 we obtain

$$\begin{aligned} \text{at } \phi = 0 \quad \max C_{\theta_p} &= \frac{\pi}{2} + \theta_p - \gamma \\ \text{at } \phi = \pi \quad \min C_{\theta_p} &= -(\frac{\pi}{2} + \gamma + \theta_p) \end{aligned}$$

When  $-\gamma < \theta_p < \gamma$  from Eq. 4.8 we obtain

$$\begin{aligned} \text{at } \phi = 0 \quad \max C_{\theta_p} &= \frac{\pi}{2} + \theta_p - \gamma \\ \text{at } \phi = \pi \quad \min C_{\theta_p} &= -\frac{\pi}{2} + \theta_p + \gamma \end{aligned}$$

When  $\gamma < \theta_p < \frac{\pi}{2}$  again from 4.8 we obtain

$$\begin{aligned} \text{at } \phi = \pi \quad \max C_{\theta_p} &= \frac{\pi}{2} + \gamma - \theta_p \\ \text{at } \phi = 0 \quad \min C_{\theta_p} &= -\frac{\pi}{2} + \gamma + \theta_p \end{aligned}$$

Due to the geometrical symmetry it will suffice to consider the case  $\theta_p > 0$ .

We distinguish two cases

$$\text{Case I} \quad \frac{\pi}{2} > \theta_p \geq \max C_{\theta_p} \quad \theta_p > \gamma$$

$$\text{Case II} \quad \max C_{\theta_p} > \theta_p \geq \min C_{\theta_p}$$

Case I -

$$\theta_p > \gamma, \frac{\pi}{2} \geq \theta_p \geq \max C_{\theta_p}$$

(see Figure 2)  $\theta_0$  does not intersect  $C_{\theta_p}$ . Let  $G_{\theta_0}$  be the surface region on the vehicle bounded below by  $\theta_0$ . Let  $P(\theta_p, \theta_0)$  denote the probability that a molecule from the point  $p$  will hit the region  $G_{\theta_0}$ .

Then with the aid of 4.15 and 4.16 we obtain

$$\begin{aligned}
 P(\theta_p, \theta_o) &= \frac{1}{\pi} \iint_{G_{\theta_o}} \sin \alpha \cos \alpha d\alpha d\beta \\
 &= \frac{\sin \theta_o \sin \gamma}{4\pi} \int_0^{2\pi} \frac{(\cos \phi - \frac{\sin \theta_p \cos \theta_o}{\sin \theta_o \cos \theta_p}) d\phi}{\cos \phi + \tan \theta_o \tan \theta_p - \frac{1 + \sin^2 \gamma}{2 \sin \gamma \cos \theta_o \cos \theta_p}}
 \end{aligned}$$

Or

$$P(\theta_p, \theta_o) = \frac{\sin \theta_o \sin \gamma}{2}$$

(4.17)

$$+ \frac{(1 + \sin^2 \gamma) \sin \theta_o - 2 \sin \gamma \sin \theta_p}{8\pi \cos \theta_o \cos \theta_p} \int_0^{2\pi} \frac{d\phi}{\cos \phi + \tan \theta_o \tan \theta_p - \frac{1 + \sin^2 \gamma}{2 \sin \gamma \cos \theta_o \cos \theta_p}}$$

In order to evaluate the integral in 4.17 we use the residue theorem by setting

$$2 \cos \phi = z + z^{-1}$$

Let

$$\lambda = \tan \theta_o \tan \theta_p - \frac{1 + \sin^2 \gamma}{2 \sin \gamma \cos \theta_o \cos \theta_p}$$

Then

$$\int_0^{2\pi} \frac{d\phi}{\cos \phi + \lambda} = \frac{2}{i} \oint \frac{dz}{z^2 + 2\lambda z + 1} \quad (4.18)$$

The roots of

$$z^2 + 2\lambda z + 1 = 0 \quad \text{are} \quad (4.19)$$

$$-\lambda \pm (\lambda^2 - 1)^{1/2}$$

Consider the equation

$$f(x) = x^2 + 2\lambda + 1$$

we obtain

$$f(1) = 1 + 2\lambda + 1 = 2(1 + \lambda)$$

$$f(-1) = 1 - 2\lambda + 1 = 2(1 - \lambda)$$

But

$$1 - \lambda = \frac{4 \sin \gamma \cos^2 \frac{\theta_o + \theta_p}{2} + (1 - \sin \gamma)^2}{2 \sin \gamma \cos \theta_o \cos \theta_p} > 0 \quad (4.20)$$

$$1 + \lambda = \frac{-4 \sin \gamma \sin^2 \frac{\theta_o - \theta_p}{2} - (1 - \sin \gamma)^2}{2 \sin \gamma \cos \theta_o \cos \theta_p} \quad (4.21)$$

Hence  $1 - \lambda^2 < 0$  or  $\lambda^2 - 1 > 0$

That is, equation 4.19 has real roots and on account of 4.20 and 4.21 we conclude

$$-1 < -\lambda - (\lambda^2 - 1)^{1/2} < 1 < -\lambda + (\lambda^2 - 1)^{1/2}$$

Hence the residue of  $\frac{1}{z^2 + 2\lambda z + 1}$  within  $|z| = 1$  is  $-\frac{1}{2(\lambda^2 - 1)^{1/2}}$

it follows  $\int_0^{2\pi} \frac{d\phi}{\cos \phi + \lambda} = \frac{-2\pi}{(\lambda^2 - 1)^{1/2}}$

Therefore

$$\begin{aligned} P(\theta_p, \theta_o) &= \frac{\sin \theta_o \sin \gamma}{2} - \frac{(1 + \sin^2 \gamma) \sin \theta_o - 2 \sin \gamma \sin \theta_p}{4 \cos \theta_o \cos \theta_p (\lambda^2 - 1)^{1/2}} \\ &= \frac{\sin \theta_o \sin \gamma}{2} - \frac{G\pi}{2} \end{aligned} \quad (4.22)$$

where

$$G = \frac{[(1 + \sin^2 \gamma) \sin \theta_o - 2 \sin \gamma \sin \theta_p] \sin \gamma}{\pi \left\{ [2 \sin \gamma \cos(\theta_o + \theta_p) + 1 + \sin^2 \gamma] [-2 \sin \gamma \cos(\theta_o - \theta_p) + 1 + \sin^2 \gamma] \right\}^{1/2}}$$

we can easily verify that when  $\theta = \frac{\pi}{2}$  and  $\theta_o$  coincides with  $C_{\theta_p}$  (i.e.  $\theta_o = \gamma$ ) that  $P(\theta_p, \theta_o) = \sin^2 \gamma$  as it is expected

When  $\theta_o = \theta_p$

$$P(\theta_p, \theta_p) = \frac{\sin \theta_p \sin \gamma}{2} - \frac{(1 - \sin \gamma) \sin \gamma \sin \theta_p}{2(1 + \sin^2 \gamma + 2 \sin \gamma \cos^2 \theta_p)^{1/2}} \quad 4.23$$

### Case II

$\theta_o$  always intersects  $C_{\theta_p}$

This occurs when  $\max C_{\theta_p} > \theta_o > \min C_{\theta_p}$  whether  $\theta_p > \gamma$  or  $\theta_p < \gamma$  see Figures 3.

The intersection of  $\theta_o$  and  $C_{\theta_p}$  is given by  $\cos \phi = \frac{\sin \gamma}{\cos \theta_o \cos \theta_p} - \tan \theta_o \tan \theta_p$

(see Eq. 4.8). Let  $\phi_o$  be the first intersection, i.e.  $0 < \phi < \pi$ . Then the other intersection is  $-\phi_o$ . Let  $G_{\theta_p}$  be the surface area on the vehicle bounded by  $\theta_o$  and  $C_{\theta_p}$  and for which  $\theta > \theta_o$ .

Then

$$P(\theta_p, \theta_o) = \frac{1}{\pi} \iint_{G_{\theta_p}} \sin \alpha \cos \alpha d\alpha d\beta =$$

$$\frac{\sin \theta_o \sin \gamma}{2\pi} \int_0^{\phi_o} \frac{(\cos \phi - \frac{\sin \theta_p \cos \theta_o}{\sin \theta_o \cos \theta_p})}{\cos \phi + \tan \theta_o \tan \theta_p - \frac{1 + \sin^2 \gamma}{2 \sin \gamma \cos \theta_o \cos \theta_p}} d\phi + \frac{\sin^2 \gamma}{\pi} \int_{\beta_o}^{\pi/2} d\beta$$

where  $\beta_o$  is given by

$$\sin \beta_o = \frac{\sin \theta_o - \sin \gamma \sin \theta_p}{\cos \gamma \cos \theta_p} \quad (\text{Eq. 4.9})$$



or

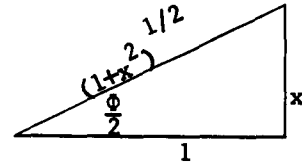
$$\begin{aligned}
 P(\theta_p, \theta_o) &= \frac{\sin \theta_o \sin \gamma}{2\pi} \Phi_o \\
 &+ \frac{(1+\sin^2 \gamma) \sin \theta_o - 2 \sin \gamma \sin \theta_p}{4\pi \cos \theta_o \cos \theta_p} \int_0^{\Phi_o} \frac{d\Phi}{\cos \Phi + \tan \theta_o \tan \theta_p - \frac{1+\sin^2 \gamma}{2 \sin \gamma \cos \theta_o \cos \theta_p}} \\
 &+ \frac{\sin^2 \gamma}{\pi} \left( \frac{\pi}{2} - \beta_o \right)
 \end{aligned} \tag{4.24}$$

To evaluate 4.24 use the following substitution

$$x = \tan \frac{\Phi}{2}$$

$$d\Phi = \frac{2dx}{1+x^2}$$

$$\cos \Phi = 2 \cos^2 \frac{\Phi}{2} - 1 = \frac{1-x^2}{1+x^2}$$



(4.25)

Then

$$\int \frac{d\Phi}{\cos \Phi + \lambda} = \frac{2}{\lambda+1} \int \frac{dx}{x^2 + \frac{\lambda+1}{\lambda-1}}$$

where

$$\lambda = \tan \theta_o \tan \theta_p - \frac{1+\sin^2 \gamma}{2 \sin \gamma \cos \theta_o \cos \theta_p}$$

Now

$$\frac{\lambda+1}{\lambda-1} = \frac{\lambda^2-1}{(\lambda-1)^2} > 0 \quad \text{since } \lambda^2-1 > 0$$

Solving 4.25 for X and setting  $\Phi = \Phi_o$  we obtain

$$X_1 = \left[ \frac{\cos(\theta_o - \theta_p) - \sin \gamma}{\cos(\theta_o + \theta_p) + \sin \gamma} \right]^{1/2}$$

where we have taken the positive root since

$$0 < \Phi_o < \pi \longrightarrow \tan \frac{\Phi_o}{2} = X_1 > 0$$

Then 4.24 becomes

$$P(\theta_p, \theta_o) = \frac{\sin \theta_o \sin \gamma}{2\pi} \phi_o + \frac{\sin^2 \gamma}{\pi} \left( \frac{\pi}{2} - \beta_o \right) - G(\theta_p, \theta_o) \tan^{-1} \left[ X_1 \left( \frac{\lambda-1}{\lambda+1} \right)^{1/2} \right] \quad (4.26)$$

where  $G$  has been defined in Eq. 4.22

$$\text{and} \quad \frac{\lambda-1}{\lambda+1} = \frac{2 \sin \gamma \cos(\theta_o + \theta_p) + 1 + \sin^2 \gamma}{-2 \sin \gamma \cos(\theta_o - \theta_p) + 1 + \sin^2 \gamma}$$

The formulas 4.22 and 4.26 should have the same value in their common region of domain.

Set  $\theta_o = \text{Max } C_{\theta_p}$  in Eq. 4.26

and  $\phi_o = \frac{\pi}{2}, \beta_o = \frac{\pi}{2}$

Then  $X_1 \rightarrow \infty$   $\frac{\lambda-1}{\lambda+1} \neq 0$

$$\text{Hence} \quad \tan^{-1} \left[ X_1 \left( \frac{\lambda-1}{\lambda+1} \right)^{1/2} \right] = \frac{\pi}{2}$$

and 4.27 reduces to 4.22.

Also when  $\theta_o = \text{min. } C_{\theta_p}$  we expect  $P(\theta_p, \theta_o) = \sin^2 \gamma$

Indeed,  $\theta_o = -\frac{\pi}{2} + \theta_p + \gamma$

$$X_1 = 0 \rightarrow \tan^{-1} \left[ X_1 \left( \frac{\lambda-1}{\lambda+1} \right)^{1/2} \right] = 0$$

$$\phi_o = 0, \beta_o = -\frac{\pi}{2}$$

$$P(\theta_p, \theta_o) = \sin^2 \gamma$$

Consider the special case where  $\theta_o = \theta_p = 0$

Then  $\sin \beta_o = 0 \quad \beta_o = 0$

Then  $P(\theta_p, \theta_o) = \frac{\sin^2 \gamma}{2}$  (what was expected)

## 4.1.2 From the Vehicle to the Chamber Wall

Consider the point P on the vehicle and the curve  $\theta_o$  on the chamber wall (Figure 4,5). Again we need consider only  $\theta_p > 0$  with two cases.

$$\text{Case I} \quad \frac{\pi}{2} > \theta_o > \max C_{\theta_p} \quad (\text{Figure 5})$$

$$\text{Case II} \quad \max C_{\theta_p} \geq \theta_o \geq \min C_{\theta_p} \quad (\text{Figure 4})$$

Let P be a point on the vehicle with position  $(0, \theta_p)$  and let A be a point on  $\theta_o$  such that  $\alpha < \frac{\pi}{2}$  (see Figure 4).

If we set up an orthogonal system at P as before and make use of Table (1.3) we obtain

$$\bar{x} = R \sin \phi \cos \theta_o \bar{a} \quad (4.27)$$

$$+ R \left[ -\cos \phi \cos \theta_o \sin \theta_p + \sin \theta_o \cos \theta_p \right] \bar{b}$$

$$+ R \left[ \cos \phi \cos \theta_o \cos \theta_p + \sin \theta_o \sin \theta_p \right] \bar{c}$$

$$\bar{y} = R \sin \phi \cos \theta_o \bar{a} \quad (4.28)$$

$$+ R \left[ -\cos \phi \cos \theta_o \sin \theta_p + \sin \theta_o \cos \theta_p \right] \bar{b}$$

$$+ R \left\{ \left[ \cos \phi \cos \theta_o \cos \theta_p + \sin \theta_o \sin \theta_p \right] - r \right\} \bar{c}$$

The intersection of the curves  $C_{\theta_p}$  and  $\theta_o$  (if they intersect) is easily found to be given by

$$\cos \phi \cos \theta_o \cos \theta_p + \sin \theta_o \sin \theta_p = 1$$

Hence

$$\cos \phi_o = \frac{\sin \gamma}{\cos \theta_o \cos \theta_p} - \tan \theta_o \tan \theta_p \quad (4.29)$$

as before.

Also

$$|\bar{y}|^2 = R^2 \left[ 1 + \sin^2 \gamma - 2 \sin \gamma (\cos \phi \cos \theta_o \cos \theta_p + \sin \theta_o \sin \theta_p) \right] \quad (4.30)$$

$$\sin^2 \alpha = \frac{1 - (\cos \phi \cos \theta_o \cos \theta_p + \sin \theta_o \sin \theta_p)^2}{1 + \sin^2 \gamma - 2 \sin \gamma (\cos \phi \cos \theta_o \cos \theta_p + \sin \theta_o \sin \theta_p)} \quad (4.31)$$

$$\sin \beta_o = \frac{\sin \theta_o - \sin \gamma \sin \theta_p}{\cos \theta_p \cos \gamma} \quad (4.32)$$

$$d\beta = \frac{\cos \theta_o \left[ \sin \theta_p \cos \theta_o - \cos \phi \sin \theta_o \cos \theta_p \right] d\phi}{1 - (\cos \phi \cos \theta_o \cos \theta_p + \sin \theta_o \sin \theta_p)^2} \quad (4.33)$$

In an analogous manner as before (sec. 4.1.1) the following relations can be derived

When  $\gamma < \theta_p < \frac{\pi}{2}$

$$\begin{aligned} \text{at } \phi = \pi \quad \text{Max } C_{\theta_p} &= \frac{\pi}{2} - \theta_p + \gamma \\ &= 0 \quad \text{Min } C_{\theta_p} = -\frac{\pi}{2} + \theta_p + \gamma \end{aligned}$$

When  $-\gamma < \theta_p < \gamma$

$$\begin{aligned} \text{at } \phi = 0 \quad \text{Max } C_{\theta_p} &= \frac{\pi}{2} + \theta_p - \gamma \\ \phi = 0 \quad \text{Min } C_{\theta_p} &= -\frac{\pi}{2} + \theta_p + \gamma \end{aligned}$$

When  $-\frac{\pi}{2} < \theta_p < -\gamma$

$$\begin{aligned} \text{at } \phi = 0 \quad \text{Max } C_{\theta_p} &= \frac{\pi}{2} + \theta_p - \gamma \\ \phi = \pi \quad \text{Min } C_{\theta_p} &= -(\frac{\pi}{2} + \theta_p + \gamma) \end{aligned}$$

Case I  $\frac{\pi}{2} > \theta_o > \text{Max } C_{\theta_p}$  (Figure 5)

It occurs when  $\theta_p > \gamma$ . Let  $G_{\theta_o}$  be the surface area on the chamber wall for which  $\theta \geq \theta_o$ .

Then

$$\begin{aligned}
 P(\theta_p, \theta_o) &= \frac{1}{\pi} \iint_{G_{\theta_o}} \sin \alpha \cos \alpha \, d\alpha \, d\beta \quad (4.34) \\
 &= \frac{\sin \theta_o}{4\pi \sin \gamma} \int_0^{2\pi} \frac{(\cos \phi - \frac{\sin \theta_p \cos \theta_o}{\sin \theta_o \cos \theta_p}) \, d\phi}{\cos \phi + \tan \theta_o \tan \theta_p - \frac{1 + \sin^2 \gamma}{2 \sin \gamma \cos \theta_o \cos \theta_p}} \\
 &= \frac{\sin \theta_o}{2 \sin \gamma} + \frac{(1 + \sin^2 \gamma) \sin \theta_o - 2 \sin \gamma \sin \theta_p}{8\pi \sin^2 \gamma \cos \theta_o \cos \theta_p} \int_0^{2\pi} \frac{d\phi}{\cos \phi + \tan \theta_o \tan \theta_p - \frac{1 + \sin^2 \gamma}{2 \sin \gamma \cos \theta_o \cos \theta_p}} \\
 &= \frac{\sin \theta_o}{2 \sin \gamma} - \frac{\pi G}{2 \sin^2 \gamma}
 \end{aligned}$$

Consider the special case where  $\theta_p = \frac{\pi}{2}$ ,  $\theta_o = \gamma$ . We expect  $P(\theta_p, \theta_o) = 1$ . A substitution easily verifies that this is indeed the case.

Case II  $\text{Max } C_{\theta_p} > \theta_o > \text{Min } C_{\theta_p}$  (Figure 4)

As before we find

$$\begin{aligned}
 P(\theta_p, \theta_o) &= \frac{\sin \theta_o}{2\pi \sin \gamma} \phi_o + \frac{1}{\pi} \left( \frac{\pi}{2} - \beta_o \right) \quad (4.35) \\
 &\quad - \frac{G(\theta_p, \theta_o)}{\sin^2 \gamma} \tan^{-1} \left[ X_1 \left( \frac{\lambda-1}{\lambda+1} \right)^{1/2} \right]
 \end{aligned}$$

where  $G$  is defined in the same way as for equation 4.26.

Formulas 4.34 and 4.35 should give the same value in their common region of domain. Indeed if  $\theta_o = \text{Max } C_{\theta_p} = \frac{\pi}{2} - \theta_p + \gamma$   $\theta_p > \gamma$

$$\phi_o = \pi, \beta_o = \frac{\pi}{2}, \tan^{-1} \left[ x_1 \left( \frac{\lambda-1}{\lambda+1} \right)^{1/2} \right] = \frac{\pi}{2}$$

4.35 reduces to 4.34.

Also when  $\theta_o = \text{Min } C_{\theta_p}$  we expect  $P(\theta_p, \theta_o) = 1$

Set  $\theta_o = -\frac{\pi}{2} + \theta_p + \gamma$ ,  $\gamma < \theta_p < \frac{\pi}{2}$  or  $-\gamma < \theta_p < \gamma$

$$\phi_o = 0, \beta_o = -\frac{\pi}{2}, \tan^{-1} \left[ x_1 \left( \frac{\lambda-1}{\lambda+1} \right)^{1/2} \right] = 0$$

and the result follows immediately.

#### 4.1.3 From the Chamber Wall to the Chamber Wall

Consider both the point P and the curve  $\theta_o$  on the chamber wall. Thus (see Figure 6)

$$\begin{aligned} \bar{y} &= -Rc + \bar{x} \\ &= R \sin \phi \cos \theta_o \bar{a} \end{aligned} \quad (4.36)$$

$$\begin{aligned} &+ R \left[ -\cos \phi \cos \theta_o \sin \theta_p + \sin \theta_o \cos \theta_p \right] \bar{b} \\ &+ R \left[ \cos \phi \cos \theta_o \cos \theta_p + \sin \theta_o \sin \theta_p - 1 \right] \bar{c} \end{aligned}$$

$$\bar{y}_1 = 2R \cos \gamma \left[ \cos \beta \sin \gamma \bar{a} + \sin \beta \sin \gamma \bar{b} - \cos \gamma \bar{c} \right] \quad (4.37)$$

For the intersection of  $\theta_o$  and  $C_{\theta_p}$  (if they do intersect) we set

$$\bar{y} = \bar{y}_1 \quad \text{Then}$$

$$a) \quad \sin \phi \cos \theta_o = 2 \cos \gamma \cos \beta \sin \gamma$$

$$b) -\cos\phi\cos\theta_o\sin\theta_p + \sin\theta_o\cos\theta_p = 2\cos\gamma\sin\beta\sin\gamma \quad (4.38)$$

$$c) \cos\phi\cos\theta_o\cos\theta_p + \sin\theta_o\sin\theta_p - 1 = -2\cos^2\gamma$$

from 4.38c) we get

$$\cos\phi = \frac{-\cos 2\gamma}{\cos\theta_o\cos\theta_p} - \tan\theta_o\tan\theta_p \quad (4.39)$$

Substituting 4.39 into 4.38b we get

$$\sin\beta = \cot 2\gamma \tan\theta_p + \frac{\sin\theta_o}{\sin 2\gamma \cos\theta_p} \quad (4.40)$$

Similarly we find

$$\sin^2\alpha = \frac{1}{2} (1 + \cos\phi\cos\theta_o\cos\theta_p + \sin\theta_o\sin\theta_p) \quad (4.41)$$

$$d\beta = \frac{\cos\theta_o \left[ \sin\theta_p \cos\theta_o - \cos\phi \sin\theta_o \cos\theta_p \right]}{1 - (\cos\phi\cos\theta_o\cos\theta_p + \sin\theta_o\sin\theta_p)^2} d\phi \quad (4.42)$$

$$\frac{\pi}{2} - 2\gamma > 0$$

$$\frac{\pi}{2} - 2\gamma < 0$$

$$\frac{\pi}{2} - 2\gamma > \theta_p > 2\gamma - \frac{\pi}{2}$$

$$2\gamma - \frac{\pi}{2} > \theta_p > \frac{\pi}{2} - 2\gamma$$

$$\text{Max } C_{\theta_p} = 2\gamma - \theta_p$$

$$\text{Max } C_{\theta_p} = \pi - (2\gamma - \theta_p)$$

$$\text{Min } C_{\theta_p} = -(\theta_p + 2\gamma)$$

$$\text{Min } C_{\theta_p} = -\pi + 2\gamma + \theta_p$$

$$2\gamma - \frac{\pi}{2} > \theta_p > -\frac{\pi}{2}$$

$$\frac{\pi}{2} - 2\gamma > \theta_p > -\frac{\pi}{2}$$

$$\text{Max } C_{\theta_p} = \pi - (2\gamma - \theta_p)$$

$$\text{Max } C_{\theta_p} = \pi - (2\gamma - \theta_p)$$

$$\text{Min } C_{\theta_p} = -(\theta_p + 2\gamma)$$

$$\text{Min } C_{\theta_p} = -(2\gamma + \theta_p)$$

$$\frac{\pi}{2} > \theta_p > \frac{\pi}{2} - 2\gamma$$

$$\text{Max } C_{\theta_p} = 2\gamma - \theta_p$$

$$\text{Min } C_{\theta_p} = -\pi + 2\gamma + \theta_p$$

$$\frac{\pi}{2} > \theta_p > 2\gamma - \frac{\pi}{2}$$

$$\text{Max } C_{\theta_p} = 2\gamma - \theta_p$$

$$\text{Min } C_{\theta_p} = -\pi + 2\gamma + \theta_p$$

Again we distinguish two cases, Case I when  $\theta_o$  does not intersect  $C_{\theta_p}$  and Case II when  $\theta_o$  does intersect  $C_{\theta_p}$

Case I  $\frac{\pi}{2} > \theta_o > \text{Max } C_{\theta_p}$

$$P(\theta_p, \theta_o) = \frac{1}{\pi} \iint_{G_{\theta_p}} \sin\alpha \cos\alpha d\alpha d\beta$$

where  $G_{\theta_o}$  is defined as previously but on the chamber wall. It is easy to see then that

$$\begin{aligned} P(\theta_p, \theta_o) &= \frac{1}{4\pi} \int_0^{2\pi} \frac{\cos\theta_o [\sin\theta_p \cos\theta_o - \cos\phi \sin\theta_o \cos\theta_p] d\phi}{1 + (\cos\phi \cos\theta_o \cos\theta_p + \sin\theta_o \sin\theta_p)} \\ &= -\frac{\sin\theta_o}{4\pi} \int_0^{2\pi} \frac{\left( \cos\phi - \frac{\sin\theta_p \cos\theta_o}{\sin\theta_o \cos\theta_p} \right)}{\cos\phi + \tan\theta_o \tan\theta_p + \frac{1}{\cos\theta_o \cos\theta_p}} d\phi \\ &= -\frac{\sin\theta_o}{2} + \frac{\sin\theta_o \sin\theta_p}{4\pi \cos\theta_o \cos\theta_p} \int_0^{2\pi} \frac{d\phi}{\cos\phi + \tan\theta_o \tan\theta_p + \frac{1}{\cos\theta_o \cos\theta_p}} \end{aligned}$$

$$\text{Let } \lambda = \tan\theta_o \tan\theta_p + \frac{1}{\cos\theta_o \cos\theta_p}$$

$$(\lambda^2 - 1)^{1/2} = \frac{\sin\theta_o + \sin\theta_p}{\cos\theta_o \cos\theta_p} > 0$$



As before

$$\left. \begin{aligned} f(1) &= 2(1+\lambda) \\ f(-1) &= 2(1-\lambda) \end{aligned} \right\} f(z) = z^2 + 2\lambda z + 1$$

$$(1+\lambda) = \frac{\cos(\theta_o - \theta_p) + 1}{\cos\theta_o \cos\theta_p} = \frac{2\cos^2 \frac{\theta_o - \theta_p}{2}}{\cos\theta_o \cos\theta_p} > 0$$

$$1-\lambda = \frac{\cos(\theta_o + \theta_p) - 1}{\cos\theta_o \cos\theta_p} < 0$$

Hence  $-\lambda - (\lambda^2 - 1)^{1/2} < -1 < -\lambda + (\lambda^2 - 1)^{1/2} < 1$

and the residue of  $\frac{1}{z^2 + 2\lambda z + 1}$  within  $|z| = 1$

is  $\frac{1}{2(\lambda^2 - 1)^{1/2}}$

It follows  $\int_0^{2\pi} \frac{d\phi}{\cos\phi + \lambda} = \frac{2}{i} \oint \frac{dz}{z^2 + 2\lambda z + 1} = \frac{2\pi}{(\lambda^2 - 1)^{1/2}}$

therefore

$$P(\theta_p, \theta_o) = \frac{1}{2} - \frac{\sin\theta_o}{2} \quad (4.43)$$

Case II  $\text{Max } C_{\theta_p} > \theta_o > \text{Min } C_{\theta_p}$

$$P(\theta_p, \theta_o) = -\frac{\sin\theta_o}{2\pi} \phi_o + \frac{1}{\pi} \left( \frac{\pi}{2} - \beta_o \right) \cos^2 \gamma$$

$$+ \frac{1}{\pi} \tan^{-1} \left[ x_1 \left( \frac{\lambda-1}{\lambda+1} \right)^{1/2} \right] \quad (4.44)$$

Where

$$\phi_o = \cos^{-1} \left[ \frac{\cos^2 \gamma + \sin \theta_o \sin \theta_p}{\cos \theta_o \cos \theta_p} \right]$$

$$\beta_o = \sin^{-1} \left[ \cot 2\gamma \tan \theta_p + \frac{\sin \theta_o}{\sin 2\gamma \cos \theta_p} \right]$$

$$X_1 = \left[ \frac{\cos(\theta_o - \theta_p) + \cos 2\gamma}{\cos(\theta_o + \theta_p) - \cos 2\gamma} \right]^{1/2}$$

$$\left[ \frac{\lambda-1}{\lambda+1} \right]^{1/2} = \frac{1 - \cos(\theta_o + \theta_p)}{\sin \theta_o + \sin \theta_p}$$

Notice that equation 4.54 reduces to equation 4.53 when  $\theta_o = \text{Max } C_{\theta_p}$  where  $\text{Max } C_{\theta_p} = 2\gamma - \theta_p$ . Since, then,

$$\phi_o = \pi, \beta_o = \frac{\pi}{2}, \tan^{-1} \left[ X_1 \left( \frac{\lambda-1}{\lambda+1} \right)^{1/2} \right] = \frac{\pi}{2}$$

When  $\theta_p = \theta_o = 0$ , then  $\phi_o = \pi - 2\gamma, \beta_o = 0$

$$\tan^{-1} \left[ X_1 \left( \frac{\lambda-1}{\lambda+1} \right)^{1/2} \right] = 0 \quad \text{and equation 4.54 gives us}$$

$$P(\theta_p, \theta_o) = \frac{1}{2} \cos^2 \gamma \quad \text{for the half illuminated sphere.}$$

## 4.2 RECAPITULATION

### A. From the Chamber Wall to the Vehicle

Extending the previous results to the whole chamber wall we define  $C_{\theta_o}$  as the surface area on the vehicle which is accessible to the point P and for which

$$\theta \geq \theta_o$$

and  $P(\theta_p, \theta_o)$  as the probability that a molecule leaving the point P will hit the region  $G_{\theta_p}$ .

$$(a) \quad G_{\theta_o}$$

$$P(\theta_p, \theta_o) = \frac{\sin \theta_o \sin \gamma}{2} - \frac{G\pi}{2} \quad (4.45)$$

$$(b) \quad \text{Min } C_{\theta_p} \leq \theta_o \leq \text{Max } C_{\theta_p}$$

$$P(\theta_p, \theta_o) = \frac{\sin \theta_o \sin \gamma}{2\pi} \phi_o + \frac{\sin^2 \gamma}{\pi} \left( \frac{\pi}{2} - \beta_o \right) \quad (4.46)$$

where

$$-G \tan^{-1} \left[ X_1 \left( \frac{\lambda-1}{\lambda+1} \right)^{1/2} \right]$$

$$\frac{\lambda-1}{\lambda+1} = \frac{2 \sin \gamma \cos(\theta_o + \theta_p) + 1 + \sin^2 \gamma}{-2 \sin \gamma \cos(\theta_o - \theta_p) + 1 + \sin^2 \gamma} \quad (4.47)$$

$$X_1 = \left[ \frac{\cos(\theta_o - \theta_p) - \sin \gamma}{\cos(\theta_o + \theta_p) + \sin \gamma} \right]^{1/2} \quad (4.48)$$

$$G = \frac{\left[ (1 + \sin^2 \gamma) \sin \theta_o - 2 \sin \gamma \sin \theta_p \right] \sin \gamma}{\pi \left\{ \left[ 2 \sin \gamma \cos(\theta_o + \theta_p) + 1 + \sin^2 \gamma \right] \left[ -2 \sin \gamma \cos(\theta_o - \theta_p) + 1 + \sin^2 \gamma \right] \right\}^{1/2}} \quad (4.49)$$

$\phi_o$  and  $\beta_o$  are given by:

$$\phi_o = \cos^{-1} \left[ \frac{\sin \gamma}{\cos \theta_o \cos \theta_p} - \tan \theta_o \tan \theta_p \right] \quad (4.50)$$

$$\beta_o = \sin^{-1} \frac{\sin \theta_o - \sin \gamma \sin \theta_p}{\cos \gamma \cos \theta_p} \quad (4.51)$$

with the restrictions that

$$0 < \phi_o < \pi$$

$$-\frac{\pi}{2} < \beta_o < \frac{\pi}{2}$$

### B. From the Vehicle to the Chamber Wall

Now  $\theta_o$  and  $\theta_p$  switch surfaces.  $G_{\theta}$  is defined as previously.  $C_{\theta}$  is the intersection of the tangent plane at  $P_o$  (of the vehicle) with the chamber wall.

- (a)  $G_{\theta_o}$  completely illuminated from P

$$P(\theta_o, \theta_o) = \frac{\sin \theta_o}{2 \sin \gamma} - \frac{\pi G}{2 \sin^2 \gamma} \quad (4.52)$$

- (b)  $\text{Min } C_{\theta_p} \leq \theta_o \leq \text{Max } C_{\theta_p}$

$$P(\theta_p, \theta_o) = \frac{\sin \theta_o}{2 \pi \sin \gamma} \phi_o + \frac{1}{\pi} \left( \frac{\pi}{2} - \beta_o \right) - \frac{G}{\sin^2 \gamma} \tan^{-1} \left[ X_1 \left( \frac{\lambda-1}{\lambda+1} \right) \right]^{1/2} \quad (4.53)$$

where  $\frac{\lambda-1}{\lambda+1}$ ,  $X_1$ ,  $G$ ,  $\phi_o$  and  $\beta_o$

are given by 4.47, 4.48, 4.49, 4.50 and 4.51 respectively.

### C. From the Chamber Wall to the Chamber Wall

Both  $\theta_o$  and  $\theta_p$  are on the chamber wall.  $G_{\theta_o}$  (now on the chamber wall) is defined as previously

- (a)  $\theta_o > \text{Max } C_{\theta_p}$

$$P(\theta_p, \theta_o) = - \frac{\sin \theta_o}{2} + \frac{1}{2} \quad (4.54)$$

- (b)  $\text{Min } C_{\theta_p} < \theta_o < \text{Max } C_{\theta_p}$

$$P(\theta_p, \theta_o) = \frac{\sin \theta_o}{2 \pi} \phi_o + \frac{1}{\pi} \left( \frac{\pi}{2} - \beta_o \right) \cos^2 \gamma + \frac{1}{\pi} \tan^{-1} \left[ X_1 \left( \frac{\lambda-1}{\lambda+1} \right) \right]^{1/2} \quad (4.55)$$

where  $\phi_o$ ,  $\beta_o$ ,  $X_1$ ,  $\left[ \frac{\lambda-1}{\lambda+1} \right]^{1/2}$  are given immediately after equation 4.44.

## 5.0 COMPUTER LOGIC

The problem of determining analytically the molecular flux distribution in the cases where discontinuous outgassing characteristics have been assumed is exceedingly difficult. Consequently we have used a digital computer to obtain solutions to the problem. The types of surface discontinuities we deal with have been explained previously (see 4.0 Single Surface Discontinuity). The procedure which is followed for a computer solution consists of partitioning the surfaces into a number of spherical zones, each spherical zone having uniform outgassing and pumping characteristics. The probability of molecular transfer from each point of a spherical zone to another spherical zone will be considered constant, thus giving rise to a step function along the meridian of a surface for the probability of transfer from a point, to a spherical zone. The molecular density of the molecules which leave a spherical zone will be taken as uniformly distributed on this spherical zone so that the molecular density along a meridian will assume the form of a step function also. Thus the exact solution of the molecular flux distribution can be better approximated by increasing the number of the spherical zones of each surface.

### 5.1 PARTITION

Both surfaces (chamber wall and vehicle) are partitioned into  $2N$  spherical zones of width  $\Delta\theta$  where  $N$  is an integer. In numbering the sequence of these spherical zones we set

$$X_r = [(r-N-1)\Delta\theta, (r-N)\Delta\theta]$$

where  $X_r$  has been defined previously.

Thus

$$X_1 = \left[ -\frac{\pi}{2}, -\frac{\pi}{2} + \Delta\theta \right]$$

$$X_2 = \left[ (1-N)\Delta\theta, (2-N)\Delta\theta \right]$$

$$X_{N+1} = \left[ 0, \Delta\theta \right]$$

$$X_{2N} = \left[ \frac{\pi}{2} - \Delta\theta, \frac{\pi}{2} \right]$$

The choice of  $N$  is such that

- a)  $N$  is reasonable large.
- b) The discontinuous line or (lines) are boundaries of spherical zones.
- c)  $\theta = \gamma$  is a boundary of a spherical zone.

Obviously, the probability from a point of a latitude  $\theta_I$  of a surface  $X$  to a spherical zone  $Y_J$  is

$$P_{X_I Y_J} = |P_{XY}(\theta_I, \theta_J) - P_{XY}(\theta_I, \theta_{J+1})| \quad (5.1.1)$$

In terms of the partition then Eq. (5.1.1) will denote the probability from a spherical zone  $X_I$  to a spherical zone  $Y_J$  producing therefore a step function for the probability distribution of a surface with respect to a spherical zone. Clearly then, a sufficient condition that

$$P_{X_I Y_J} = P_{X_K Y_r}$$

is that

$$K = 2N - I + 1, \quad r = 2N - J + 1$$

Hence

$$P_{X_I Y_J} = P_X(2N - I + 1) Y(2N - J + 1) \quad (5.1.2)$$

Hence, in view of Eq. (5.3.2) it is sufficient to calculate  $P_{X_I Y_J}$  for  $J \geq N+1$

## 5.2 PROBABILITY EQUATIONS

The probability equations which will be used in the computer solutions have been derived previously and appear in section (4.2). In regrouping these equations for computer use we have

$$P_{CV}(\theta_I, \theta_J) = \text{as given by (4.45)} \quad \left. \begin{array}{l} \text{from chamber} \\ \text{wall to} \end{array} \right\} \quad (5.2.1)$$

$$P_{CV}(\theta_I, \theta_J) = \text{as given by (4.46)} \quad \left. \begin{array}{l} \text{vehicle} \end{array} \right\} \quad (5.2.2)$$

$$P_{CC}(\theta_I, \theta_J) = \frac{1 - \sin \theta_J}{2} \quad (5.2.3)$$

$$P_{CC}(\theta_I, \theta_J) = \frac{1 - \sin \theta_J}{2} - \sin^2 \gamma \quad \left. \begin{array}{l} \text{from chamber} \\ \text{wall to} \\ \text{chamber wall} \end{array} \right\} \quad (5.2.4)$$

$$P_{CC}(\theta_I, \theta_J) = \text{as given by (4.55)} \quad (5.2.5)$$

Equations (5.2.1) and (5.2.2) pertain to the case "From Chamber Wall to Vehicle" while Eqs. (5.2.3)-(5.2.5) pertain to the case "From Chamber Wall to Chamber Wall". Here we have omitted the case "From Vehicle to Chamber Wall" in view of the relation

$$P_{VC}(\theta_I, \theta_J) = P_{CV}(\theta_I, \theta_J) / \sin^2 \gamma \quad (5.2.6)$$

Thus there are actually two probability matrices which have to be determined, one for the chamber-vehicle case and the other for the chamber-chamber case.

### 5.3 PROBABILITY FLOW CHARTS

In all cases we determine the probabilities  $(P_{XY}(\theta_I, \theta_J))$  for  $J \geq N+1$ . In differencing the results by means of Eq. (5.1.1) and extending the domain of  $J$  to  $J < N+1$  by means of Eq. (5.1.2) we obtain the probability matrices  $P_{CV}$  and  $P_{CC}$ .

#### 5.3.1 From Chamber Wall to Vehicle

Since it is sufficient to start with  $\theta \leq \theta_J$  in view of the relation (5.1.2) we may begin with  $\theta_I > \gamma - \pi/2$ . For each  $\theta_I$  we have

$$\begin{aligned} \overline{\text{Lim}} C_{\theta_I} &= \theta_I + \pi/2 - \gamma \quad \text{if } \theta_I - \gamma < 0 \\ &= -\theta_I + \pi/2 + \gamma \quad \text{if } \theta_I - \gamma > 0 \end{aligned}$$

As for the  $\underline{\text{Lim}} C_{\theta_I}$ , we are only interested in the value of  $\underline{\text{Lim}} C_{\theta_I}$  when  $\underline{\text{Lim}} C_{\theta_I} > 0$ . This occurs when  $\theta_I > \pi/2 - \gamma$  yielding

$$\begin{aligned} \underline{\text{Lim}} C_{\theta_I} &= \theta_I + \gamma - \pi/2 \\ \text{For } \theta_I - \gamma < 0 \end{aligned}$$

the domain of  $\theta_J$  for a non zero probability is  $0 \leq \theta_J < \theta_I + \pi/2 - \gamma$   $\underline{\text{Lim}} C_{\theta_I} < 0$

$$\theta_I + \gamma - \pi/2 \leq \theta_J < \theta_I + \pi/2 - \gamma \quad \overline{\text{Lim}} C_{\theta_I} > 0$$

and  $P_{CV}(\theta_I, \theta_J)$  is determined from Eq. (5.2.2)

$$\text{For } \theta_I - \gamma > 0$$

the domains of  $\theta_J$  are

$$a) \quad 0 \leq \theta_J < -\theta_I + \pi/2 + \gamma \quad \underline{\text{Lim}} C_{\theta_I} < 0$$

$$\text{or } \theta_I + \gamma - \pi/2 \leq \theta_J < -\theta_I + \pi/2 + \gamma \quad \underline{\text{Lim}} C_{\theta_I} > 0$$

$$b) \quad -\theta_I + \pi/2 + \gamma \leq \theta_J \leq 2N$$

and  $P_{CV}(\theta_I, \theta_J)$  is determined by Eq. (5.2.2) for case a) and by (5.2.1) for case b). In the flow chart we have been using spherical zone sequential numbers. The corresponding angles to these numbers are:

$$N - N_2 + I \longrightarrow \theta = \pi/2 - \gamma + \theta_I = \overline{\text{Lim}} C_{\theta_I} \quad \theta_I - \gamma < 0$$

$$N + N_2 + 1 \longrightarrow \theta = \gamma$$

$$2N - N_2 + 1 \longrightarrow \pi/2 - \gamma$$

$$N_2 - N + I \longrightarrow \theta = \gamma - \pi/2 + \theta_I = \underline{\text{Lim}} C_{\theta_I}$$

$$3N + N_2 + 2 - I \longrightarrow \theta = \pi/2 + \gamma - \theta_I = \overline{\text{Lim}} C_{\theta_I} \quad \theta_I - \gamma > 0$$

### 5.3.2 From Chamber Wall to Chamber Wall

We distinguish two cases I and II

Case I  $\pi/4 - \gamma > 0$

We start with  $\theta_J = 0$  and  $\theta_I = -\pi/2$

We have

$$\begin{aligned} \overline{\text{Lim}} C_{\theta_I} &= \theta_I + \pi - 2\gamma & \theta_I < 2\gamma - \pi/2 \\ &= 2\gamma - \theta_I & \theta_I > 2\gamma - \pi/2 \end{aligned}$$

As for  $\underline{\text{Lim}} C_{\theta_I}$  we notice that  $\underline{\text{Lim}} C_{\theta_I} = -(\theta_I + 2\gamma) > 0$  when  $-\pi/2 < \theta_J < -\gamma$  and for  $\theta_I > -\gamma$ ,  $\underline{\text{Lim}} C_{\theta_I} < 0$  in all cases.

a) For  $\theta_I < 2\gamma - \pi/2$

the domains of  $\theta_J$  are

$$\left. \begin{aligned} i) \quad 0 \leq \theta_J < -(\theta_I + 2\gamma) \\ ii) \quad -(\theta_I + 2\gamma) \leq \theta_J < \theta_I + \pi - 2\gamma \end{aligned} \right\} \text{ if } \underline{\text{Lim}} C_{\theta_I} > 0$$



or

$$\text{iii)} \quad 0 \leq \theta_J < \theta_I + \pi - 2\gamma \quad \text{if } \underline{\text{Lim}} C_{\theta_I} < 0$$

In case Ia, the Probabilities  $P_{CC}(\theta_I, \theta_J)$  are determined by Eq. (5.2.4) for i) and by (5.2.5) for ii) and by Eq. (5.2.5) for iii)

b) For  $\theta_I > 2\gamma - \pi/2$

the domains of  $\theta_J$  are

$$\left. \begin{array}{l} \text{iv)} \quad 0 \leq \theta_J < -(\theta_I + 2\gamma) \\ \text{v)} \quad -(\theta_I + 2\gamma) \leq \theta_J < 2\gamma - \theta_I \\ \text{vi)} \quad 2\gamma - \theta_I \leq \theta_J < \pi/2 \end{array} \right\} \quad \text{if } \underline{\text{Lim}} C_{\theta_I} > 0$$

or

$$\left. \begin{array}{l} \text{vii)} \quad 0 \leq \theta_J < 2\gamma - \theta_I \\ \text{viii)} \quad 2\gamma - \theta_I \leq \theta_J < \pi/2 \end{array} \right\} \quad \begin{array}{l} \underline{\text{Lim}} C_{\theta_I} < 0 \\ \overline{\text{Lim}} C_{\theta_I} > 0 \end{array}$$

or

$$\text{ix)} \quad 0 \leq \theta_J < \pi/2 \quad \text{if } \overline{\text{Lim}} C_{\theta_I} < 0$$

Then Eq. (5.2.3) for calculating  $P_{CC}(\theta_I, \theta_J)$  is used in the cases iv) while Eq. (5.2.4) is used for the cases v) and vii) and Eq. (5.2.5) for the cases vi), viii) and ix).

The corresponding angles to the sequential numbering which appears in the flow chart are

$$2(N+1-N_2)-I \longrightarrow \theta = -(\theta_I + 2\gamma) = \underline{\text{Lim}} C_{\theta_I}$$

$$2(N-N_2)+I \longrightarrow \theta = \pi - 2\gamma + \theta_I = \overline{\text{Lim}} C_{\theta_I}, \quad \theta_I < 2\gamma - \pi/2$$

$$2N_2+1 \longrightarrow \theta = 2\gamma - \pi/2$$

$$N-2N_2+1 \longrightarrow \theta = -2\gamma$$

Case II  $\pi/4 - \gamma < 0$

In this case we start with  $\theta_J = 0$  and  $\theta_I > 2\gamma - \pi$

We have

$$\begin{aligned}\overline{\text{Lim}} C_{\theta_I} &= \theta_I + \pi - 2\gamma & \theta_I < 2\gamma - \pi/2 \\ &= 2\gamma - \theta_I & \theta_I > 2\gamma - \pi/2\end{aligned}$$

As for  $\underline{\text{Lim}} C_{\theta_I}$  we have

$$\begin{aligned}\underline{\text{Lim}} C_{\theta_I} &= -(\theta_I + 2\gamma) & \text{if } \theta_I + 2\gamma < \pi/2 \\ &= \theta_I + 2\gamma - \pi & \text{if } \theta_I + 2\gamma > \pi/2\end{aligned}$$

c)  $\theta_I < 2\gamma - \pi/2$

The domain of  $\theta_J$  is

$$\text{x) } 0 \leq \theta_J < \theta_I + \pi - 2\gamma \quad \underline{\text{Lim}} C_{\theta_I} < 0$$

$$\text{xi) } \theta_I + 2\gamma - \pi \leq \theta_J < \theta_I + \pi - 2\gamma \quad \underline{\text{Lim}} C_{\theta_I} > 0$$

d)  $\theta_I > 2\gamma - \pi/2$

The domain of  $\theta_J$  is

$$\begin{aligned}\text{xii) } 0 \leq \theta_J < 2\gamma - \theta_I \\ \text{xiii) } 2\gamma - \theta_I \leq \theta_J < \pi/2\end{aligned} \quad \left. \vphantom{\begin{aligned} \text{xii) } 0 \leq \theta_J < 2\gamma - \theta_I \\ \text{xiii) } 2\gamma - \theta_I \leq \theta_J < \pi/2 \end{aligned}} \right\} \quad \underline{\text{Lim}} C_{\theta_I} < 0$$

or

$$\begin{aligned}\text{xiv) } \theta_I + 2\gamma - \pi \leq \theta_J < 2\gamma - \theta_I \\ \text{xv) } 2\gamma - \theta_I \leq \theta_J < \pi/2\end{aligned} \quad \left. \vphantom{\begin{aligned} \text{xiv) } \theta_I + 2\gamma - \pi \leq \theta_J < 2\gamma - \theta_I \\ \text{xv) } 2\gamma - \theta_I \leq \theta_J < \pi/2 \end{aligned}} \right\} \quad \underline{\text{Lim}} C_{\theta_I} > 0$$

Eq. (5.2.3) is used for the cases xiii) and xv) while (5.2.5) is used for all the other cases in c) and d).

The corresponding angles to the sequential numbering which appears in the flow chart are

$$\begin{aligned}
 2(N-N_2)+I &\longrightarrow \theta = \theta_I + \pi - 2\gamma = \overline{\text{Lim}} C_{\theta_I} & \theta_I < 2\gamma - \pi/2 \\
 2N_2+1 &\longrightarrow \theta = 2\gamma - \pi/2 \\
 3N-2N_2+1 &\longrightarrow \theta = \pi - 2\gamma \\
 2(N_2-N)+I &\longrightarrow \theta = \theta_I + 2\gamma - \pi = \underline{\text{Lim}} C_{\theta_I} & \theta_I + 2\gamma > \pi/2 \\
 2(N+N_2+1)-I &\longrightarrow \theta = 2\gamma - \theta_I = \overline{\text{Lim}} C_{\theta_I} & \theta_I > 2\gamma - \pi/2
 \end{aligned}$$

#### 5.4 MOLECULAR TRANSFER FLOW CHARTS

(single discontinuity on the chamber wall)

The area of a spherical zone of width  $\Delta\theta$  on a sphere of radius  $r$  is

$$4\pi r^2 \sin \frac{\Delta\theta}{2} \cos(\theta + \frac{\Delta\theta}{2}) \quad (5.4.1)$$

If, however,  $\Delta\theta$  is small we may set

$$\sin \frac{\Delta\theta}{2} = \frac{\Delta\theta}{2}$$

and the spherical zone area will be

$$2\pi r^2 \cos(\theta + \frac{\Delta\theta}{2}) \Delta\theta \quad (5.4.2)$$

Thus, the flow which will hit a spherical zone  $Y_I$  due to the flow which leaves a spherical zone  $X_J$  is (Area of  $X_J$ )(density of flow leaving  $X_J$ ) $P_{X_J Y_I}$  where  $X, Y$  are any combination of  $C, V$  except the combination  $V, V$ .

The flow which leaves a spherical zone  $V_I$  in the time interval  $(n+1)\tau \leq t < (n+2)\tau$  is

$$2\pi r_v^2 \cos \theta_I \rho(V_I)_{n+1} \Delta\theta = (1 - \alpha_v) \sum_{J=1}^{2N} 2\pi r_c^2 \cos \theta_J \Delta\theta \rho(C_J)_n P_{C_J V_I} \quad (5.4.3)$$

Similarly, the flow which leaves the spherical zone  $C_I$  during the time interval  $(n+1)\tau \leq t < (n+2)\tau$  is

$$2\pi r_c^2 \cos \theta_I \rho(C_I)_{n+1} \Delta\theta = (1 - \alpha_c) \sum_{J=1}^{2N} \left[ 2\pi r_c^2 \cos \theta_J \Delta\theta \rho(C_J)_n P_{C_J C_I} + 2\pi r_v^2 \cos \theta_J \Delta\theta \rho(V_J)_n P_{V_J C_I} \right] \quad (5.4.4)$$

where

$$\cos\theta_J = \cos(\theta_J + \frac{\Delta\theta}{2}) \quad (5.4.5)$$

$$K = \begin{cases} 1 & 1 \leq I < N_1 \\ 2 & N_1 \leq I < 2N \end{cases} \quad (5.4.6)$$

Noting that  $r_v^2/r_c^2 = \sin^2\gamma$ ,  $P_{V_J C_I} = P_{C_J V_I} / \sin^2\gamma$  (see Equation 5.2.6) and denoting  $\cos\theta_{I\rho}(X_I)_n$  by  $\sigma(X_I)_n$ , Eqs. (5.4.3) and (5.4.4) are rewritten as follows:

$$\sigma(V_I)_{n+1} = (1-\alpha_v)/\sin^2\gamma \sum_{J=1}^{2N} \cos\theta_{J\rho}(C_J)_n P_{C_J V_I} \quad (5.4.7)$$

$$\sigma(C_I)_{n+1} = (1-a_K \sum_{J=1}^{2N} \cos\theta_J \left[ \rho(C_J)_n P_{C_J C_I} + \rho(V_J)_n P_{C_J V_I} \right]) \quad (5.4.8)$$

where K is defined by (5.4.6). The flow chart for the molecular transfer is self-explanatory. The molecular incidence for each spherical zone  $X_I$  is found by the relation

$$R_{X_I} = \frac{2 r_X^2 \Delta\theta \sum_{n=0}^{\infty} \sigma(X_I)_{n+1}}{2 r_X \Delta\theta \cos\theta_I (1-a_{X_I})} = \frac{\sum_{n=0}^{\infty} \sigma(X_I)_{n+1}}{(1-a_{X_I}) \cos\theta_I} \quad (5.4.9)$$

The infinite series, however, is very rapidly converging and in most cases it is sufficient to take  $n=10$  or less.

## 5.5 MODIFIED APPROACH TO THE COMPUTER SOLUTION

This approach is formulated in matrix notation and has the following advantages over the approach described previously.

- There are no limitations to the number of surface discontinuities of the parallel type.
- It is sufficient to know only the initial flows. Thus, calculations of flows which leave the surfaces in subsequent time intervals are unnecessary.
- The final solution to the flux distribution is not the result of a chopped off summation of an infinite series.
- It is free of errors introduced in the calculations of the flows which leave the surfaces during  $n\tau \leq t < (n+1)\tau$ ,  $n \geq 2$ .

### 5.5.1 Matrix Notation

$$P_{XY} = \begin{pmatrix} P_{X_1 Y_1}, P_{X_1 Y_2}, & P_{X_1 Y_{2N}} \\ P_{X_2 Y_1} & \\ & \\ & \\ P_{X_{2N} Y_1}, & P_{X_{2N} Y_{2N}} \end{pmatrix}$$

$$F_X(n) = \begin{pmatrix} F_{X_1}(n) \\ F_{X_2}(n) \\ \\ \\ F_{X_{2N}}(n) \end{pmatrix} \quad F_X = \begin{pmatrix} F_{X_1} \\ F_{X_2} \\ \\ \\ F_{X_{2N}} \end{pmatrix}$$

$$A_X = \begin{pmatrix} 1-\alpha_{X_1} & 0 & & 0 \\ 0 & 1-\alpha_{X_2} & & \\ & \ddots & \ddots & \\ 0 & & 0 & 1-\alpha_{X_{2N}} & 0 \end{pmatrix}$$

$$E = \begin{pmatrix} \cos\theta_1 & 0 & 0 \\ 0 & \cos\theta_2 & 0 \\ 0 & 0 & \ddots \\ 0 & 0 & 0 \cos\theta_{2N} \end{pmatrix}$$

$$H_X = \begin{pmatrix} H_{X_1} \\ H_{X_2} \\ \vdots \\ H_{X_{2N}} \end{pmatrix}$$

$$R_X = \begin{pmatrix} R_{X_1} \\ R_{X_2} \\ \vdots \\ R_{X_{2N}} \end{pmatrix}$$

$$\text{where } \theta_I = \theta_I + \frac{\Delta\theta}{2}$$

$\theta_I$  being the lower latitude of the I'th spherical zone.

## 5.5.2 Molecular Transfer

The following difference equations are easily derived

$$F_V(n+1) = (1-a_{V_J}) \sum_{I=1}^{2N} P_{C_I V_J} F_{C_I}(n) \quad (5.5.2.1)$$

$$F_C(n+1) = (1-a_{C_J}) \sum_{I=1}^{2N} \left[ P_{V_I C_J} F_{V_I}(n) + P_{C_I C_J} F_{C_I}(n) \right] \quad (5.5.2.2)$$

In matrix notation the above two equations take the form

$$F_V(n+1) = A_V P'_{CV} F_C(n) \quad (5.5.2.3)$$

$$F_C(n+1) = A_C \left[ P'_{VC} F_V(n) + P'_{CC} F_C(n) \right] \quad (5.5.2.4)$$

where the primes denote transpose matrices.

The boundary conditions then are

$$F_V(0) = 2\pi r_V^2 \Delta\theta A_V E F_V \quad (5.5.2.5)$$

$$F_C(0) = 2\pi r_C^2 \Delta\theta A_C E F_C \quad (5.5.2.6)$$

From (5.5.2.3) and (5.5.2.4) in view of (5.5.2.5) and (5.5.2.6) we obtain

$$F_V(1) = 2\pi r_C^2 \Delta\theta A_V P'_{CV} A_C E F_C \quad (5.5.2.7)$$

$$F_C(1) = A_C \left[ 2\pi r_V^2 \Delta\theta P'_{VC} A_V E F_V + 2\pi r_C^2 \Delta\theta P'_{CC} A_C E F_C \right] \quad (5.5.2.8)$$

Substituting (5.5.2.3) into (5.5.2.4) we obtain

$$F_C(n+2) = A_C \left[ P'_{VC} A_V P'_{CV} F_C(n) + P'_{CC} F_C(n+1) \right] \quad (5.5.2.9)$$

Summing up (5.5.2.9) from  $n = 0$  to  $N = \infty$  and solving for  $H_C$  we obtain

$$H_C = \left\{ I - A_C \left[ \frac{P'_{CV} A_V P'_{CV}}{\sin^2 \gamma} + P'_{CC} \right] \right\}^{-1} \left\{ F_C(1) + \frac{A_C P'_{CV} A_V P'_{CV} F_C(0)}{\sin^2 \gamma} \right\} \quad (5.5.2.10)$$

where  $I$  is the unit matrix.

Similarly, summing up (5.5.2.3) from  $n = 0$  to  $n = \infty$  we obtain

$$H_V = A_V P'_{CV} \left[ H_C + F_C(0) \right] \quad (5.5.2.11)$$

### 5.5.3 Molecular Flux Distribution

Since the area of the  $I$ 'th spherical zone on surface  $X$  is  $2\pi r_X^2 \cos\theta_I \Delta\theta$  where  $\theta_I = (I-N-\frac{1}{2})\Delta\theta = \theta_I + \frac{\Delta\theta}{2}$

the rate of incidence on this spherical zone is

$$R_{X_I} = \frac{H_{X_I}}{2\pi r_X^2 \cos\theta_I \Delta\theta (1-a_{X_I})} \quad (5.5.3.1)$$

Hence, in matrix form

$$R_X = \frac{(EA_X)^{-1} H_X}{2\pi r_X^2 \Delta\theta} \quad (5.5.3.2)$$

Then from (5.5.2.10) and (5.5.3.2) we obtain

$$R_C = \left\{ EA_C - A_C \left[ \frac{P'_{CV} A_V P'_{CV}}{\sin^2 \gamma} + P'_{CC} \right] EA_C \right\}^{-1} T \quad (5.5.3.3)$$

$$T = A_C \left\{ P'_{CV} A_V E_F + \left[ P'_{CC} + \frac{P'_{CV} A_V P'_{CV}}{\sin^2 \gamma} \right] A_C E_F \right\}$$

Similarly, from (5.5.2.11) and (5.5.3.2) we obtain

$$\begin{aligned} R_V &= \frac{(EA_V)^{-1}}{\sin^2 \gamma} A_V P'_{CV} \left[ EA_C R_C + A_C E_F \right] \\ &= \frac{E^{-1}}{\sin^2 \gamma} P'_{CV} EA_C \left[ R_C + F_C \right] \end{aligned} \quad (5.5.3.4)$$



## 6.0 COMPUTER RESULTS

For studying general trends in the molecular flux distribution on the chamber-vehicle surfaces, a variety of cases were chosen and the results were plotted on semilog paper (see figures 16-26). Each of these figures contains two graphs for the molecular flux distributions, one for the chamber wall (dotted curve) and the other for the vehicle (circle curve). The cases under study were chosen in terms of the following parameters.

- a) Size of sun (large and small)
- b) Size of vehicle (large and small)
- c) Pumping coefficients
- d) Source of outgassing

The size of the sun is determined by the discontinuous line  $N_1$  while the size of the vehicle is determined by the magnitude of  $N_2$ . For the size of the sun and the vehicle there were chosen two values for  $N_1$  and  $N_2$

$$\begin{aligned} N_1 &= 30 \text{ Large size sun} \\ &= 33 \text{ Small size sun} \end{aligned}$$

$$\begin{aligned} N_2 &= 6 \text{ Large size vehicle } (\gamma=30^\circ) \\ &= 3 \text{ Small size vehicle } (\gamma=15^\circ) \end{aligned}$$

The different combinations of a), b), c), and d) making up the different test cases are shown in the following table.

TABLE OF TEST CASES

2N = 36

Case	$N_1$	$N_2$	$a_1$	$a_2$	$a_v$	$q_1$	$q_2$	$q$	$m$
1	30	6	.9	0	0	0	1	0	10
2	33	6	.9			0	1	0	10
3	33	3	.9			0	1	0	10
4	30	6	.95			0	1	0	10
5	30	6	.8			0	1	0	15
6	30	6	.9			1	0	0	10
7	30	6	.9			0	0	1	10
8	30	6	.8			0	0	1	15
9	33	3	.9			0	0	1	10
10	30	6	.9	.1	.1	.3	.5	1	10
11	30	6	.9	.1	.1	.01	.1	1	10

Looking at these graphs we can point out a number of interesting phenomena. Generally speaking, in the cases of a non-outgassing vehicle the flux distributions on the chamber wall and on the vehicle cross each other at a point. It is not as much the size of the sun as it is the size of the vehicle which affects this crossing point. A comparison between cases 1) and 2) (Figures 16 and 17) shows that the crossing point has been affected by less than  $5^\circ$  while between cases 2) and 3) (Figures 18 and 19) the crossing point has been displaced by  $20^\circ$ . Also a slight increase in the pumping coefficient on the chamber wall will hardly affect the crossing point as it can be seen from cases 1) and 4) (Figures 16 and 19). An interesting phenomenon is presented in case 6 (Figure 21). The two flux distributions almost coincide. If the area of the sun shrinks to zero we have the uniform case of outgassing chamber wall. Then the molecular flux on the unpumping areas is  $F_C(1-a_C)/a_C$  on both the chamber wall and the vehicle as it can be seen from equation 3.2.5. Setting  $F_C = 1$  and  $a_C = .9$  we find

$$\frac{F_C(1-a_C)}{a_C} = \frac{1}{9}$$

Thus in case 6 the flux distributions on both surfaces of the chamber wall and of the vehicle are equal and 10 times as much the flux distributions in the uniform case. From this observation it appears that the presence of a non-pumping non-outgassing sun will have a very slight effect on the uniformity of molecular flux distribution. Of course, this cannot be the case for all sizes of vehicle. From the ratio of the area of the sun to the area of the vehicle in case 6 we can state safely that both fluxes are equal to a constant depending on the size of the sun as long as

$$\frac{\text{sun area}}{\text{vehicle area}} \leq .2$$

As we have implied above, in the cases of predominantly outgassing vehicle the two fluxes do not cross each other. Further, the flux distribution on the chamber wall remains practically uniformly distributed, apart from a slight negligible variation, while the flux on the vehicle, increases from a minimum at  $\theta = -\pi/2$  to a point between  $0^\circ$  and  $30^\circ$  above the equation at a constant rate and from that point on at a higher rate leveling off around  $\theta = \pi/2$ .

Case 7 is the superposition of cases 1, 6 and 10 each multiplied by an appropriate factor if we neglect the pumping coefficient  $a_{C2}$  and  $a_V$ . Thus if we multiply case 1 by .5 and case 6 by .3 and subtract the sum of these two results from case 10 we will obtain approximately case 7. To see this let us select three points  $\theta = -\pi/2, 0, \pi/2$   $1+d_1$  denotes the flux of the 1'th case at any  $\theta$  we must have  $d_7 = d_{10} - (.5d_1 + .3d_6)$  either on the chamber wall or on the vehicle. Consider the flux on the chamber wall at  $\theta = \pi/2$ .

$$d_1 = 4.9248 \times 10^{-3}, d_6 = 1.0238, d_{10} = 5.4276 \times 10^{-1} \quad d_7 = 2.4138 \times 10^{-1}$$

$$d_{10} - (.5d_1 + .3d_6) = .23316$$

$$\text{At } \theta = 0$$

$$d_1 = 9.1821 \times 10^{-2}, d_6 = 1.0154, d_{10} = 6.2723 \times 10^{-1}$$

$$d_7 = 2.9613 \times 10^{-1}$$

$$d_{10} - (.5d_1 + .3d_6) = 2.7670 \times 10^{-1}$$

$$\text{At } \theta = \pi/2$$

$$d_1 = 1.9230 \times 10^{-1}, d_6 = 1.0107, d_{10} = 6.527 \times 10^{-1}$$

$$d_7 = 2.8306 \times 10^{-1}$$

$$d_{10} - (.5d_1 + .3d_6) = .25334$$

The agreement is better at  $\theta = \pi/2$  and becomes less accurate with increasing  $\theta$ . This is of course due to the fact that we have discarded the pumping coefficient  $a_{C_2}$  and  $a_V$  in case 10. The flux distribution on the vehicle can be considered in a similar way. Thus, if  $N_1$ ,  $a_{C_1}$ ,  $a_{C_2}$  and  $a_V$  are kept fixed, the results of any combination of source outgassing can be obtained from a linear combination of the following three cases

- i)  $q_1 = 1, q_2 = q = 0$
- ii)  $q_1 = 0, q_2 = 1, q = 0$
- iii)  $q_1 = q_2 = 0, q = 1$

The superposition principle becomes also useful in the cases where many types of gases are considered with independent pumping and outgassing characteristics for each type of gas. The solution then in that case is obtained by superimposing the individual solutions for each type of gas.

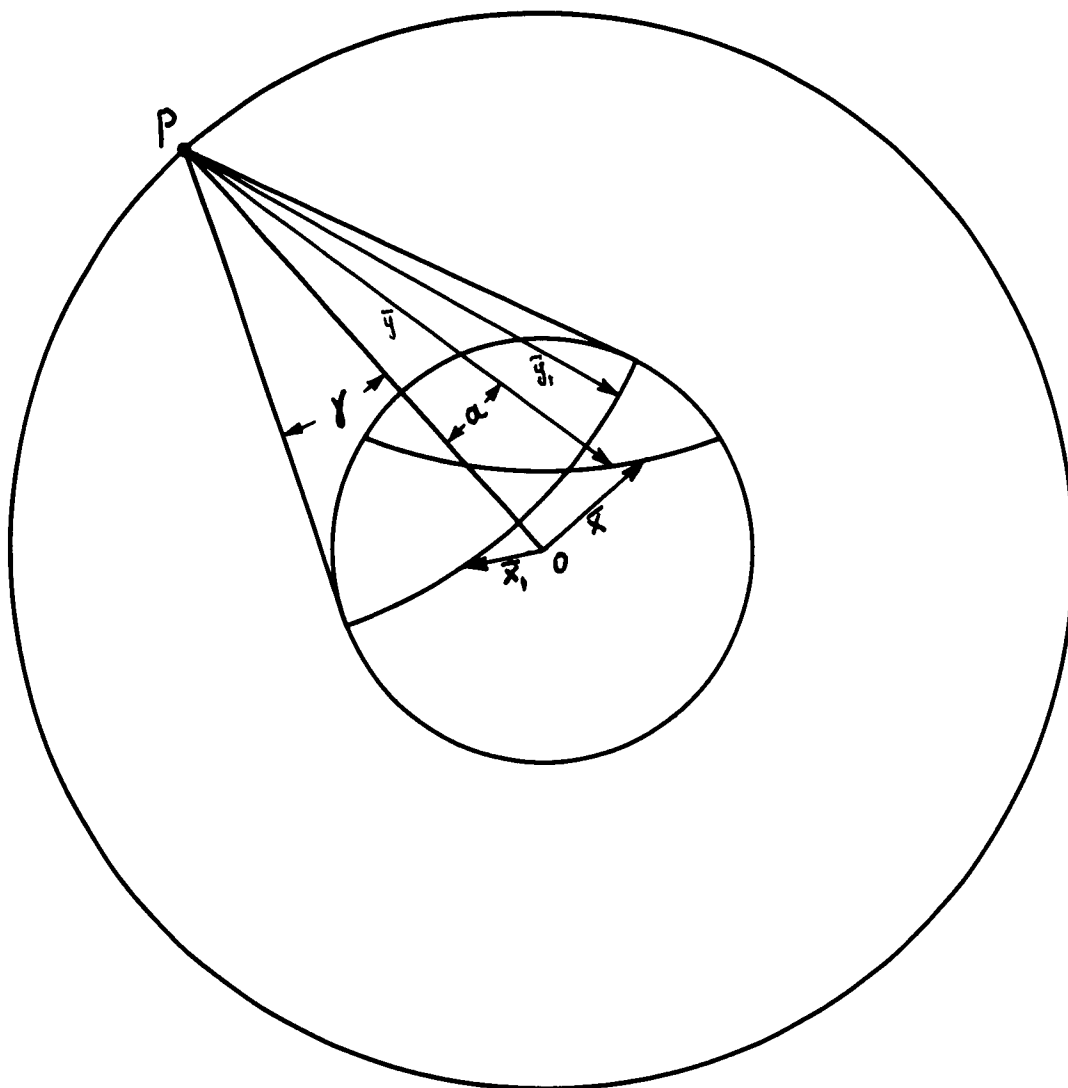


FIGURE 1

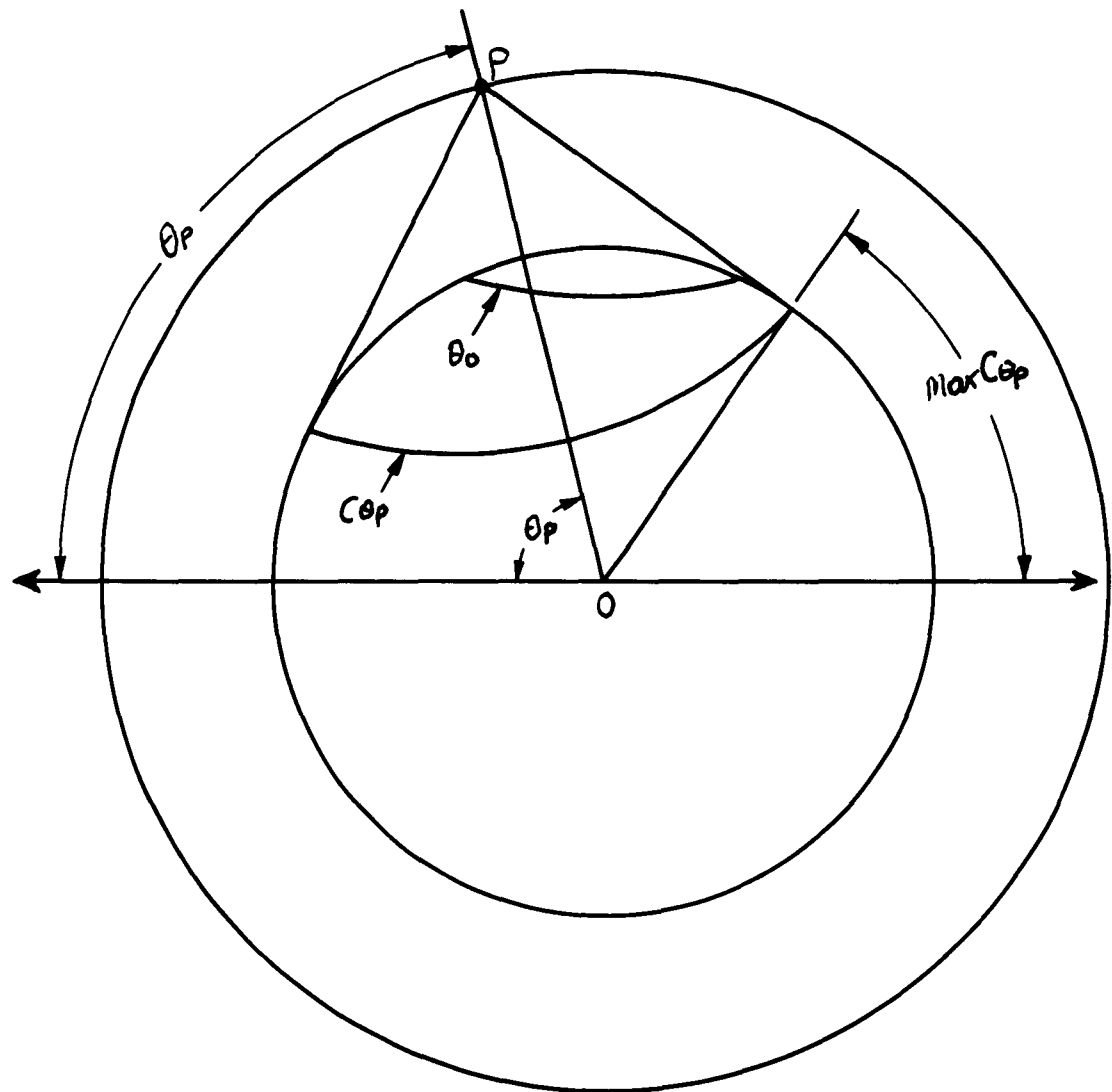


FIGURE 2

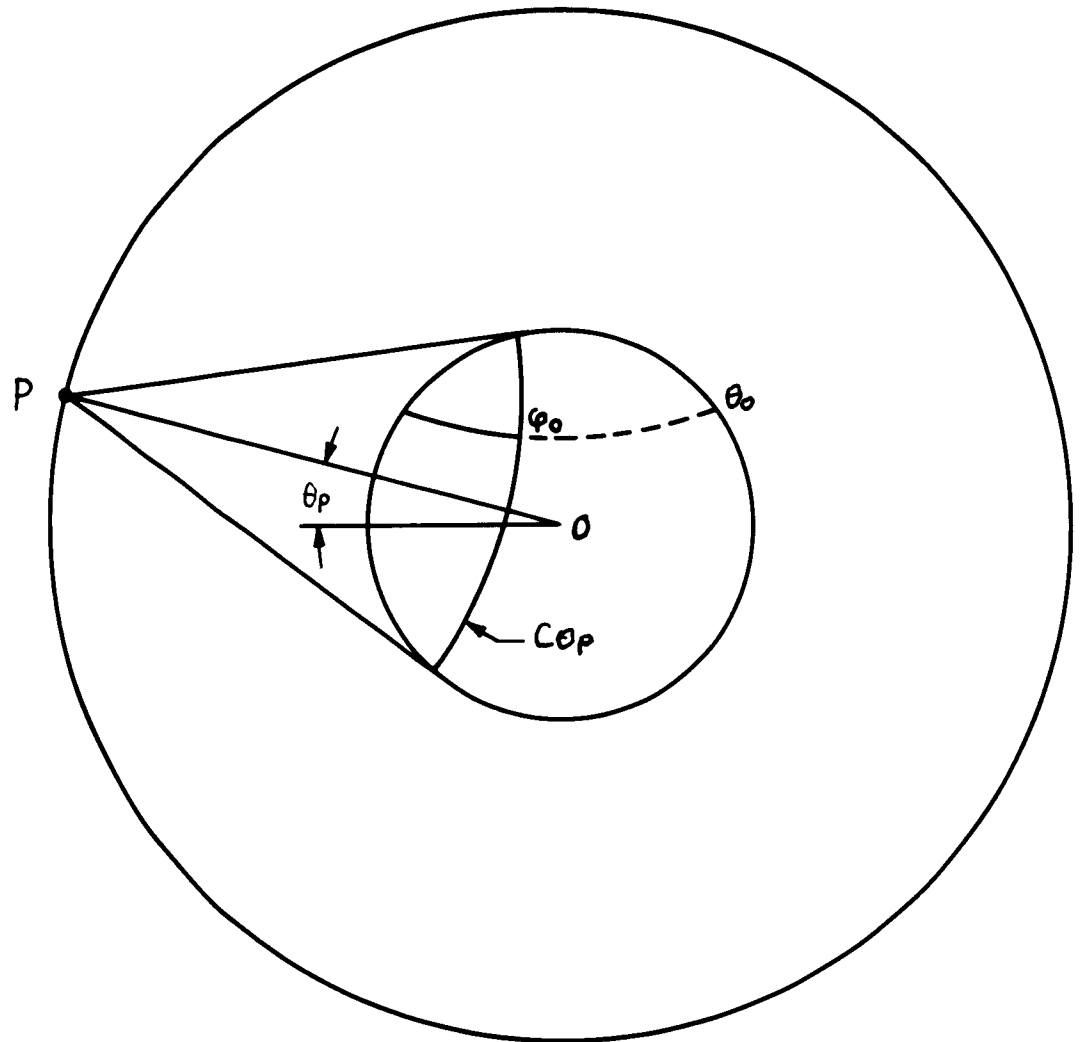


FIGURE 3

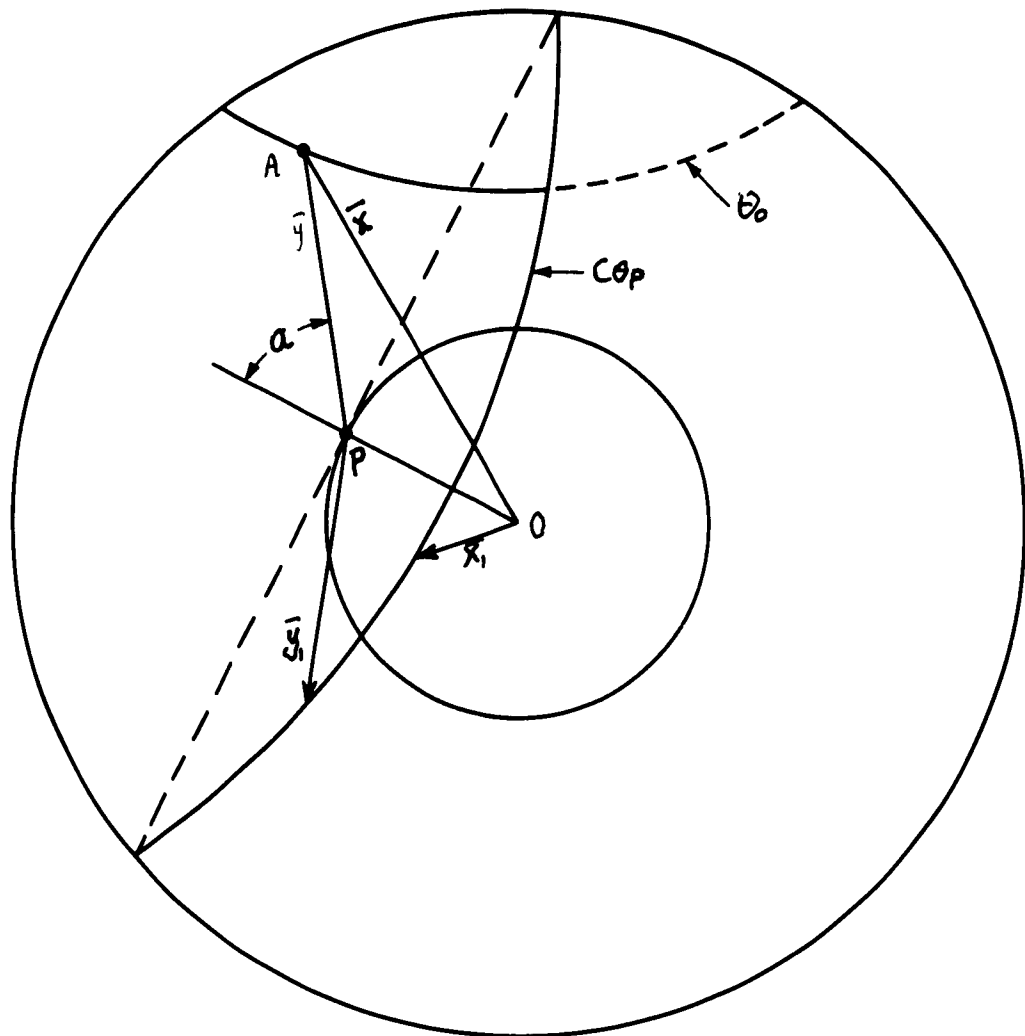


FIGURE 4

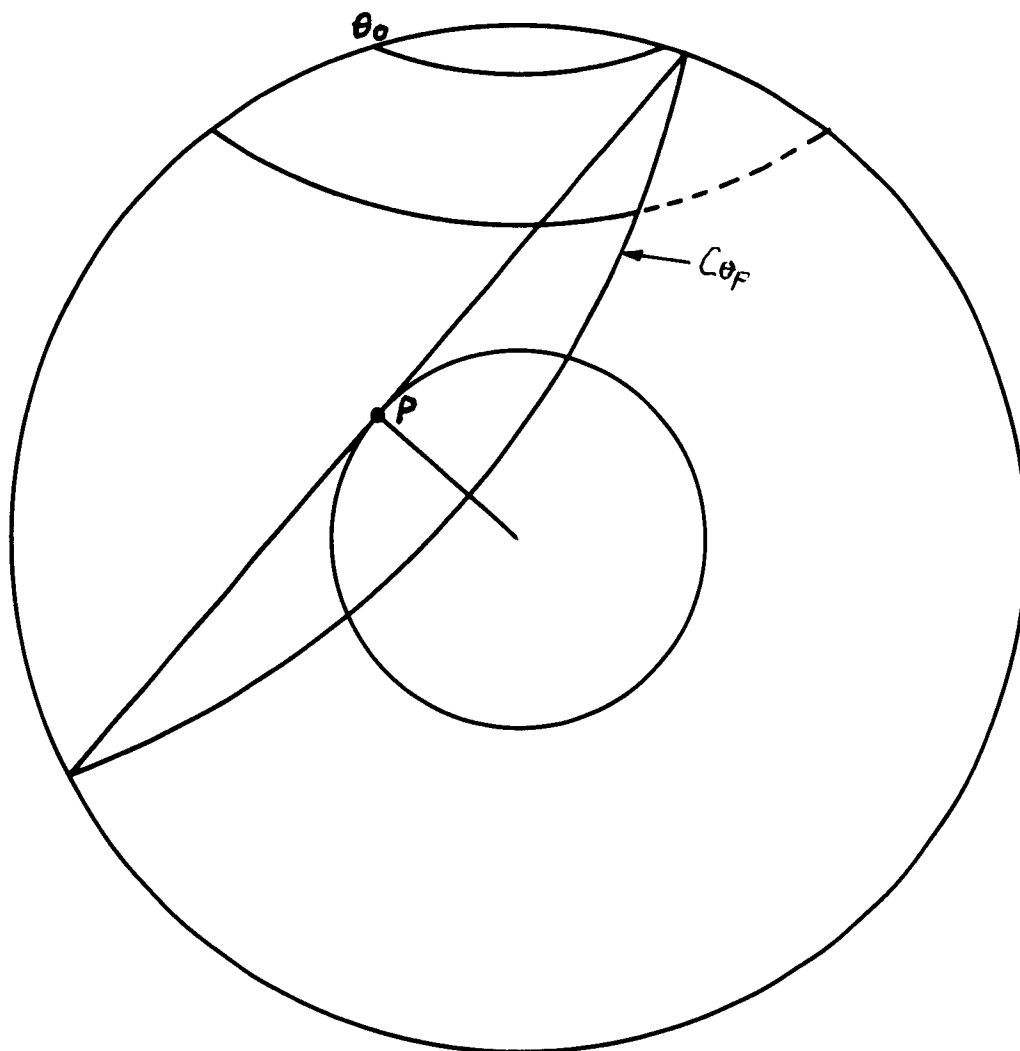


FIGURE 5





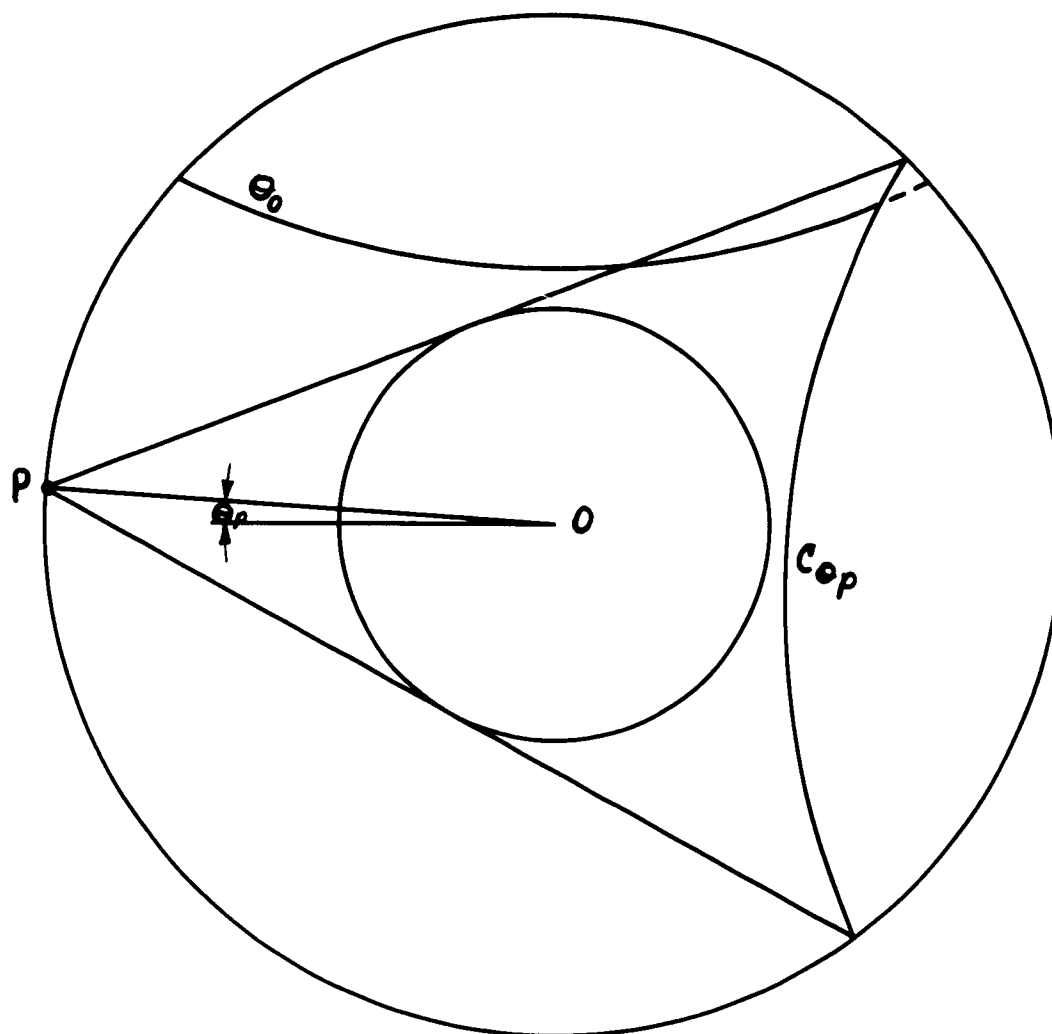


FIGURE 7

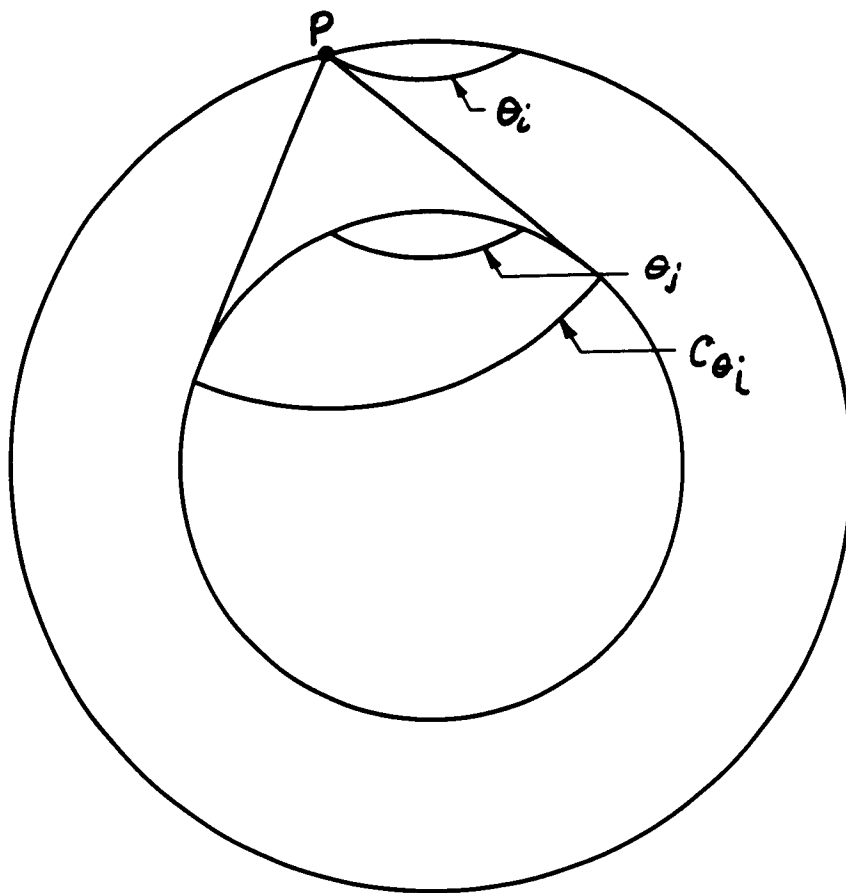


FIGURE 8

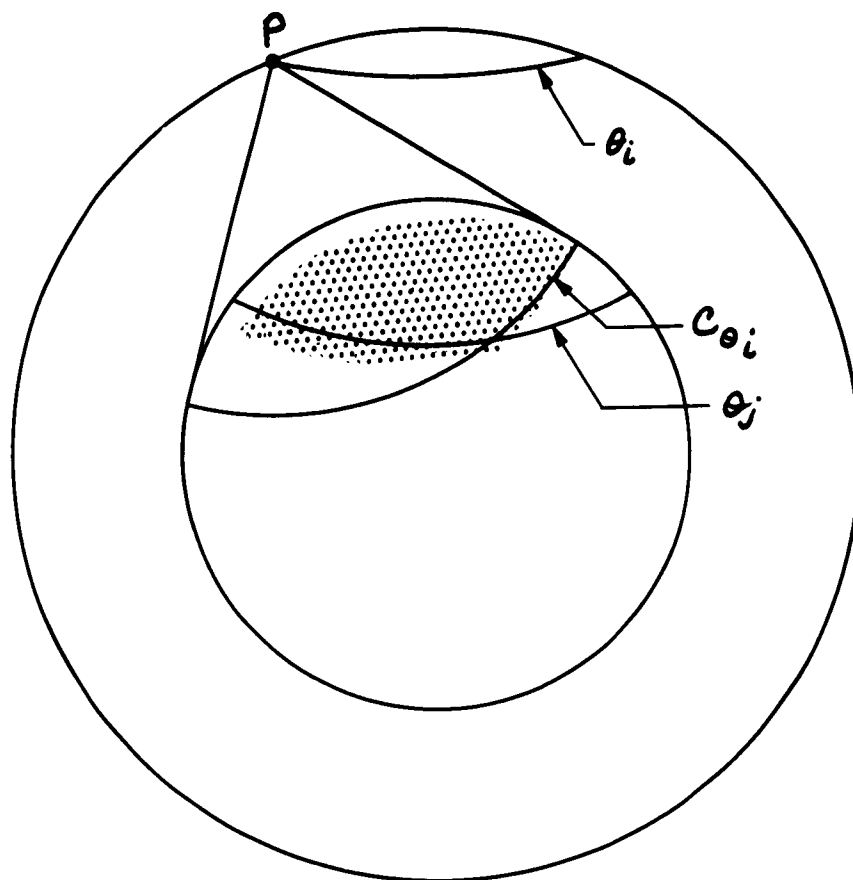


FIGURE 9

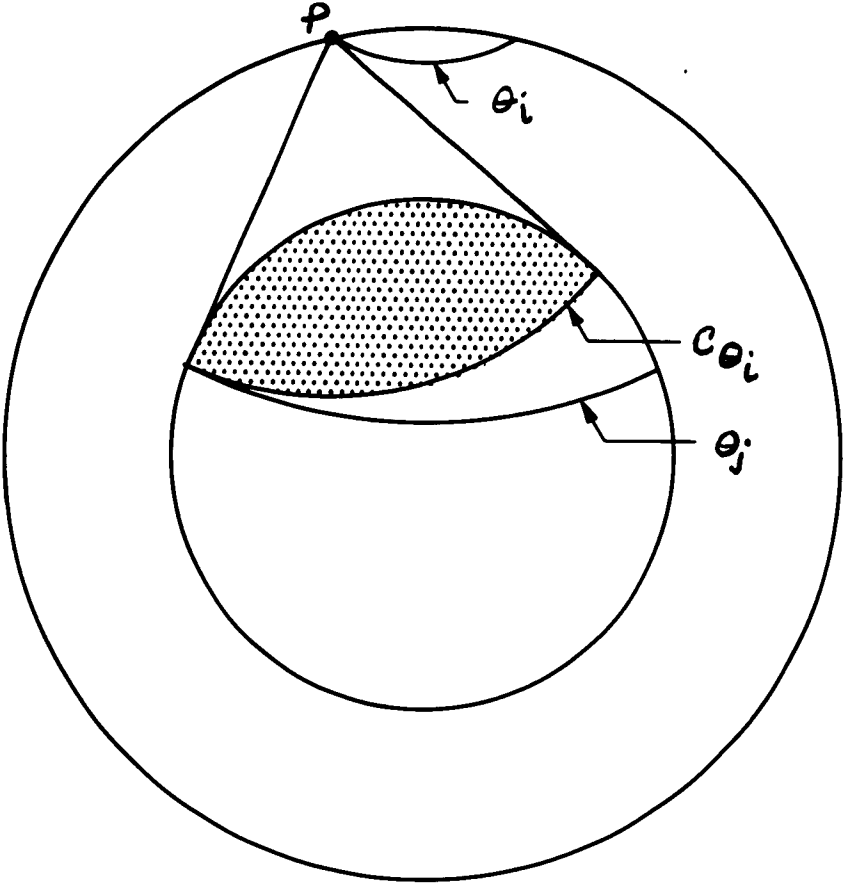


FIGURE 10

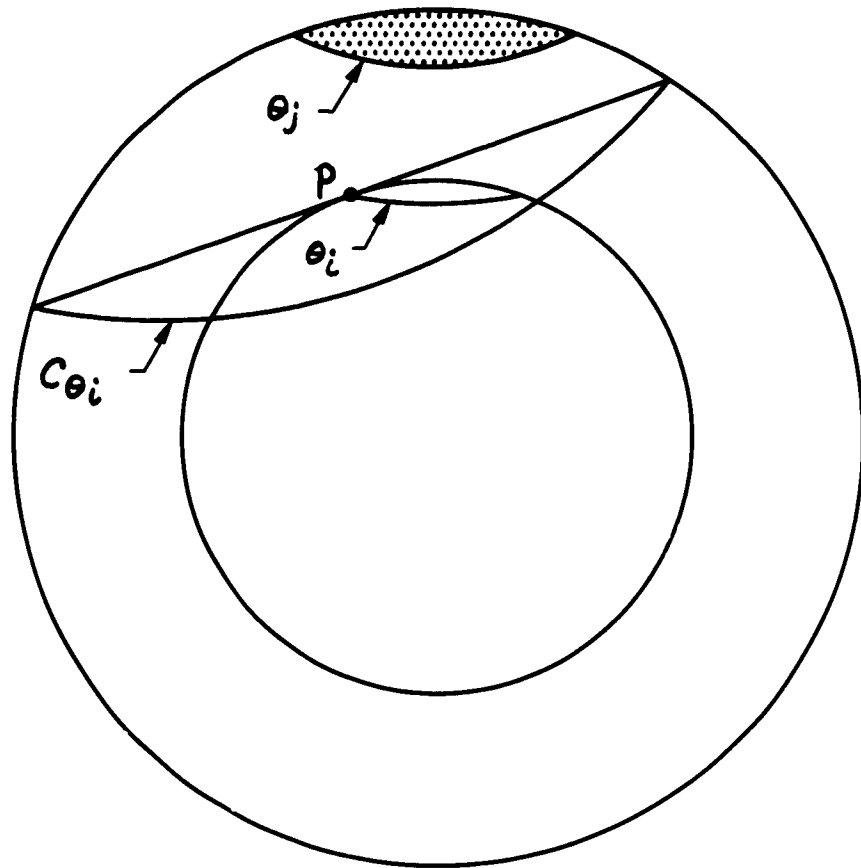


FIGURE 11

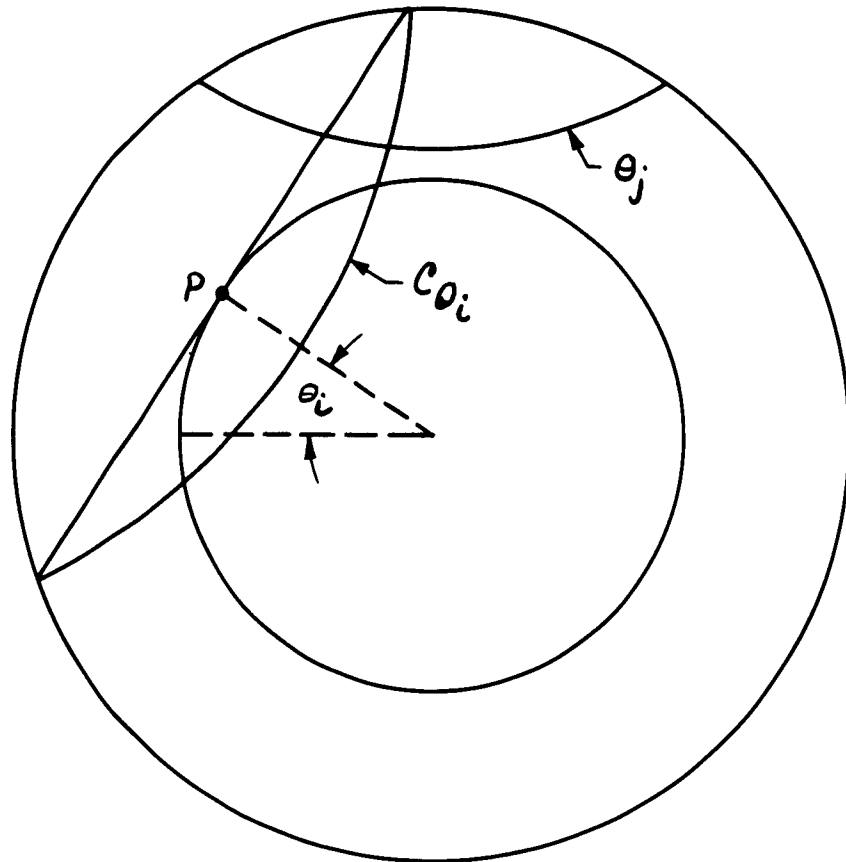


FIGURE 12

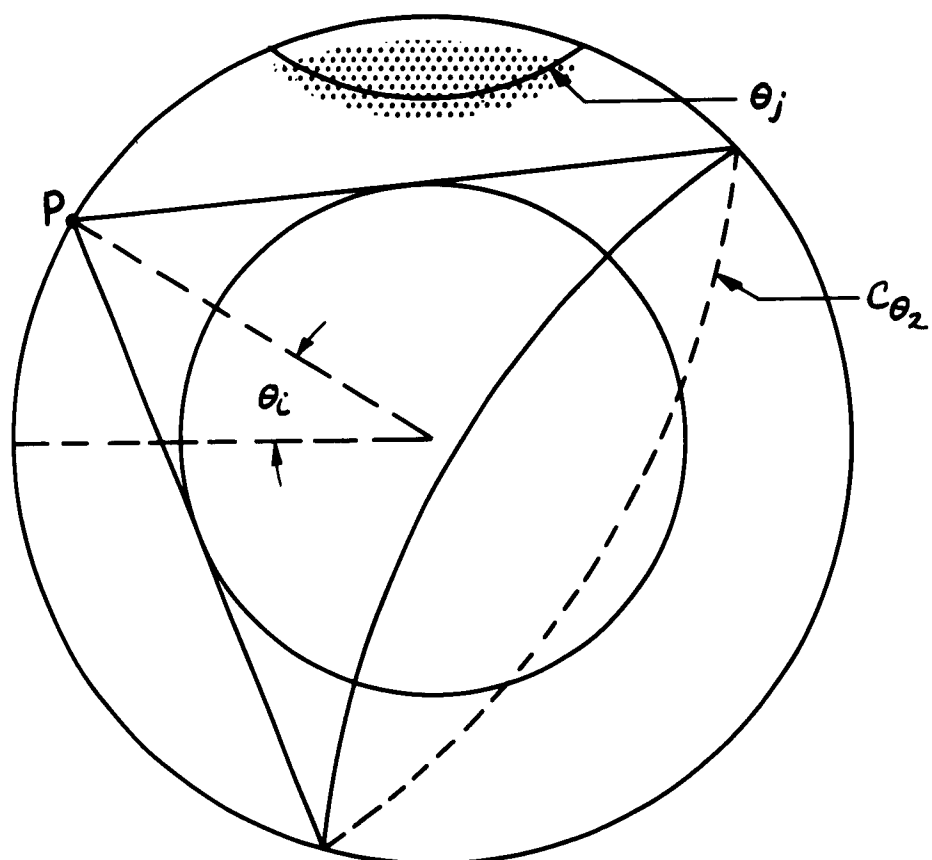


FIGURE 13



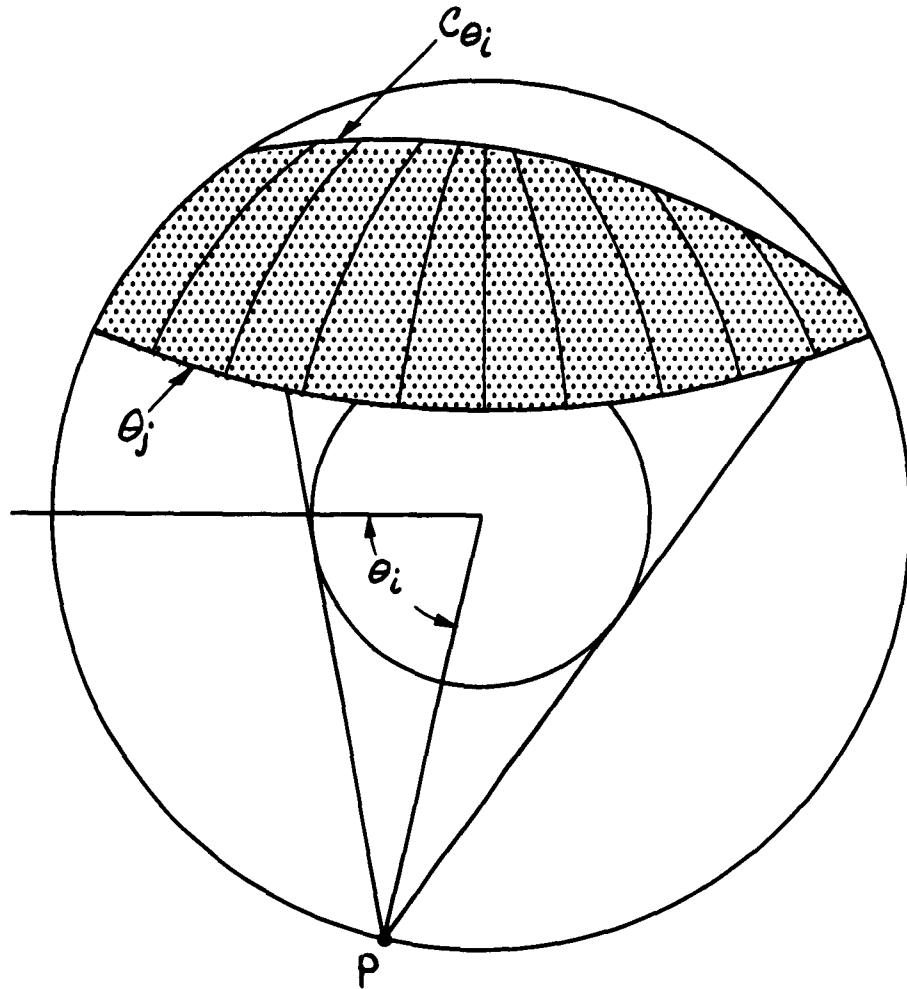


FIGURE 14

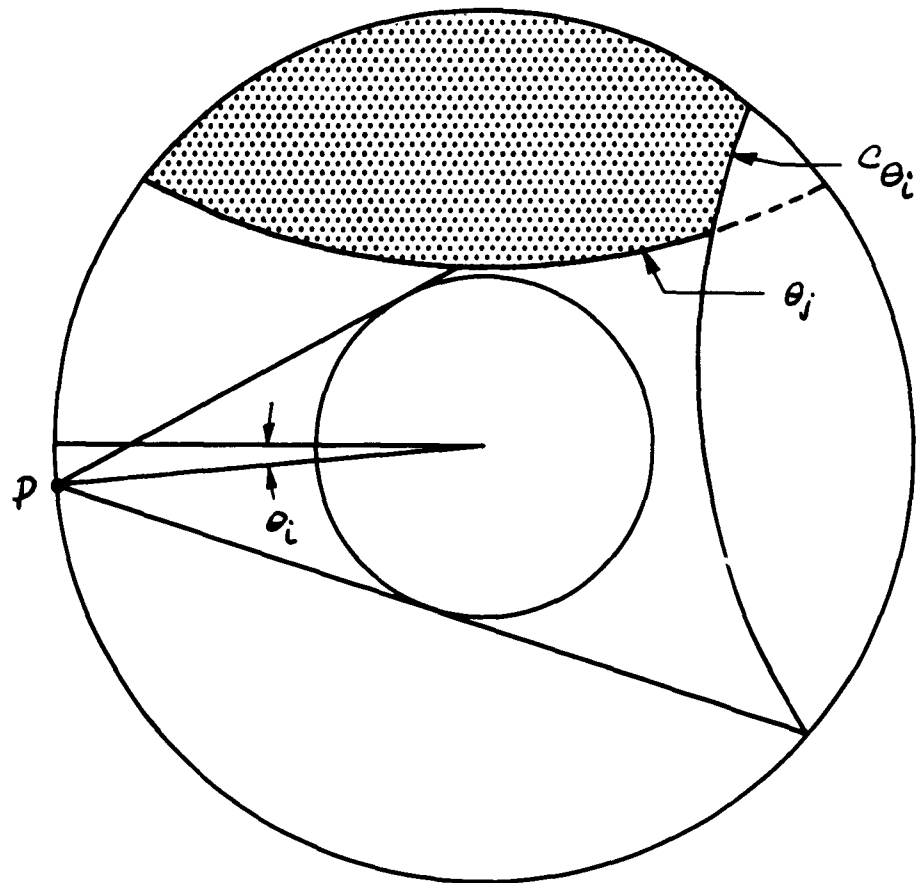


FIGURE 15

## CASE NO. 1 TOTAL HITS PER UNIT AREA

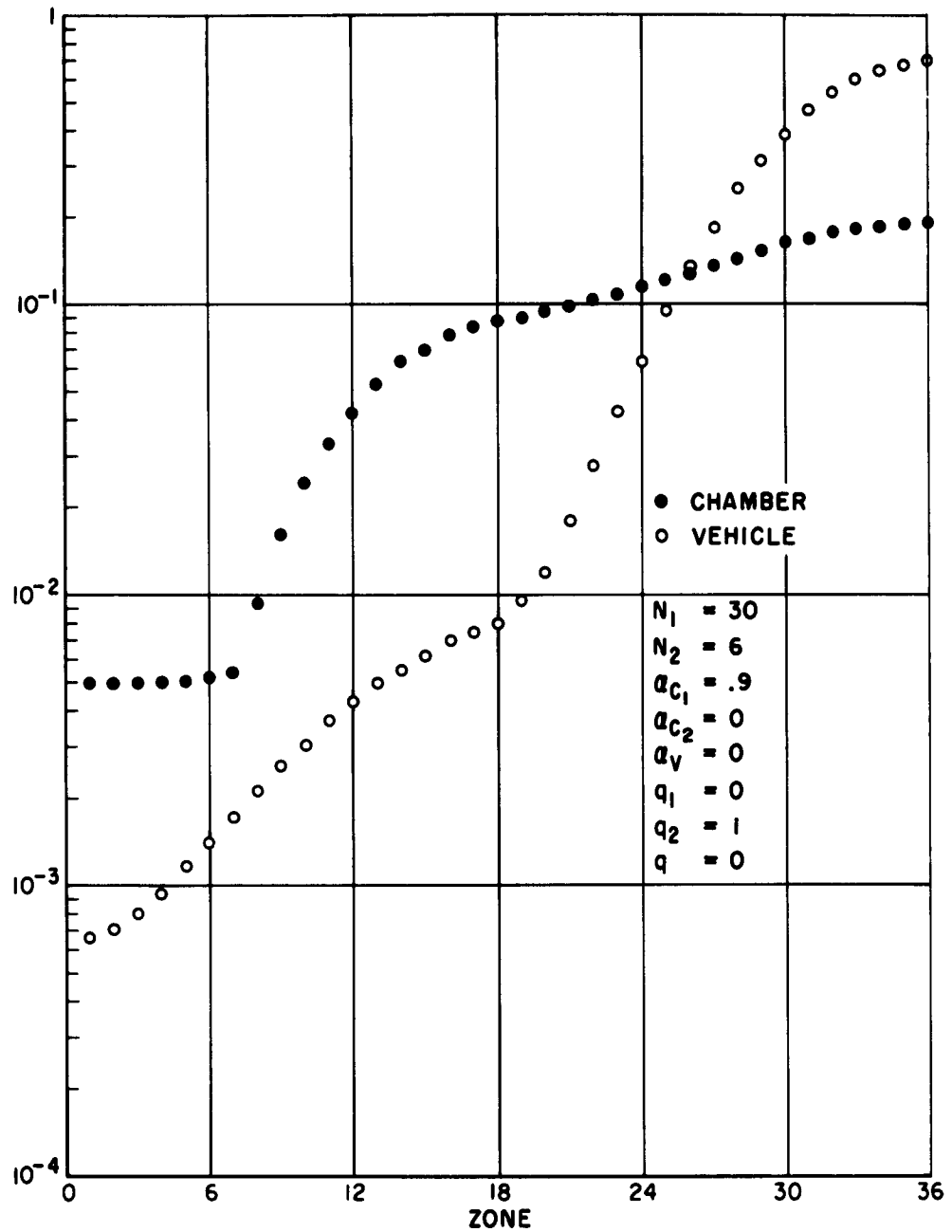


FIGURE 16

## CASE NO. 2 TOTAL HITS PER UNIT AREA

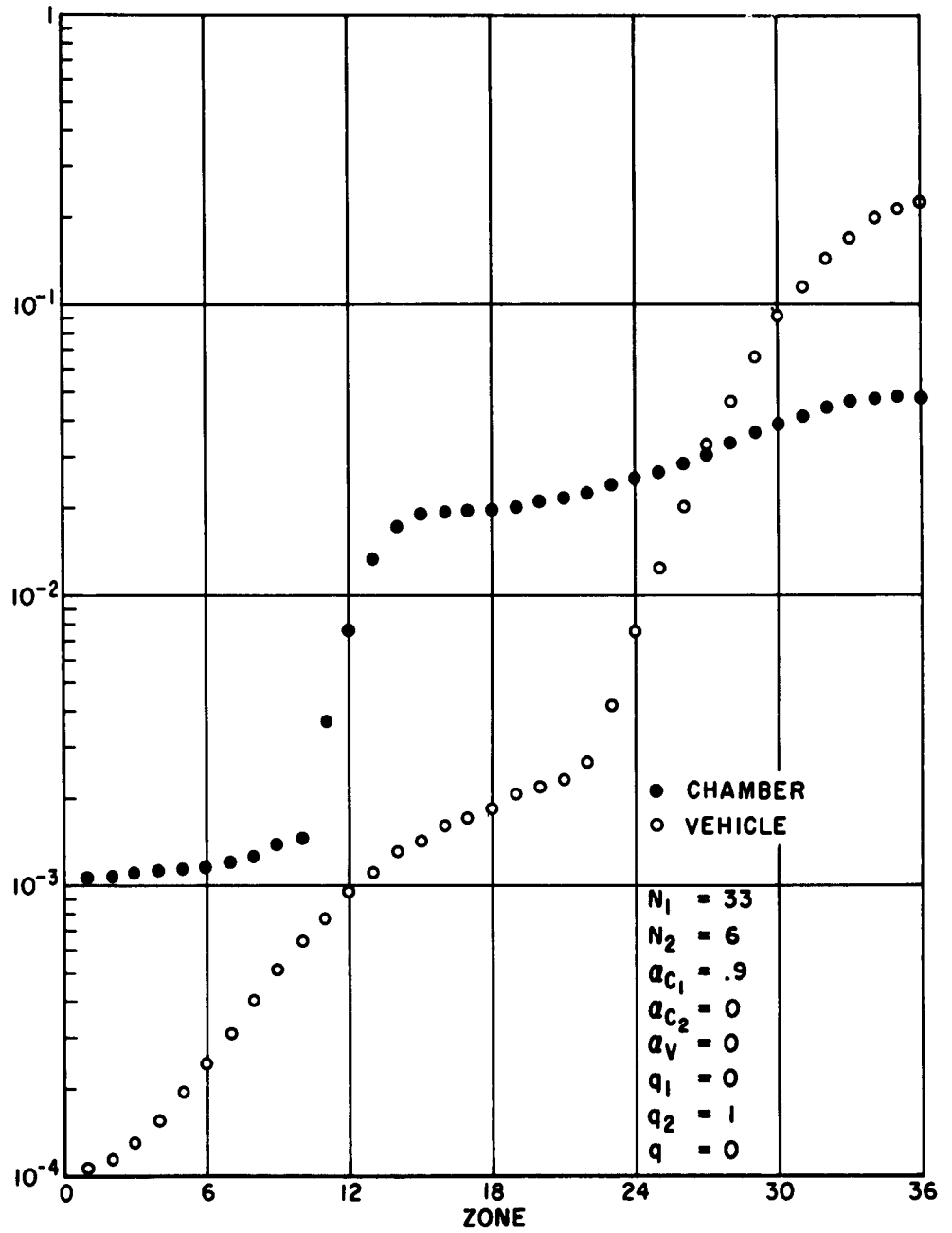


FIGURE 17

CASE NO.3 TOTAL HITS PER UNIT AREA

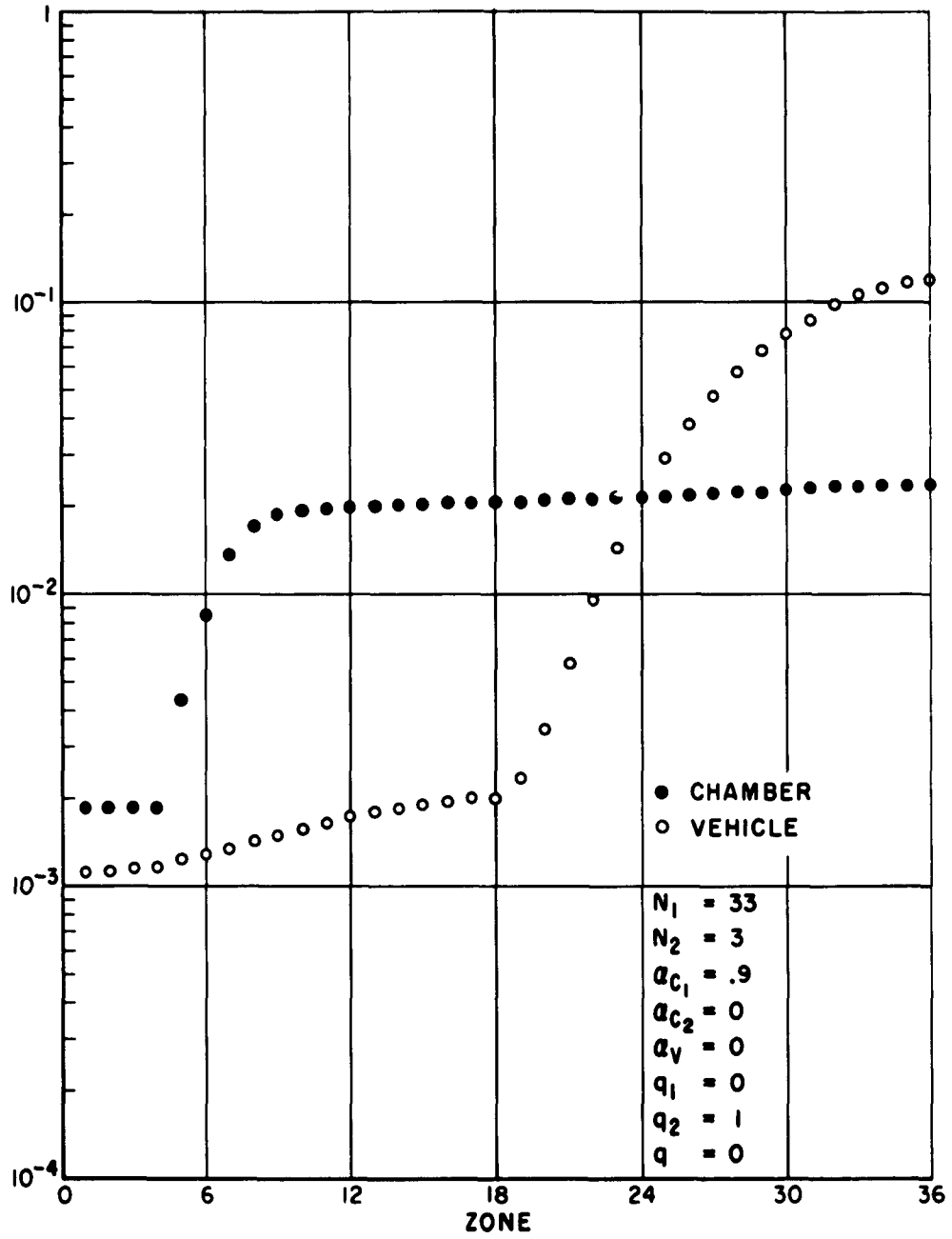


FIGURE 18

## CASE NO. 4 TOTAL HITS PER UNIT AREA

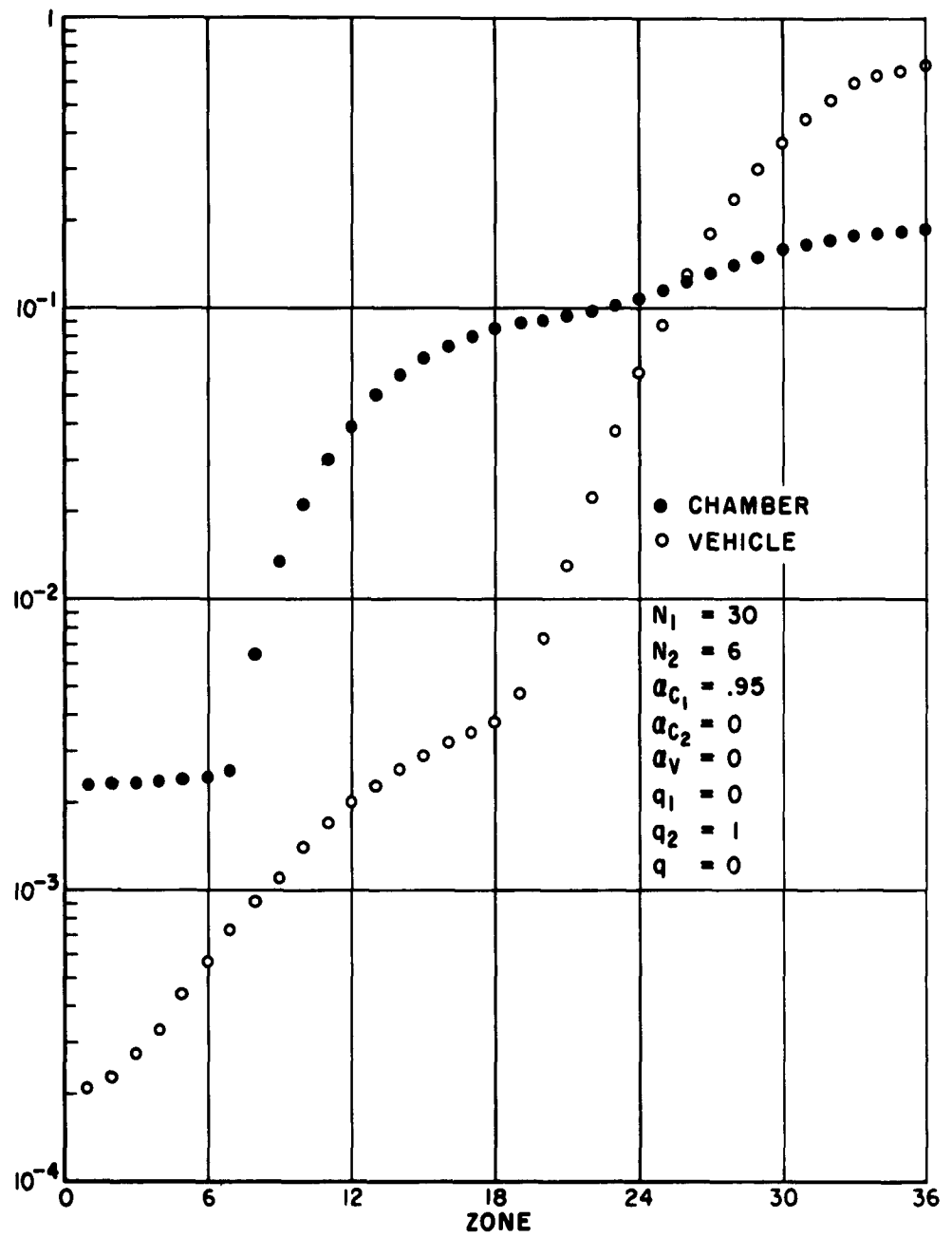


FIGURE 19

CASE NO. 5 TOTAL HITS PER UNIT AREA

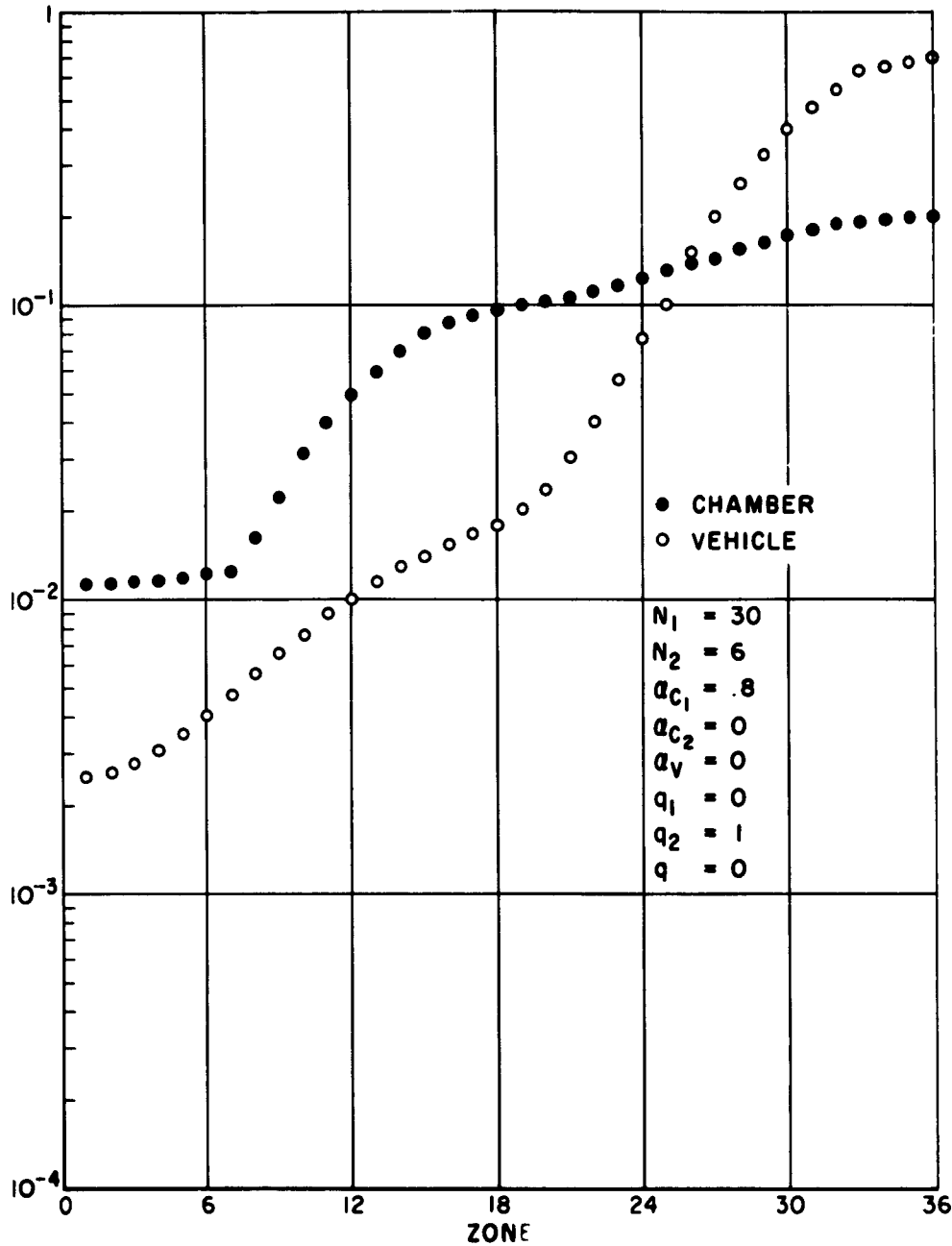


FIGURE 20

## CASE NO. 6 TOTAL HITS PER UNIT AREA

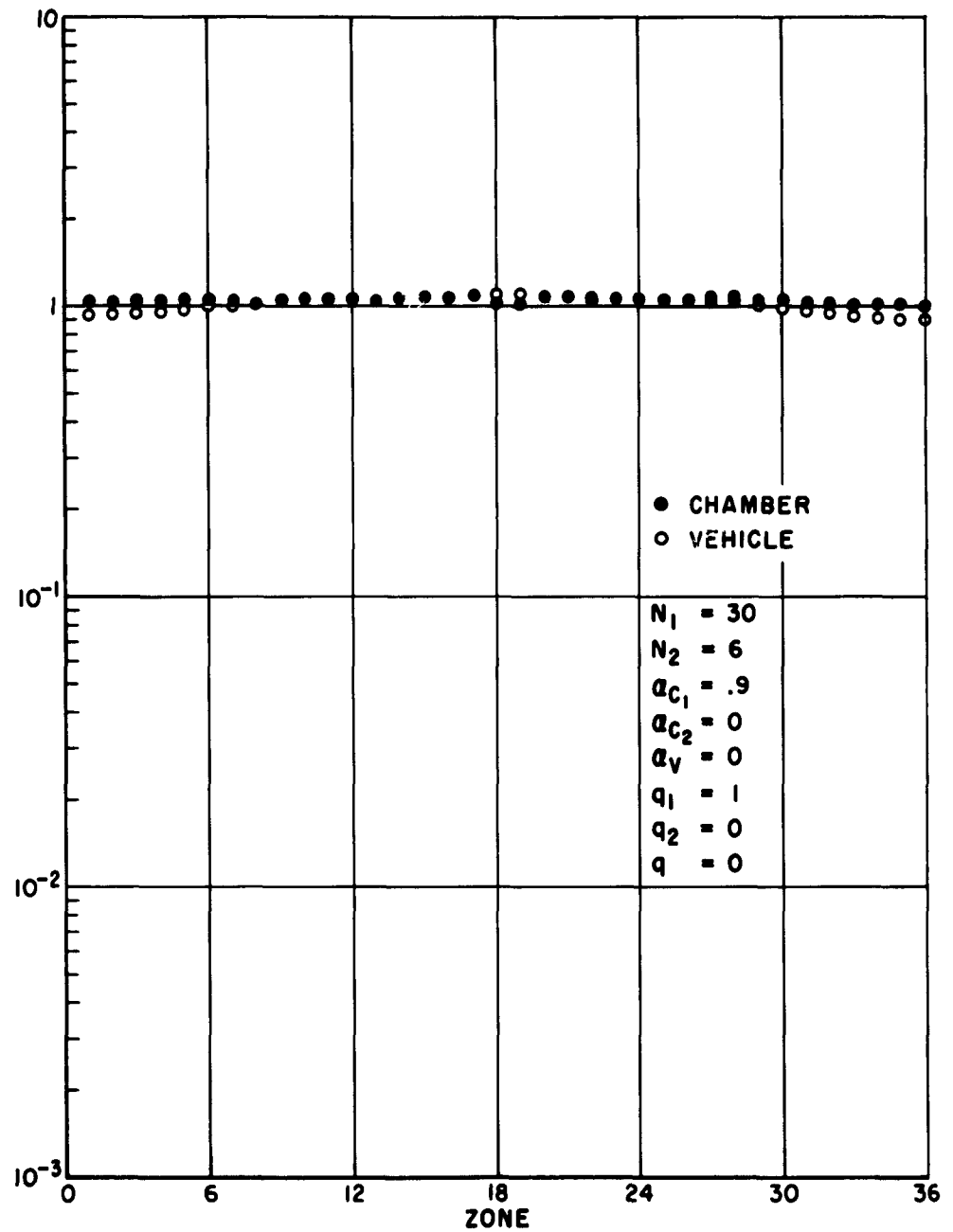


FIGURE 21



## CASE NO. 7 TOTAL HITS PER UNIT AREA

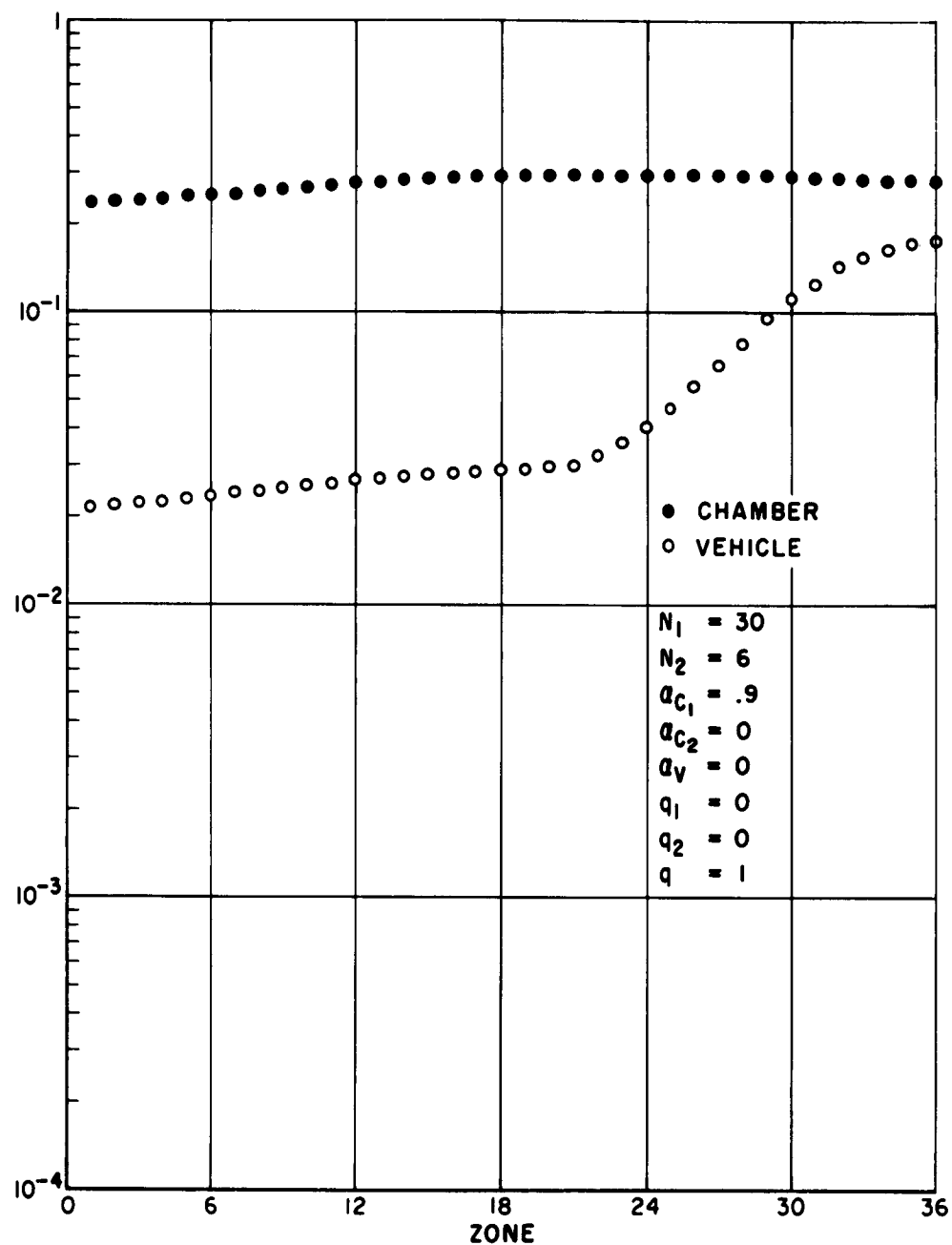


FIGURE 22

## CASE NO. 8 TOTAL HITS PER UNIT AREA

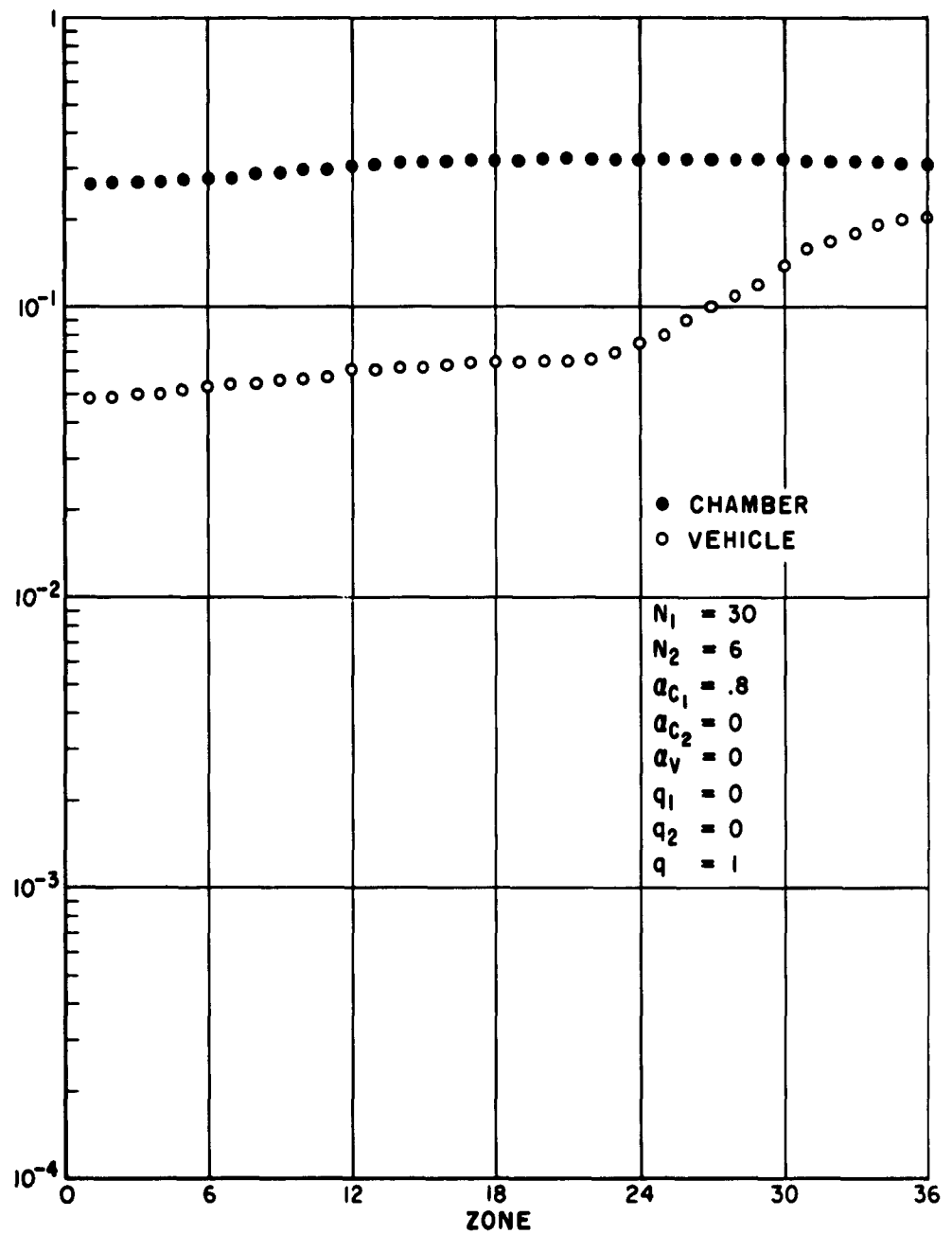


FIGURE 23

## CASE NO. 9 TOTAL HITS PER UNIT AREA

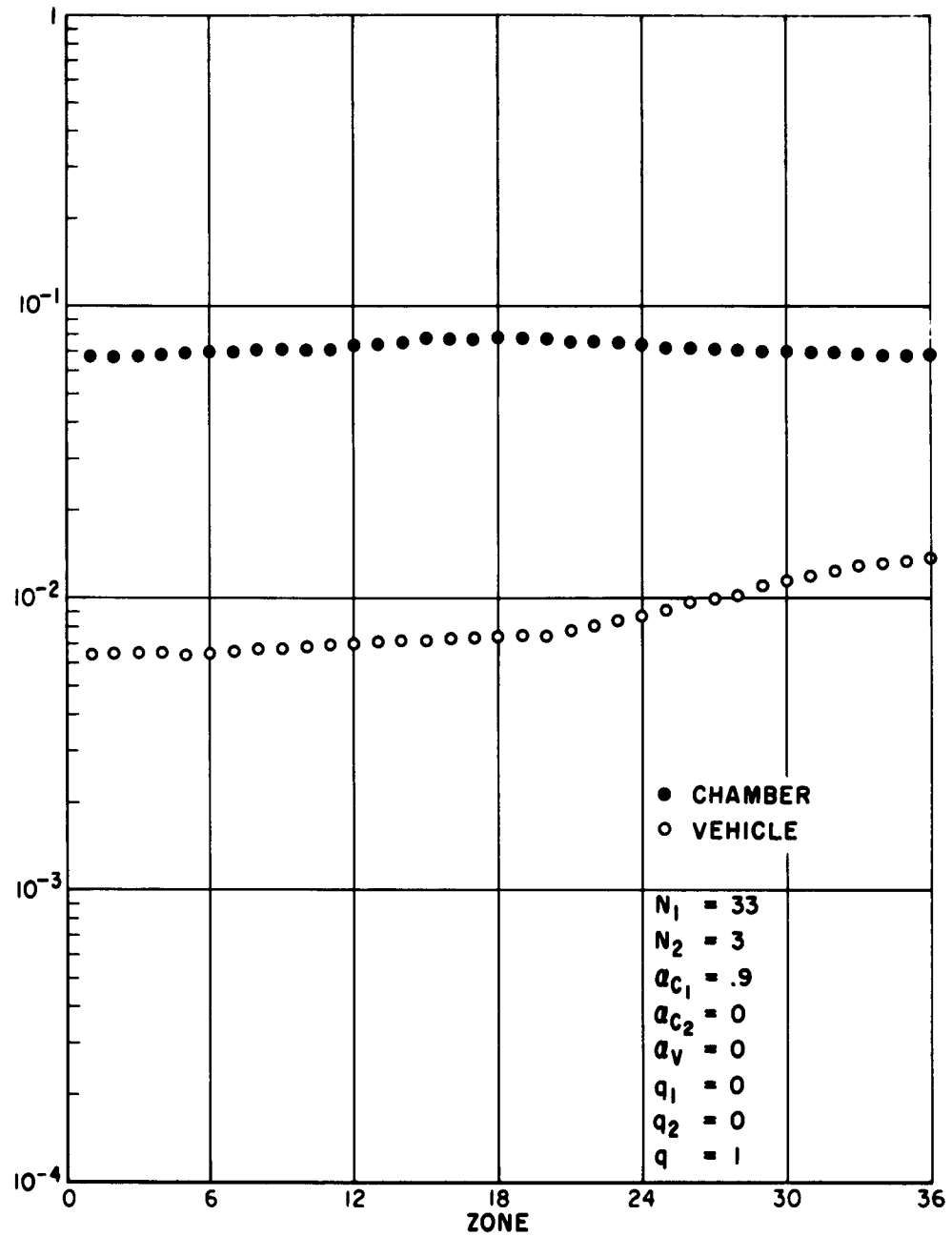


FIGURE 24

## CASE NO. 10 TOTAL HITS PER UNIT AREA

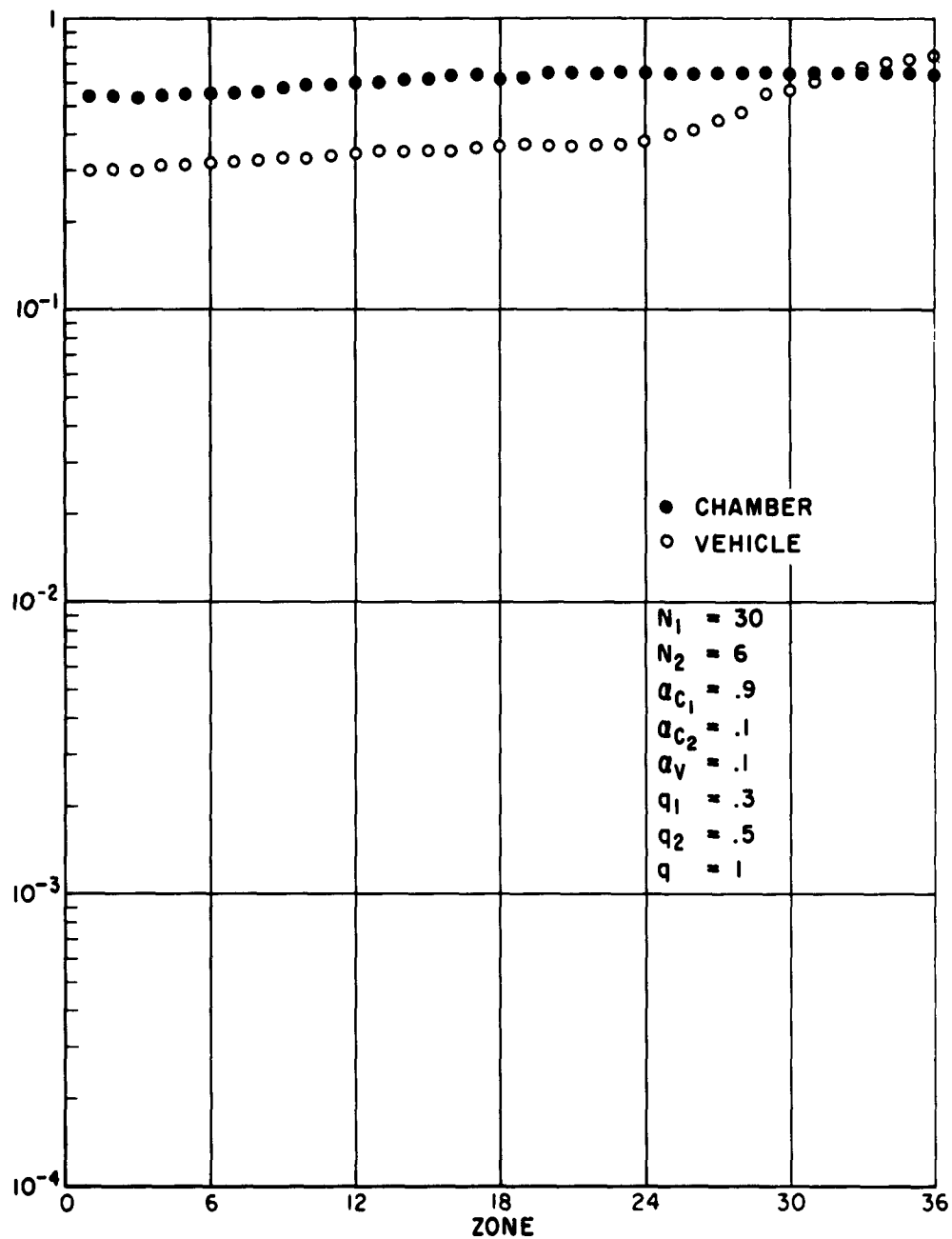


FIGURE 25

## CASE NO. 11 TOTAL HITS PER UNIT AREA

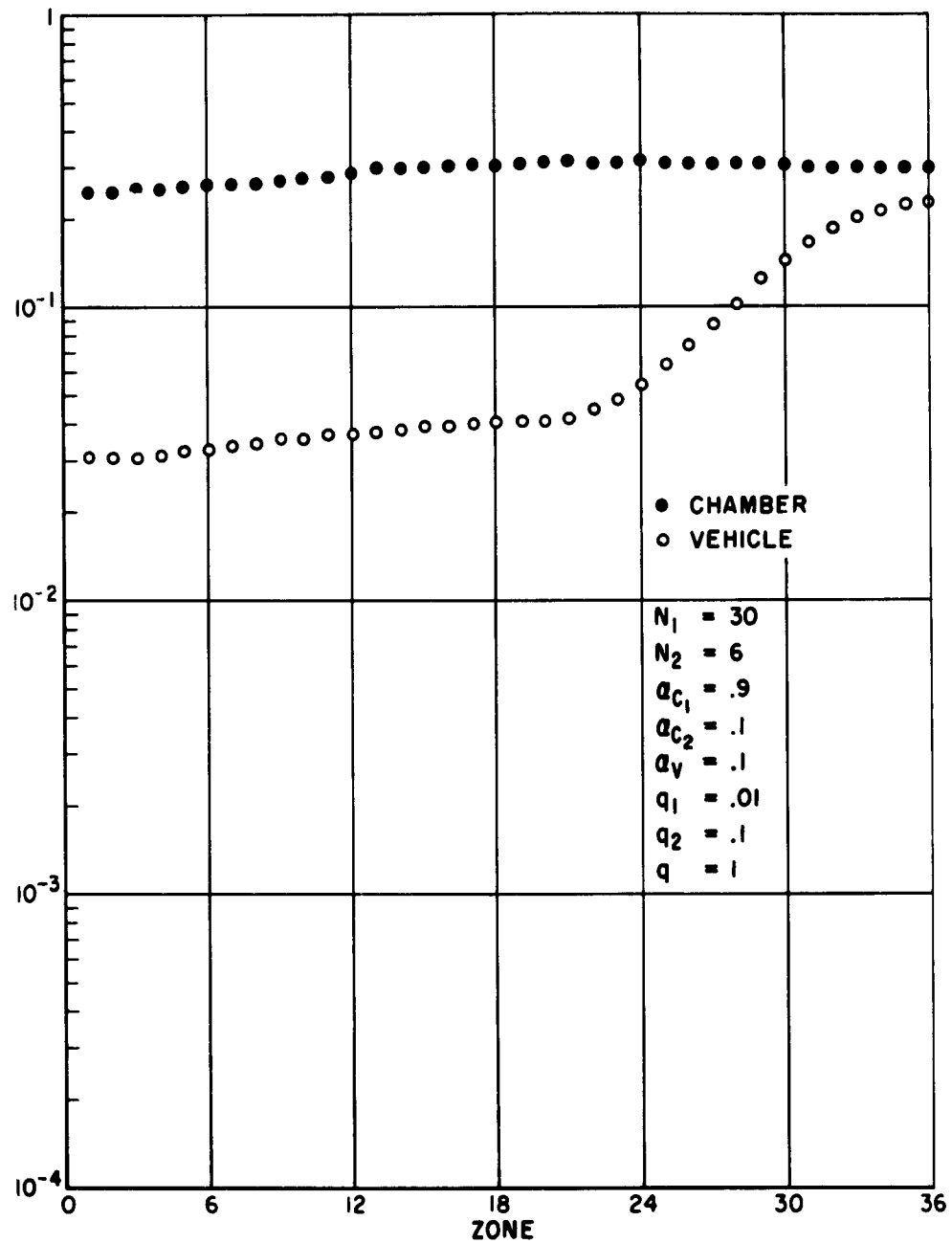


FIGURE 26

**PROBABILITY FLOW CHART  
FROM CHAMBER WALL TO VEHICLE AND FROM VEHICLE TO CHAMBER WALL**

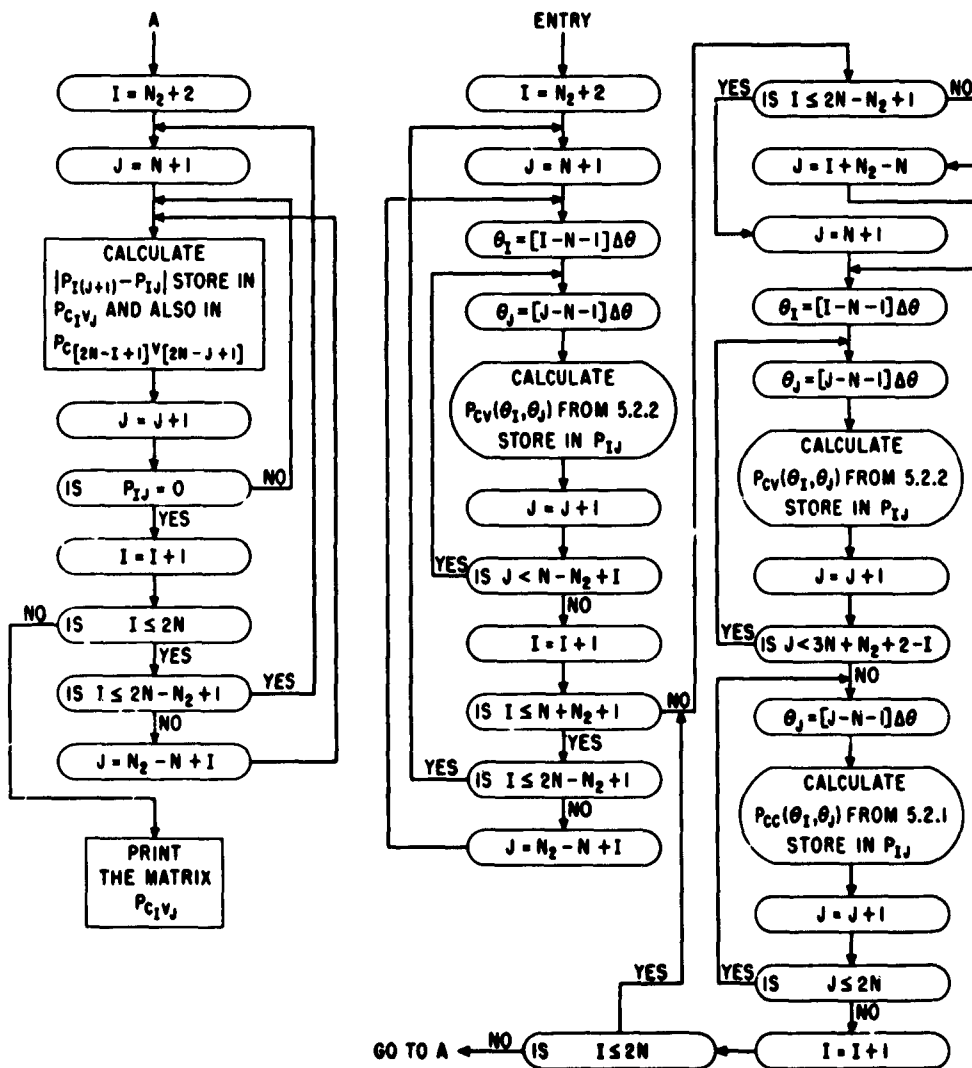


FIGURE 27

**PROBABILITY FLOW CHART  
FROM CHAMBER WALL TO CHAMBER WALL WHEN  $\pi/2 - 2\gamma \leq 0$**

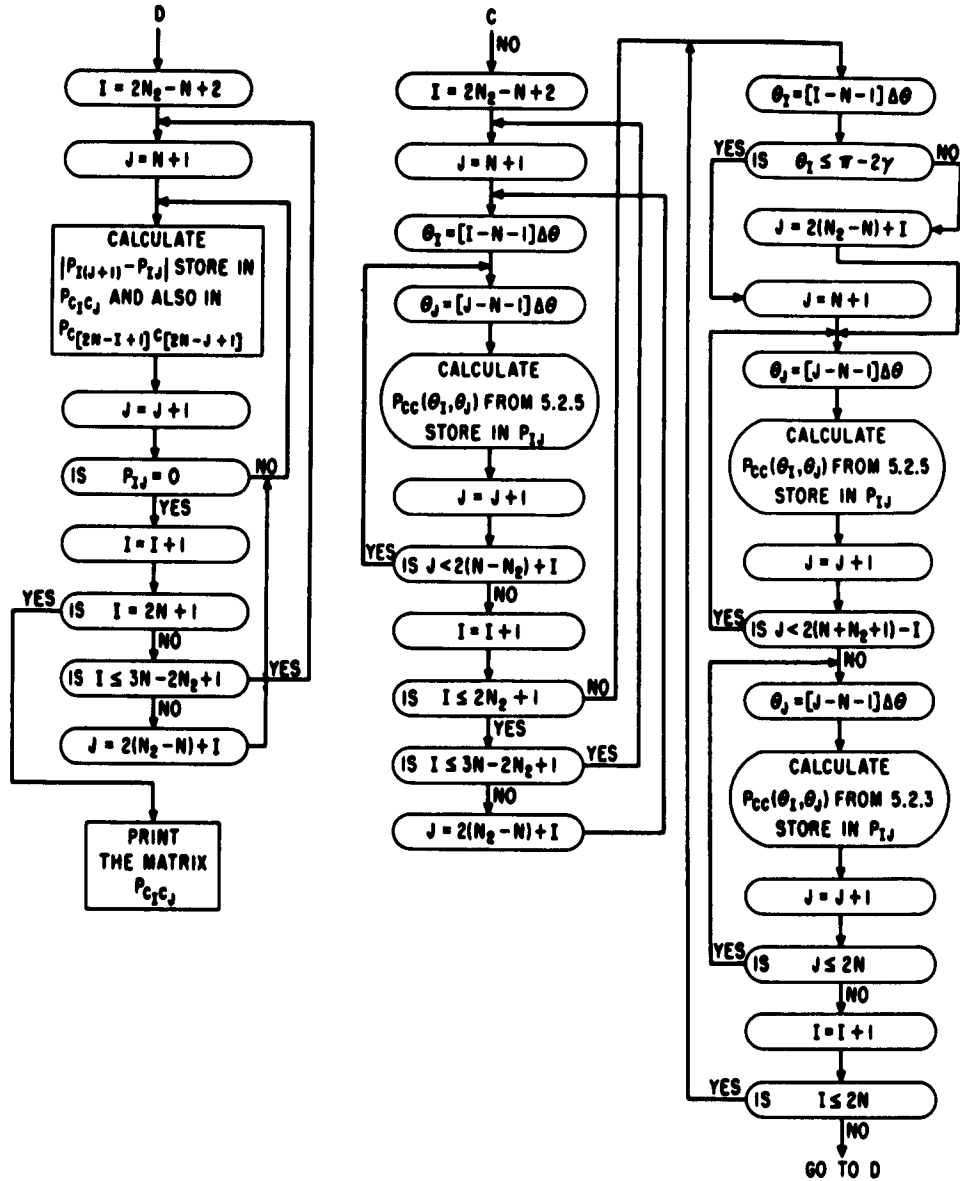
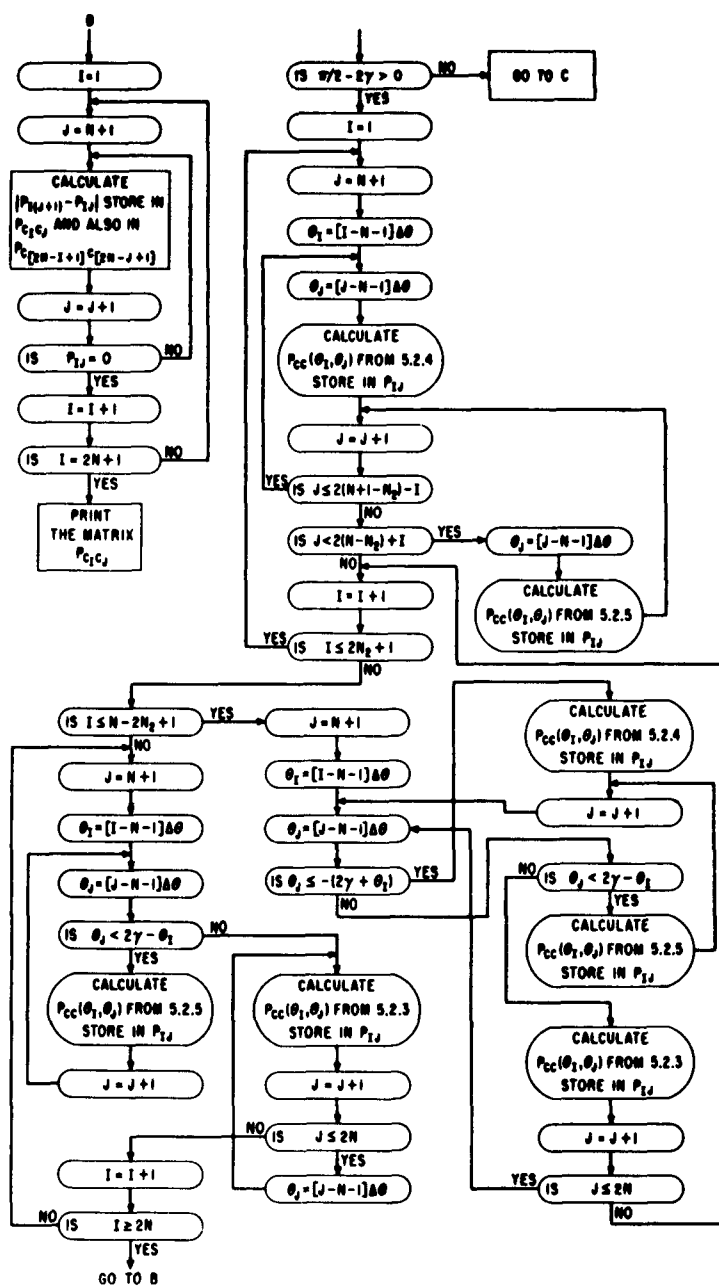


FIGURE 28

**PROBABILITY FLOW CHART  
FROM CHAMBER WALL TO CHAMBER WALL WHEN  $\pi/2 - 2\gamma > 0$**

**FIGURE 29**



## MOLECULAR TRANSFER FLOW CHART

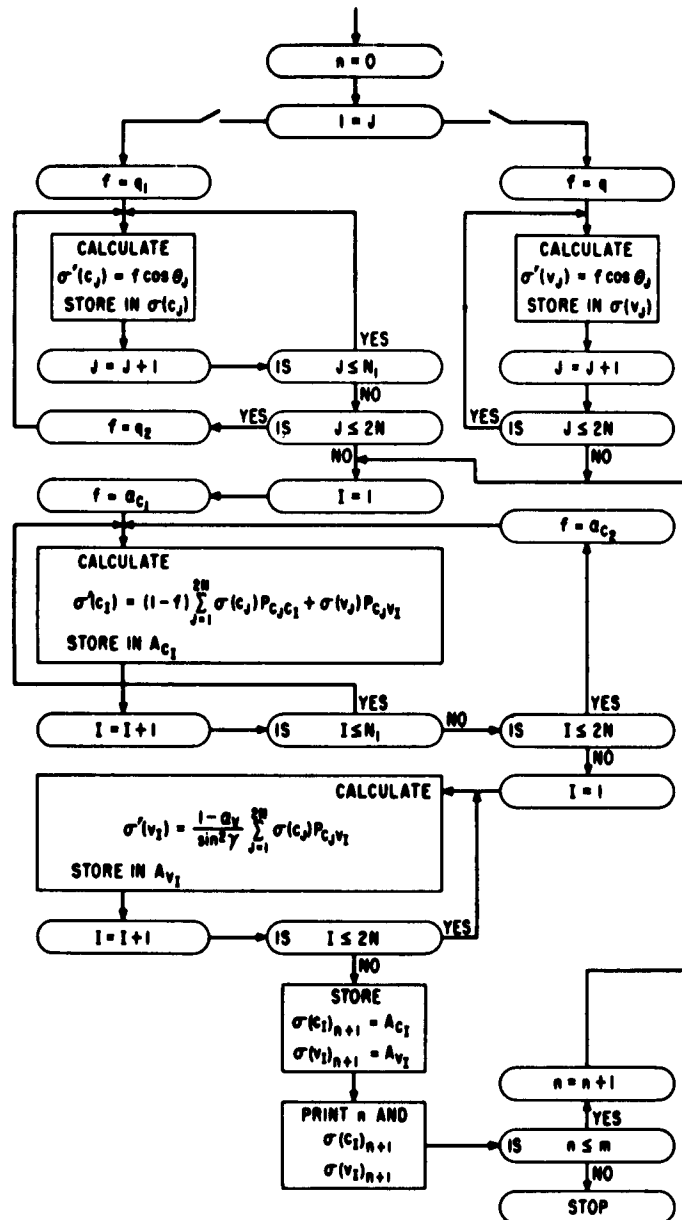


FIGURE 30

PROBABILITY FLOW CHART (REVISED)  
FROM CHAMBER WALL TO VEHICLE

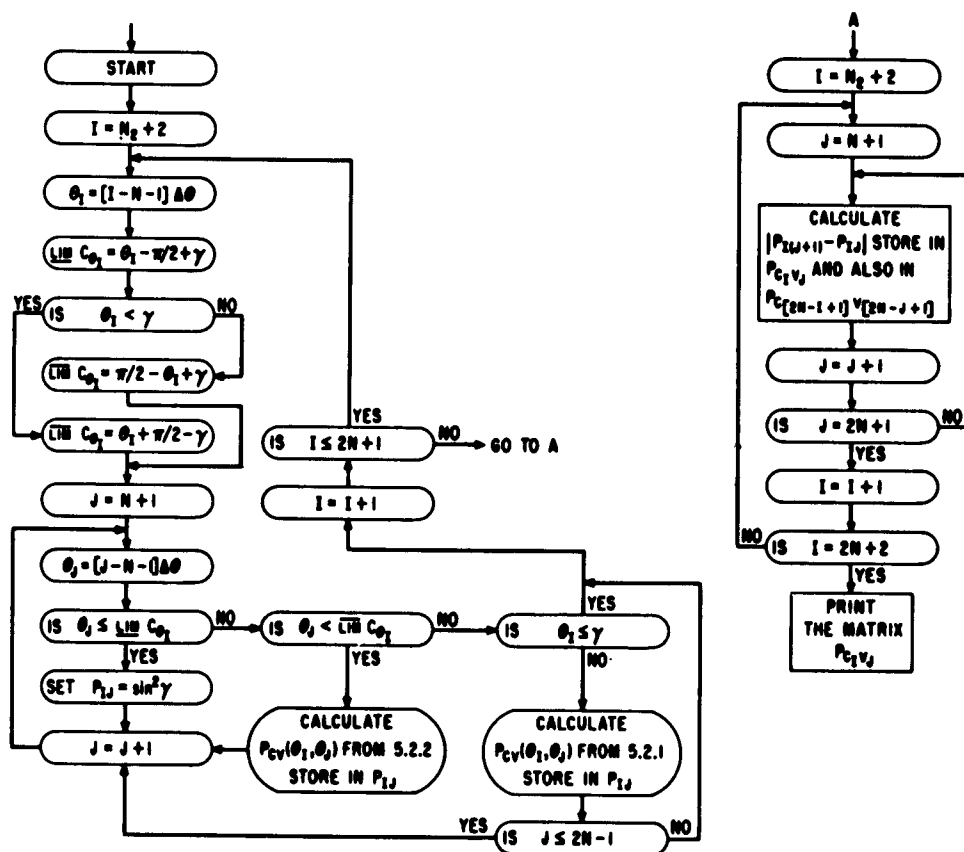


FIGURE 31

**PROBABILITY FLOW CHART (REVISED)**  
**FROM CHAMBER WALL TO CHAMBER WALL WHEN  $\gamma > \pi/4$**

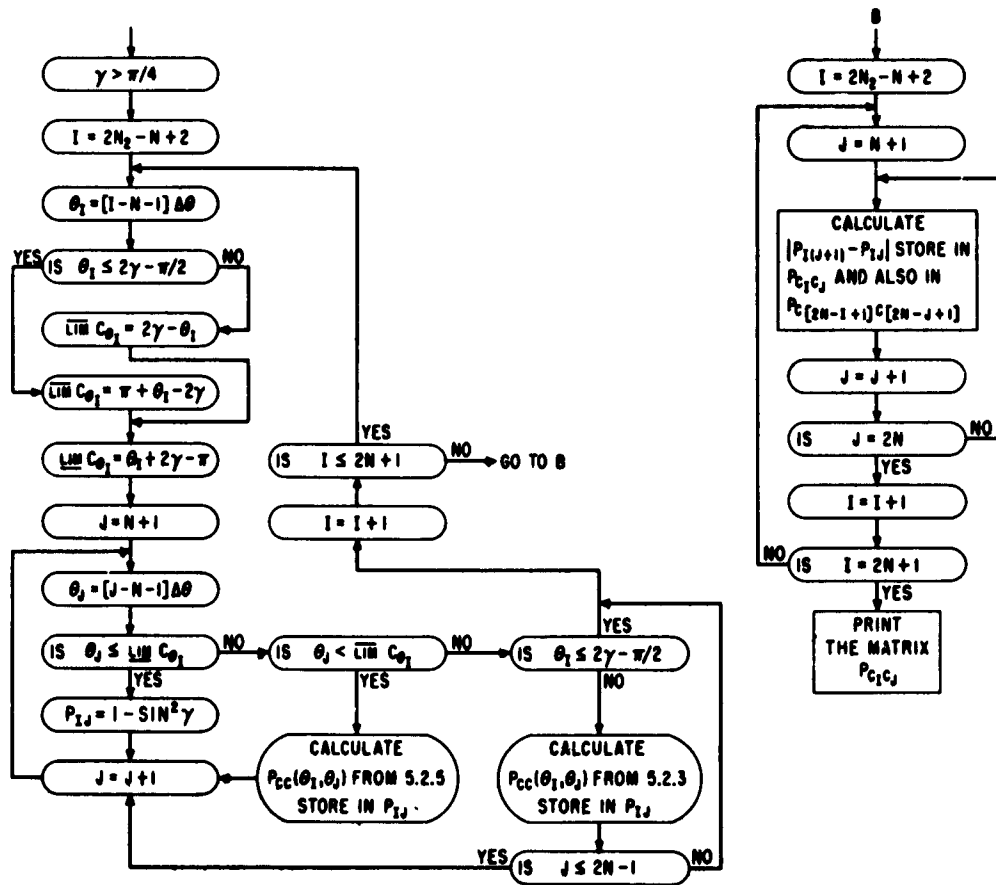


FIGURE 32

<p>Arnold Engineering Development Center Arnold Air Force Station, Tennessee Rpt. No. AEDC TDR-63-88. MOLECULAR FLUX DISTRIBUTION IN AN AEROSPACE CHAMBER - ANALYSIS OF GAS KINETICS - SUMMARY REPORT. April 1963, 81 p. incl illus.</p> <p>Unclassified Report</p> <p>The purpose of this investigation was to determine analytically the molecular incidence rates on the various surfaces of the space simulator. The mathematical model of the space simulator consists of two concentrically located spherical surfaces corresponding to the chamber wall outside and to the vehicle inside. The analysis is divided into two phases. Phase I deals with conditions of uniform pumping and outgassing on each surface. A square pulse of outgassing is assumed to occur and the total number of molecular hits is determined for each surface. These results are extended to a steady state uniform flow and the</p>	<p>1. Space environmental conditions 2. Simulation 3. Test facilities 4. Molecular properties 5. Gas flow 6. Dynamics 7. Analysis</p> <p>I. AFSC Program Area 850E, Project 7778, Task 777801 II. Contract AF 40(600)-954 III. General Engineering Lab., General Electric Co., Schenectady, N. Y. IV. C. A. Tsonis V. Available from OTS VI. In ASTIA Collection</p>	<p>Arnold Engineering Development Center Arnold Air Force Station, Tennessee Rpt. No. AEDC TDR-63-88. MOLECULAR FLUX DISTRIBUTION IN AN AEROSPACE CHAMBER - ANALYSIS OF GAS KINETICS - SUMMARY REPORT. April 1963, 81 p. incl illus.</p> <p>Unclassified Report</p> <p>The purpose of this investigation was to determine analytically the molecular incidence rates on the various surfaces of the space simulator. The mathematical model of the space simulator consists of two concentrically located spherical surfaces corresponding to the chamber wall outside and to the vehicle inside. The analysis is divided into two phases. Phase I deals with conditions of uniform pumping and outgassing on each surface. A square pulse of outgassing is assumed to occur and the total number of molecular hits is determined for each surface. These results are extended to a steady state uniform flow and the</p>	<p>1. Space environmental conditions 2. Simulation 3. Test facilities 4. Molecular properties 5. Gas flow 6. Dynamics 7. Analysis</p> <p>I. AFSC Program Area 850E, Project 7778, Task 777801 II. Contract AF 40(600)-954 III. General Engineering Lab., General Electric Co., Schenectady, N. Y. IV. C. A. Tsonis V. Available from OTS VI. In ASTIA Collection</p>
<p>molecular incidence rates are obtained. Phase II is an analysis of the nonuniform case introduced by surface discontinuities of axisymmetric type. The procedure followed is to determine the various probabilities that a molecule leaving a surface will hit spherical zones on either surface. Using these probabilities the molecular incidence rates can be determined. While the probabilities have been found, analytic expressions for molecular incidence determination are very difficult to obtain. The problem, therefore, was approached from a computer point of view enabling us to obtain computer solutions with a high degree of accuracy.</p>		<p>molecular incidence rates are obtained. Phase II is an analysis of the nonuniform case introduced by surface discontinuities of axisymmetric type. The procedure followed is to determine the various probabilities that a molecule leaving a surface will hit spherical zones on either surface. Using these probabilities the molecular incidence rates can be determined. While the probabilities have been found, analytic expressions for molecular incidence determination are very difficult to obtain. The problem, therefore, was approached from a computer point of view enabling us to obtain computer solutions with a high degree of accuracy.</p>	